

NORTHWESTERN UNIVERSITY

Qualification of Autonomous Crack Monitoring Systems

A Thesis

Submitted to the Graduate School In Partial Fulfillment of the Requirements

For the Degree

MASTER OF SCIENCE

Field of Civil Engineering

By

Brandon G. Hughes

EVANSTON, IL

June 2006

Table of Contents

Acknowledgements.....	V
Abstract.....	VII
List of Figures.....	VIII
List of Tables.....	XII
Chapter 1 – Introduction.....	1
Chapter 2 – Installation, Software and Literature of Crack Monitoring System X.....	4
Installation.....	4
Geophone Monitor.....	5
Crack Monitor.....	7
Sensors.....	9
Geophone Sensors.....	9
Crack Sensors.....	11
Noise Levels and Electromagnetic Interference (EMI).....	12
Computer Interface and Software.....	14
System X Programming and Connection.....	15
Data Analysis Software.....	21
Literature and Manuals.....	23
Chapter 3 – Lab Testing of Crack Monitoring System X.....	25
Long Term or Static Response.....	25
Calibration.....	26
Long Term or Static Testing Equipment Setup.....	29
Long Term or Static Response Results.....	31
Short Term or Dynamic Response.....	33
Dynamic Testing Equipment Setup.....	34
Dynamic Qualification Results – Amplitude Comparison.....	38
Dynamic Qualification Results – Frequency Comparison.....	40
Dynamic Qualification Results – Offsets.....	42
Chapter 4 – Field Testing of Crack Monitoring System X.....	43
Field Trial Blast Vibrations.....	43

Level I Operation.....	44
Level I Equipment Setup.....	44
Level I Data Collection.....	45
Level II Operation.....	51
Level II Equipment Setup.....	52
Level II Data Collection.....	52
Level II Performance.....	55
Level III Operation.....	61
Level III Equipment Setup.....	63
Level III Data Collection.....	64
Level III Performance.....	66
Chapter 5 – Installation, Software and Literature of Crack Monitoring System Y.....	74
Installation.....	74
Geophone.....	75
Crack Monitor.....	76
Sensors.....	79
Geophone Sensors.....	79
Crack Sensors.....	80
Noise Levels and Electromagnetic Interference (EMI).....	82
Computer Interface and Software.....	84
System Y Programming and Connection.....	84
Data Analysis Software.....	88
Literature and Manuals.....	89
Chapter 6 – Lab Testing of Crack Monitoring System Y.....	91
Long Term or Static Response.....	91
Long Term or Static Testing Equipment Setup.....	92
Long Term or Static Response Results.....	94
Short Term or Dynamic Response.....	96
Dynamic Testing Equipment Setup.....	97
Dynamic Qualification Results – Amplitude Comparison.....	101
Dynamic Qualification Results – Frequency Comparison.....	104

Dynamic Qualification Results – Offsets.....	105
Chapter 7 – Field Testing of Crack Monitoring System Y.....	107
Field Trial Blast Vibrations.....	107
Level I Operation.....	108
Level I Equipment Setup.....	108
Level I Data Collection.....	109
Level II Operation.....	114
Level II Equipment Setup.....	114
Level II Data Collection.....	115
Level II Performance.....	116
Chapter 8 – Conclusions.....	123
References.....	130

Acknowledgments

Without the assistance of so many gracious and patient people, this thesis could not have been accomplished. First and foremost, I would like to thank my advisor Professor Charles Dowding for his expertise, conversation, support, motivation and guidance during this process. Without Professor Dowding, this thesis would certainly not have been possible. I would also like to thank Professor Richard Finno for his geotechnical instruction and to both professors for allowing me to pursue my graduate degree at Northwestern University.

I would like to thank the Infrastructure Technology Institute for funding my research. I must thank the ITI staff members; Dan Hogan, Dan Marron, Dave Kosnik and Matthew Kotowsky for whom I am grateful to for their technical assistance and education in all matters electronic. The remote monitoring of these commercial systems could not have been done without the help of Civil Data Systems.

I would also like to thank my fellow geotech graduate students, specifically Greg Andrianis, Wan-Jei Cho, Luke Erickson, Cecilia Rechea and Mike Waldron. For those who were lucky enough to be my fearless roommates, I thank-you for putting up with me at both school and home. Without these people my graduate school experience at Northwestern would not have been nearly as enjoyable, and I would not have had the honor of calling myself an Aquitard.

Finally, I would like to thank my family and friends for all the support they have given during this adventure. Specifically, I could not have done this without my parents, Jim and Patty, who have always instilled in me the importance of higher education. I am truly grateful for their undivided attention, encouragement and constant support during this task. Additionally, I would like to thank Michael Wysockey and the Wysockey family for encouraging me to strive for a graduate degree. Their friendship, encouragement and support while I pursued my graduate degree were greatly appreciated.

Abstract

This thesis summarized the qualification and testing of two commercial Autonomous Crack Monitoring (ACM) systems for use in measuring micrometer displacement of cracks. Qualification involved the assessment of both laboratory and field performance in a residential structure subjected to nearby quarry blasting for the production of roadway aggregate. Aggregate and construction industries are dependant on procedures that cause vibratory ground motion and would benefit from a commercial ACM system. Currently, only research grade equipment is available for ACM monitoring which is expensive, unwieldy and requires specialized knowledge to operate.

Performance at three levels of monitoring has been evaluated. During level I monitoring only long term crack displacement response to environmental effects was recorded. During level II monitoring both long term and dynamic (triggered by ground motion) crack displacements are recorded. At the highest level of monitoring, level III, long term and dynamic crack displacements are recorded with dynamic response triggered by crack response and/or ground motion. Crack displacement triggering allows recording of crack responses to occupant activities or other non ground motion events such as wind gusts.

Qualification showed that each system was able to sufficiently operate at monitoring and collecting level I crack and environmental responses. Additionally, each system also showed continued progress towards adequate level II operation. Finally, one of the systems was evaluated as a level III system and captured both occupant and environmentally induced crack responses during qualification.

List of Figures

2.1	System X wiring diagram.....	5
2.2	Installation of the geophone (left) and the downstairs data logger (right).....	6
2.3	Installation of the system X crack and null lvdt's on the crack. The core being epoxied (left), the final installation (middle) and a close-up of sensor showing the size relation to the crack.....	8
2.4	Typical ground motion record by the system X geophone. Blast occurred on May 27, 2005.....	10
2.5	Typical system X noise level visible in the crack velocity-time history with and without NU system in operation.....	14
2.6	External key pad for on-site programming of the system X crack monitor.....	16
2.7	System TTY mode layout for programming.....	19
2.8	Detailed description of the trigger settings for system X.....	20
2.9	System X, Event Manager Software interface.....	21
2.10	Seismic Analysis Software Screenshot when creating a Crack Time History.....	22
3.1	Kaman calibration equipment setup used to test the system X LVDT's.....	27
3.2	Voltage vs. displacement for calibration of the Transtek LVDTs.....	28
3.3	Static response qualification equipment layout.....	30
3.4	Independent temperature and displacement recorded during static testing.....	32
3.5	Measured and calculated displacement vs. temperature for sensor 1 and 2.....	33
3.6	Modified dynamic testing apparatus.....	36
3.7	Description of how a phase shift was created in the waveforms, during dynamic testing.....	37
3.8	Typical waveform recording during the dynamic testing of system X.....	39
3.9	Frequency comparison of system X to the control system.....	41
3.10	Typical waveform time history of the control system and system X during a baseline shift.....	42
4.1	Environmental data from a three-month monitoring period. Gray jagged lines are a one-hour rolling average while the black lines are 24-hour rolling average.....	46

4.2	Comparison of the displacement time histories for the NU LVDT, System X LVDT crack gauge and indoor temperature. Gray jagged lines are a 1 hour rolling average; and the black lines are a 24-hour rolling average. (red dots, indicate points used to calculate the long term static ratio.).....	48
4.3	Long term system X versus NU LVDT data used to determine the system X long term or static ratio.....	49
4.4	Comparison of the System X Crack and Null gauges over two-month duration of testing.....	50
4.5	Temperature versus crack displacement data compared to the theoretical thermal expansion of gypsum, the main component of drywall.....	51
4.6	Direct comparison of crack time histories for system X, and NU LVDT, blast April 18, 2005. System X, data filtered to remove all content greater than 50 Hz....	55
4.7	(Top) Comparison of the displacements of system X to the NU LVDT sensor during dynamic recording. (Five individual blasts denoted by symbols.) (Bottom) Example of how the dynamic ratio was selected for a given filtered waveform.....	57
4.8	System X, recorded crack displacement from a blast occurring June 9, 2005 were a temporary offset occurred.....	58
4.9	Comparison of the crack displacement captured by system X dynamically during blasting on June 9, 2005 and long term crack displacement during three weeks of the month of June.....	60
4.10	System X, recorded crack displacement from a blast occurring June 20, 2005 during which the crack responded to primarily to the air blast.....	61
4.11	Example of the crack triggering logic for system X, when operating as level III system.....	62
4.12	Number of events recorded by system X as function of the trigger level. Specific to the Milwaukee test house, data collected on July 8-9, 2005, with a trigger level of 0.36 μm	65
4.13	Example of the typical system X noise during monitoring in comparison to the smallest crack trigger level. Trigger level of 0.036 μm shown in red.....	66

4.14	Examples of created occupancy activity recorded on the NU system, for comparison of the actual events from system X. (Waldron 2006).....	67
4.15	Low frequency (4 Hz or less) crack triggered movement recorded during system X, monitoring in Milwaukee, WI.....	68
4.16	Average hourly and gust wind speed data collect from the Mitchell Airport weather station, Milwaukee, WI.....	69
4.17	Peak to peak crack displacement as function of wind speed for data collected by Aimone-Martin in Henderson NV, and during this study.....	70
4.18	High frequency crack triggered movement recorded during system X monitoring in Milwaukee, WI.....	71
4.19	Number of events occurring in the Milwaukee test house as function of time of day. Data collected from June 30 to July 11, 2005.....	73
5.1	System Y wiring diagram.....	75
5.2	Installation of the geophone in the downstairs of the test house.....	76
5.3	Installation of the system Y crack and null linear potentiometers on the cracked and uncracked drywall.....	77
5.4	Typical ground motion record by the system Y geophone. Blast occurred on May 19, 2005.....	80
5.5	Typical system Y noise level visible in the crack velocity-time history with and without NU system in operation.....	83
5.6	External key pad for on-site programming of the system Y crack monitor.....	85
5.7	System Y command layout when programming with the keypad. (Company Y Operator Manual).....	87
5.8	System Y, Event Management software interface.....	88
5.9	Software screenshot of a ground motion and a crack time history.....	89
6.1	Static testing equipment layout for system Y.....	93
6.2	Correlation showing the comparison of the temperature and displacement recorded during static testing.....	95
6.3	Measured and calculated displacement vs. temperature for system Y.....	96
6.4	Modified dynamic testing apparatus for System Y testing.....	99

6.5	Description of how a phase shift was created in the waveforms, during dynamic testing.....	100
6.6	Typical waveform recording during the dynamic testing of system Y.....	102
6.7	Maximum and minimum displacements of the Kaman and system Y sensors during dynamic testing.....	103
6.8	Frequency comparison of system Y to the control system.....	105
6.9	Typical waveform time history of the control system and system Y during a baseline shift.....	106
7.1	Comparison of the displacement time histories for the NU LVDT, System Y linear potentiometer crack gauge and indoor temperature. Gray jagged lines are a 1 hour rolling average; and the black lines are a 24-hour rolling average. (red dots, indicate points used to calculate the long term static ratio.).....	111
7.2	Long term system Y versus NU LVDT data used to determine the system X long term or static ratio.....	112
7.3	Comparison of the System Y Crack and Null gauges over two-month duration of testing.....	113
7.4	Direct comparisons of the crack time histories for system Y, NU LVDT and NU Kaman. Blast June 2, 2005. System Y data filtered to remove all frequency content greater than 50 Hz.....	117
7.5	(Top) Comparison of the maximum and minimum displacements of system Y with the NU LVDT sensor during dynamic recording. These four events (denoted by symbols) occurred on June 2, 2005. (Bottom) Example of how the dynamic ratio was selected for a given filtered waveform.....	119
7.6	System Y recorded crack displacement from a blast occurring June 9, 2005 where a temporary offset occurred.....	121
7.7	Comparison of the crack displacement captured by system Y both long term and dynamically during blasting on June 9, 2005 where an insignificant temporary offset occurred.....	122
7.8	System Y recorded crack displacement from a blast occurring June 30, 2005 during which the crack responded primarily to the air blast.....	122

List of Tables

2.1	Specifications comparison for the Transtek LVDT to the Kaman eddy current Sensor.....	12
2.2	Historic noise levels for system X during testing.....	13
3.1	Calibration test summary data, equation slope, average slope, R ² and standard deviation.....	29
3.2	Summary of the dynamic tests completed for system X.....	39
4.1	System X and NU LVDT calculated changes in displacement from the data collected in figure 4.2.....	49
4.2	Summary of blast data collected during Level II testing of system X *Denotes events that did not require noise filtering. (NU system inactive).....	54
5.1	Specification comparison for the StructureMetrix linear potentiometer to the Kaman eddy current sensor.....	81
5.2	Historic noise levels for system Y during testing.....	83
5.3	System Y relationship between the number of channels recorded and the number of events the unit can record per monitoring period.....	86
6.1	Summary of the dynamic tests completed for system Y.....	103
7.1	System Y and NU LVDT calculated changes in displacement from the data collected in figure 7.1.....	112
7.2	Summary of blast data collected during level II testing of system Y. ¹ Denotes events record with the gain set to 1x. *Denotes events that did not require noise filtering. (NU system inactive).....	116

Chapter 1

Introduction

This thesis describes the qualification and testing of two commercial Autonomous Crack Monitoring (ACM) systems for use in measuring micrometer displacement of cracks. Qualification involved the assessment of both laboratory and field performance. The commercial ACM systems were installed in a residential structure subjected to nearby quarry blasting for the production of roadway aggregate. Aggregate and construction industries are dependant on procedures that cause vibratory ground motion and would benefit from a commercial ACM system. Currently, only research grade equipment is available for ACM monitoring, which is expensive, unwieldy and requires specialized knowledge to operate. This research was sponsored by the Infrastructure Technology Institute (ITI) at Northwestern University through a grant from the United States Department of Transportation.

ACM equipment includes hardware such as geophones for monitoring ground motion, crack sensors for determining one dimensional crack response and data loggers for recording and transmitting the results. An ACM system also includes software for transforming the data into a useful format. As ACM technology has been developed, three levels of monitoring have been created to optimize system capability. Level I monitoring records only the long term crack response to environmental effects at low sampling rates to determine daily or weekly trends. At this level of performance blast effects manifest themselves by a change in the crack response at the time of the blast. Level II monitoring records both long

term crack displacement and high sample rate dynamic data during seismic events. Level II monitoring requires a geophone to monitor ground vibration and then trigger the system to measure crack displacement during an event. Level III monitoring records long term crack displacement and high sample rate data during events triggered by ground motion and/or crack response. Crack response can include that resulting from occupant's activity or other non-seismic dynamic events such as wind gust induced response. Crack triggered response from these other dynamic events can then be compared to blast induced movements.

Previous work with ACM systems has included the development and installation of experimental systems in blasting and construction environments. Past work by (Louis, 2000; Siebert, 2001; McKenna 2002; Baillot 2004; Waldron 2006) have demonstrated the effectiveness of research grade ACM technology in monitoring crack displacement during level I and II operation. Previous work by (Petrina 2004; Ozer 2005; Waldron 2006) has further developed laboratory methods for the qualification of ACM sensors and equipment for various modes of monitoring. The thrust of this thesis, the commercialization of ACM systems, is another step in moving ACM technology from the laboratory to practice.

This thesis which describes the commercialization of two ACM systems is divided into seven Chapters. There is not a background Chapter included in this work since the information can be found in the many previous theses enumerated above. The first commercial ACM system, system X, was evaluated in Chapters 2 through 4. The second commercial ACM system, system Y, was evaluated in Chapters 5 through 7. Chapters 2 and 5, describe the equipment and installation procedures followed for systems X and Y, respectively. Additionally, the software and manuals included with each system are evaluated for ease of use. Chapters 3 and 6 describe the laboratory qualification of systems

X and Y, respectively. Laboratory qualification included evaluation of both long term and dynamic capabilities of the system. Long term qualification was completed by mounting the sensors on a homogeneous plate with a known linear thermal expansion coefficient. The recorded displacement of the sensor was then compared to the theoretical expansion of the plate. Chapters 4 and 7 describe the field qualification of systems X and Y, respectively. During field qualification, each system was installed in a residential structure to determine the system's capability to measure crack response from blasting. System X was evaluated to monitor crack displacement during operation as a level I, II and III system. System Y was evaluated to monitor crack displacement during operation as a level I and II system. The final Chapter of this thesis, Chapter 8, summarizes the conclusions made for each system.

Chapter 2

Installation, Software and Literature of Crack Monitoring System X

In this chapter, the installation, software and literature of a commercial Autonomous Crack Monitoring (ACM) system X are summarized. Specifically software and manuals of system X, were reviewed to ascertain their ease of use by the average field technician. Additionally, electromagnetic noise interference was measured and methods for reducing and removing noise were evaluated

Installation

This section describes the general installation method that was followed for installation in both the laboratory and field. The physical installation of system X including the crack sensor can be completed in one day. Figure 2.1 shows the wiring diagram for the two component system X crack monitor as it was installed in the test house. The first component measures ground motion and air blast and the other measures crack response. Each component consists of a processor (computer), data logger and sensors. Transducers for the first component measure ground motion, while those for the second, measure the crack response. The ground motion component triggers the crack sensor component when the system obtains both long-term and dynamic crack response (level II operation).

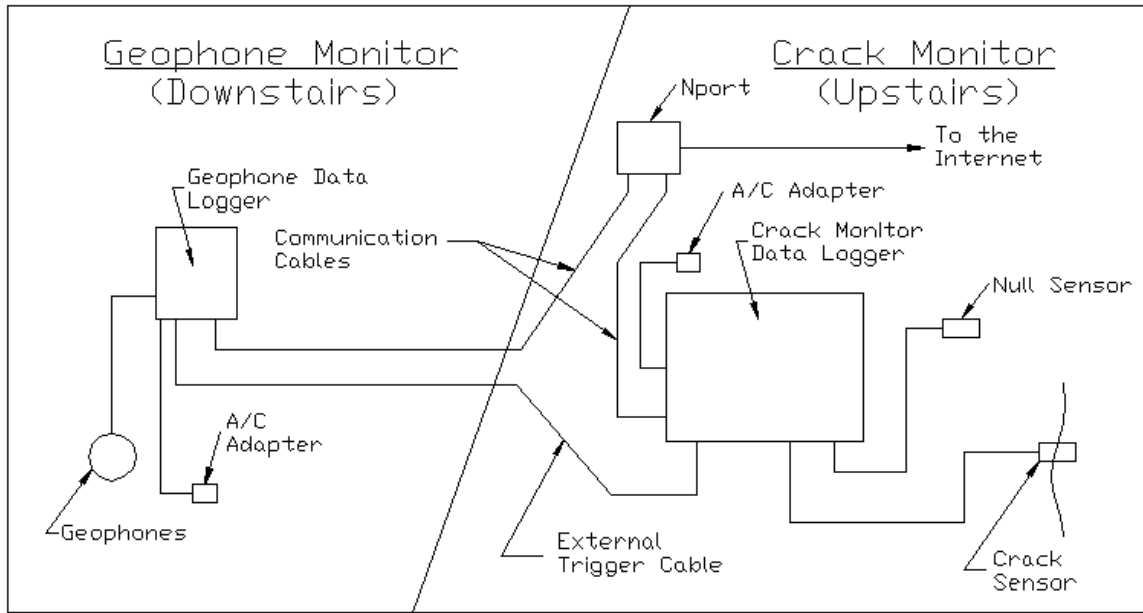


Figure 2.1 System X wiring diagram

Geophone Monitor

Installation began by the placement of the geophones and related equipment in the basement of the test house. An out of the way location for the geophone was needed to minimize triggering by activity from the house’s residents. A storage area under the stairway was selected. Normally, the geophone would be installed by burying, anchoring, sandbagging or spiking in the ground outside. However, in this case since it was not employed to ensure regular compliance, it was installed in the basement. Other measurements of ground motion were available to establish compliance. The geophone can be anchored to a concrete surface, and in this case, a plaster coating on the bottom of the geophone block was used. Figure 2.2 shows the completed installation of the geophone. Plaster was advantageous because after the testing was completed, the remaining plaster can be scraped away without leaving any residue or mounting holes.

Once the geophone was mounted, the downstairs data logger was then placed on the floor under the stairway within 5 feet of the geophone. The geophone cable was then connected to geophone port on the side of the geophone data logger. The geophone data collector contained an internal battery that could be used for short term monitoring or an A/C adapter for long term deployment. Since system X was to be deployed in the test house for at least six months, the unit was powered by the A/C adapter. The internal battery remained useful as a backup power supply in case of a power outage or a accidental unplugging of the unit. The trigger cable, attached to the auxiliary port on the geophone data logger, was routed to the auxiliary port on the crack monitor upstairs. A standard serial cable was then employed to connect the geophone data logger to an “Nport”, to allow remote communication and control via the internet. Figure 2.2 shows the installation of the geophone and geophone data logger.

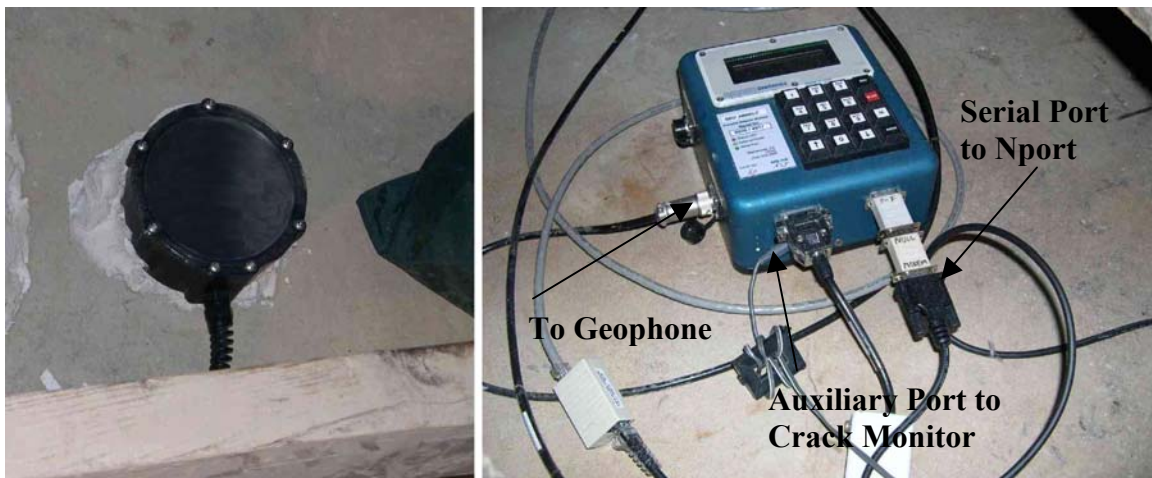


Figure 2.2 Installation of the geophone (left) and the downstairs data logger (right).

Crack Monitor

The second step of installation was attachment of the crack sensors across the crack. Two LVDTs supplied with the system were mounted at the crack. The first LVDT was mounted directly across the crack to measure crack movement; and the second LVDT was mounted on a nearby uncracked section of the drywall to measure environmental effects of the sensor and uncracked wall materials. LVDTs were attached to the wall surface with a 90 second quick setting epoxy. The sensors were placed at least 30 centimeters apart to prevent interference between the sensors.

The system X literature recommended the use of hot glue to attach the crack sensor across the crack on the wall. Previous work by (Petrina, 2004) found that using an adhesive such as hot glue was found to be deformable, have nonlinear expansion, and have a high coefficient of expansion. The hot glue was replaced with the 90 second epoxy to reduce these effects. According to lab testing done by (Petrina, 2004) the 90 second epoxy was found to be both stable and quick setting.

LVDT displacement sensors were mounted across a crack in a drywall ceiling as shown in Figure 2.3. The coil housings of the LVDTs were first epoxied in place and then connected to the crack monitor. The monitor was turned on and the core was centered in the coil housing to allow maximum travel of the sensor during operation in both directions. The crack monitor was then placed in setup mode and a voltmeter was placed across the test points to determine the exact location of the core inside the attached coil housing. The core assembly was then joined by threading the shaft of the core into the core bracket. Jam nuts, were also used for subsequent adjustment of the core position. The core assembly was then fixed in position with the quick-set epoxy. As the epoxy was setting, slight adjustments were

made to move the core assembly within the coil to the manufacturer's specified position. Adjustments were made by sliding the assembly in the setting epoxy based on the readout of the voltage meter. Finally, Loctite adhesive was applied to the jam nuts to prevent them from loosening over time. Figure 2.3 shows the completed LVDTs mounted across the crack and on the uncracked drywall.

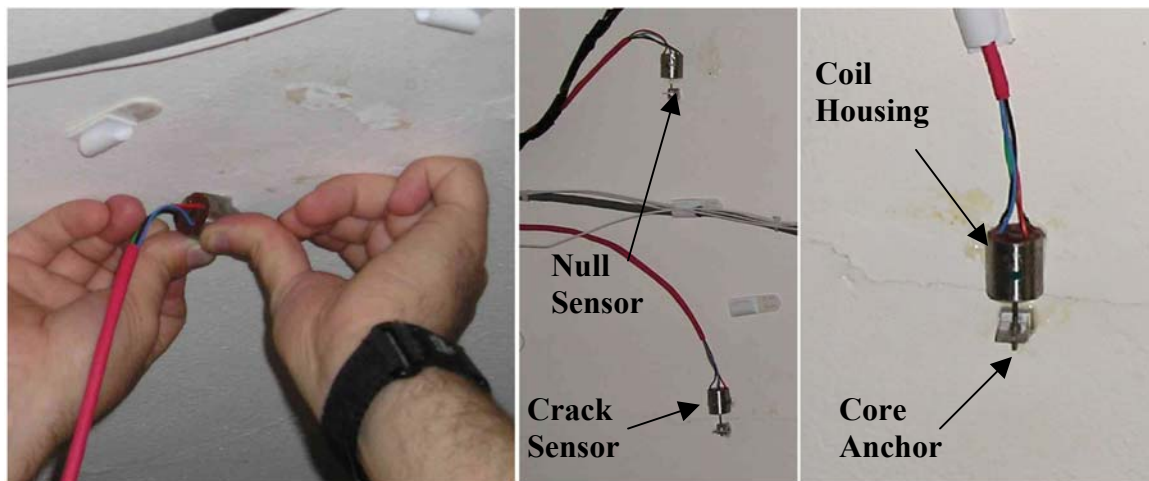


Figure 2.3 Installation of the system X crack and null lvdt's on the crack. The core being epoxied (left), the final installation (middle) and a close-up of sensor showing the size relation to the crack.

The crack and null displacement sensors were connected to the crack monitor data logger and placed in a small closet. Another data logger similar to the one in Figure 2.2 was placed on the bottom shelf of the closet and the crack sensor cables were then routed through a small hole in the wall and connected. The crack monitor data logger, like the geophone data logger, can be powered by both an internal battery and A/C adapter, and like the geophone data logger, was powered by the A/C adapter. The auxiliary port on the crack monitor received the external trigger cable from the geophone data logger. As with the

geophone data logger, a standard serial cable was employed to connect with the Nport for internet communication.

Sensors

System X crack monitors employ LVDT sensors to measure micrometer opening and closing of the crack and geophones to measure the particle velocity of the ground motion. All LVDT displacement sensors were exercised in the laboratory both statically and dynamically to ensure that they operated properly and that their response compared to previously calibrated sensors. External SUPCO temperature and humidity sensors were used to monitor the environmental effects during selected testing. Future ACM systems should include integrated temperature and humidity sensors.

Geophone Sensors

Geophones measure ground motion in terms of particle velocity. Since there are longitudinal, transversal and vertical principal directions; three geophones are necessary. In this case all three components are housed in a single geophone block. During a dynamic event, a geophone records the time history of the ground motion for a preset duration. During normal monitoring, the geophone is programmed to monitor ground motion constantly. When the ground motion exceeds a user defined trigger value, the geophone data logger then records for a preset duration. In addition to recording the particle velocity-time history after triggering, the geophone data logger will also record a preset amount of time prior to triggering. This is called the pretrigger. A pretrigger of 0.5 seconds was set for all

measurements. The particle velocity trigger level was set to 1.02 mm/sec. The unit records ground motion at 1000 samples per second for the preset pre and post trigger record time. For blast monitoring, the recorded time length for an event is normally three seconds. Figure 2.4 compares the typical three components of the particle velocity during a time history. During this blast, the geophone was triggered on the vertical channel and the maximum peak particle velocity (PPV) was 4.75 mm/second.

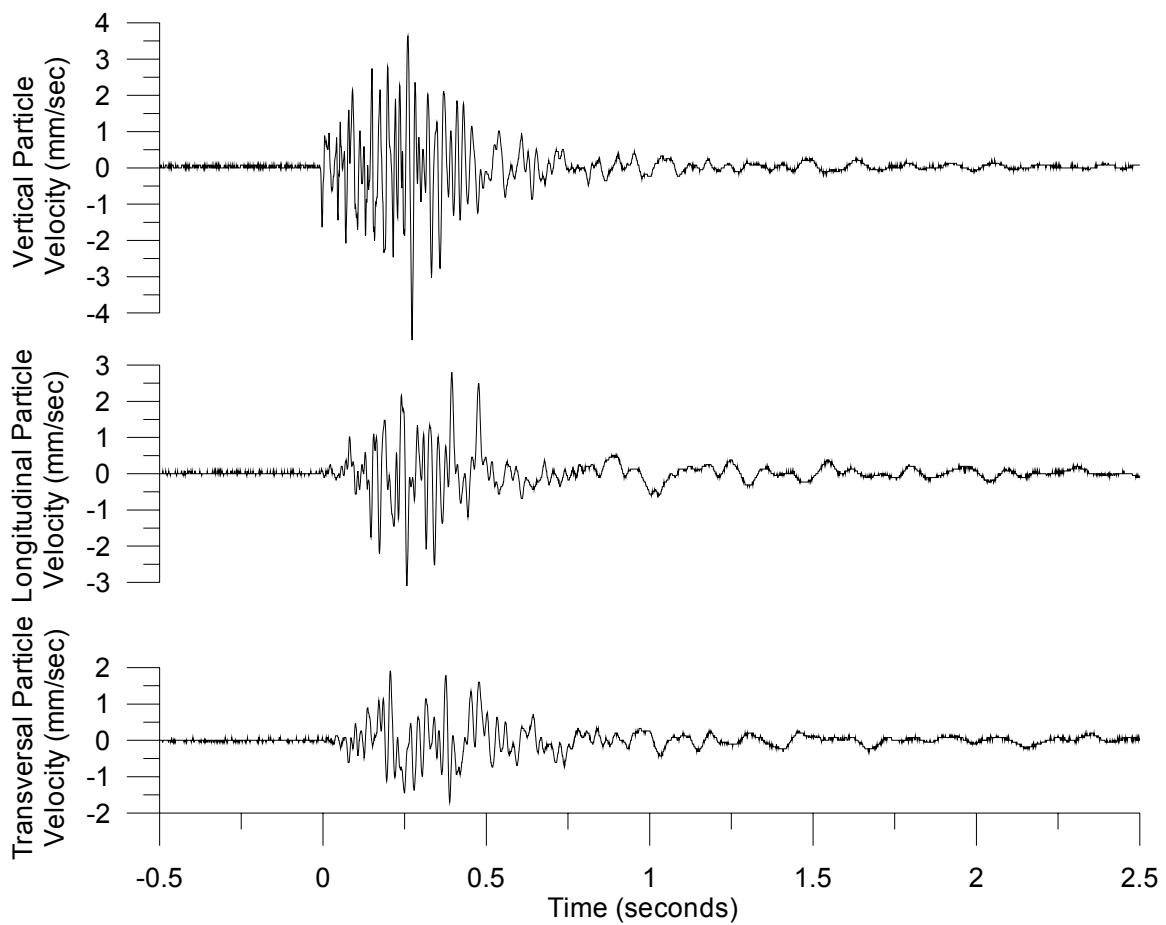


Figure 2.4 Typical ground motion record by the system X geophone. Blast occurred on May 27, 2005.

Crack Sensors

The opening and closing of a crack during a blast event are very small and often only a few micrometers of displacement will be recorded. System X was qualified with Transtek series 200 LVDTs to collect crack displacement. Thus, the crack displacement sensors must have a small range and a high resolution. The range of the Transtek sensor was approximately 2.5 times the benchmark Kaman sensor (McKenna ,2001). A direct comparison of the specifications of Transtek LVDT with the Kaman eddy current sensor is shown in Table 2.1 The Transtek sensors proved to be easy to install with little disturbance to the home owner. According to Petrina, (2004) the displacement sensors were selected based on surface attachment, mechanical design and operational configuration. Qualification of the Transtek LVDTs dynamically and statically and a comparison with the Kaman sensors is presented in Chapter 3.

The crack sensor on system X, is monitored on both a AC and DC coupled channels. The null sensor is only monitored on a DC channel. AC coupled channels measure only dynamic response while DC coupled channels measure both long term and dynamic response. The AC coupled channel should be employed versus the DC coupled channel to define the dynamic response time histories because it is highly resolved. DC coupled channels follow the long term displacement response in reference to the initial value.

Manufacturer	Transtek	Kaman
Model	Series 200	SMU-9000-2U
Type of Sensor	DC-DC LVDT	Eddy Current
Range (μm)	± 1270	± 500
Resolution (μm)	0.089 AC & 0.89 DC	0.045
Input, (Volts DC)	7 max, 5 min	30 max, 7.5 min
Input, (Current mA)	20	15mA
Output, full Scale (DC)	± 1.5	0 to 5
Scale factor (V/μm)	0.00118	0.01
Linearity, % Full Scale	± 0.5	± 10
Output Impedance	2.2 (1000 Ω)	100 Ω
Temperature Range ($^{\circ}\text{C}$)	-54 to 60	-55 to 105

Table 2.1 Specifications comparison for the Transtek LVDT to the Kaman eddy current sensor.

Noise Levels and Electromagnetic Interference (EMI)

Electromagnetic Interference (EMI) can mask the signal from a sensor measuring crack displacement in an Autonomous Crack Monitoring (ACM) system. EMI induces voltage fluctuations, which are superimposed over the sensor output. ACM systems employ highly sensitive sensors that produce a voltage proportional to changes in displacement. Thus, small crack movements result in small voltage changes. Any introduction of EMI during these measurements results in significant voltage spikes and noise as shown in Figure 2.5. Crack displacement recorded during a transient event can be obscured by noise. EMI is emitted from most electronic devices and therefore measuring equipment should be designed to operate in a noisy environment. Most EMI occurs at the 60 Hz frequency, common for AC power in residential and commercial buildings.

Initial testing of system X in the test house was completed with the NU system operating at the same time. With the NU system operating, system X noise was 2.3 μm peak

to peak. It was found during testing that the high noise levels were directly related to EMI production by the NU system. For this reason testing was completed on system X with and without the concurrent operation of the NU system. Table 2.2 shows the noise levels of the system with and without the operation of the NU system. System X was found to operate at an acceptable noise level of 0.8 μm peak to peak in a standard residential environment.

The most significant reduction of the noise levels of system X was attained when the NU System was deactivated. While the cause of noise in this testing environment was easy to pinpoint and eliminate, in some field environments this may not be possible. Figure 2.5 demonstrates the noise levels before and after the NU equipment was disabled.

System X Historical Noise Levels		
Date	Noise Level (μm)	Notes
1/20/2005	2.2	Blast Triggered Event NU System running
6/9/2005	0.8	Blast Triggered, NU System Off
6/30/2005	0.8	Crack Triggered, NU System Off

Table 2.2 Historic noise levels for system X during testing

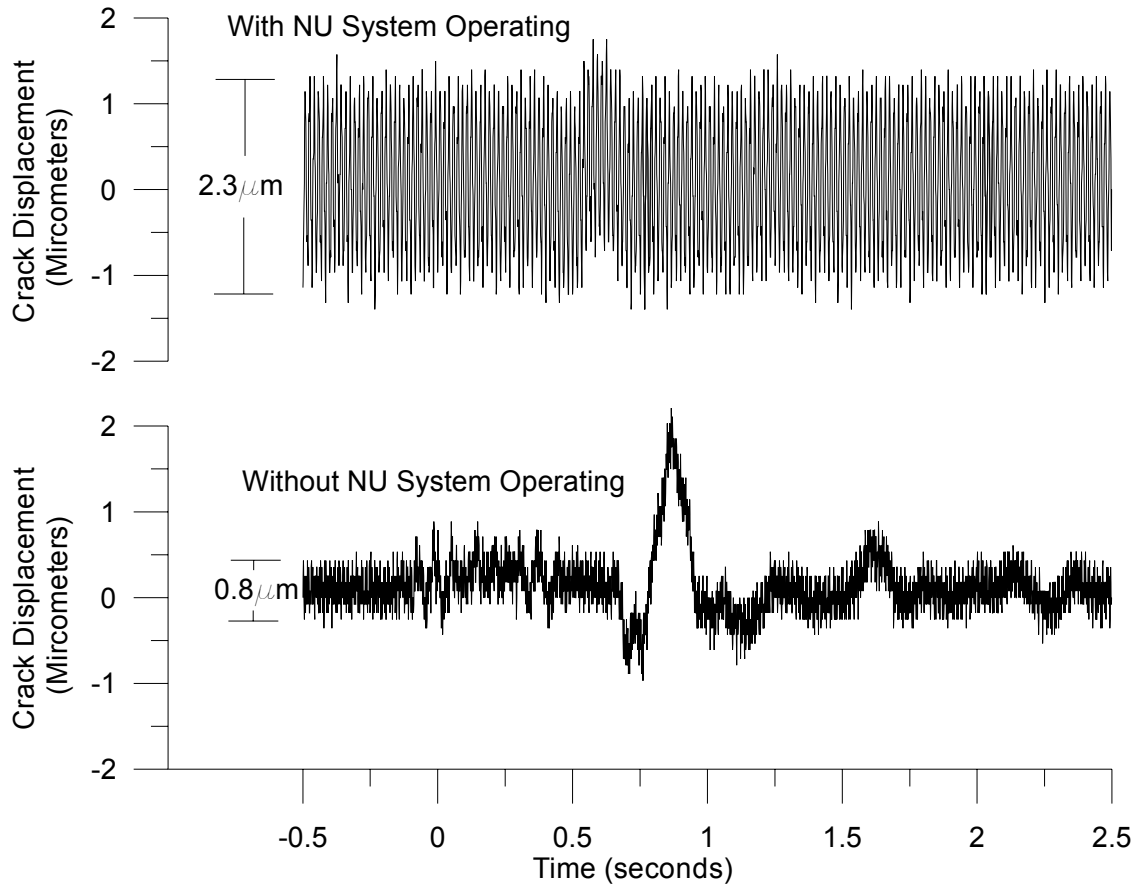


Figure 2.5 Typical system X noise level visible in the crack velocity-time history with and without NU system in operation.

Computer Interface and Software

In this section the computer interface and software supplied with system X are evaluated to determine adequacy and ease of use. After the long-term and dynamic data have been collected by an ACM system, it must be displayed properly to allow comparison. The primary function of the computer interface and software for the equipment is to allow the operator to organize, sort, store, remove and process the data. A well designed ACM system should include quality software, which would aid in automating typical data processing tasks and reduce the amount of time spent working with data by the operator. Poorly designed or

insufficient software would cause the operator of a system to spend a large amount of time and expense processing the data before it could be used as intended.

System X Programming & Connection

System X can be programmed both on-site and remotely. A serial connection is used by system X to send and receive data from the unit. On-site, the unit can be programmed with the external key pad and LCD screen located on the crack monitor by cycling through the system menus and changing setting points such as monitoring modes, trigger levels and text notes. In Figure 2.6 the external key pad on the crack monitor is shown. The system can also be programmed on-site with a computer connected to the serial port. Using a serial port to program the unit may require a USB to serial converter, since most laptop computers do not have a native serial port. Programming is accomplished through the Microsoft program HyperTerminal, which is standard with most windows operating systems. There are two methods for programming the system with a computer. The first method, called TTY, simulates the LCD screen on the crack monitor. The computer keyboard is used to program the unit. The second method for programming the unit from a computer is called “gets and sets.” A get command followed by a parameter code will return the current value stored in that field. A set command followed by a parameter code and value will store the new value in that field. A get command should always follow a set command to confirm that a setting change has been made.



Figure 2.6 External key pad for on-site programming of the system X crack monitor.

Remote communication with system X can be accomplished with a modem or over the internet. To connect to the system over a modem, both the crack and geophone unit require a serial to telephone conversion cable, external modem and an active phone line. Once the system has been connected to a modem any computer with a modem can dial into the system. For security, both the crack and geophone units require a password before setting changes or data removal can take place. During field testing, data was retrieved from the unit over the internet connection. The serial cable from the unit was connected to an Nport (Moxa), to allow access over the internet. The Nport creates a virtual serial port for the unit over the internet. The virtual serial port can be accessed using HyperTerminal on a remote computer. Once connected to the unit by modem or over the internet the TTY or get and set method can be used to program the unit.

HyperTerminal can also start, stop and retrieve data from system X. HyperTerminal allows an operator to collect data from the unit remotely and limit costly site visits.

Additionally, the remote download process can also be automated to further reduce the operating cost, limit human interaction and enable downloads when events are least likely to occur. During field testing, data were downloaded in the middle of the night when blast events and occupant activity were least likely to occur.

Programming system X, with the keypad or TTY mode was found to be the simplest and is the recommended method for programming because it does not require a list of parameter codes, as does the “get and set” method. One advantage of the “get and set” method of programming is that it allows the user to change and review settings quickly. The manufacturer of system X recommends only using TTY mode when on-site. If an interruption in communication occurs during programming in the TTY mode, the unit can become “lost” or lock up, and require a manual restart. For this reason, when simple setting changes are programmed remotely, the user should employ the “get and set” method. During the six months of evaluation of system X, a “lost” or locked up unit was only encountered once during heavy remote operation using the TTY mode.

Layout and display of the command settings in the TTY mode allowed for easy access to the different settings. Figure 2.7 shows the complete layout of the command windows an operator would see during programming in the TTY mode. Most commonly used sections of the TTY windows shown in Figure 2.7 are sections A and B. Section A shows the windows used to set the monitoring mode, record lengths and trigger levels. A detailed description of the menus found in section A is presented in Figure 2.8. The window shown in Section B is where an operator can change the text displayed on each event. Text

notes included information such as equipment ID, client name, operator and location.

Sections of the TTY layout used less frequently include sections C, D, E and F. Section C shows the menu used to set the timer and to turn the unit on and off. Utilities such as displaying the time and date in the unit and to clear the memory are located in section D. Utilities for communication and alarms are shown in section E. Section F includes commands for selecting recording templates and shutting the unit off.

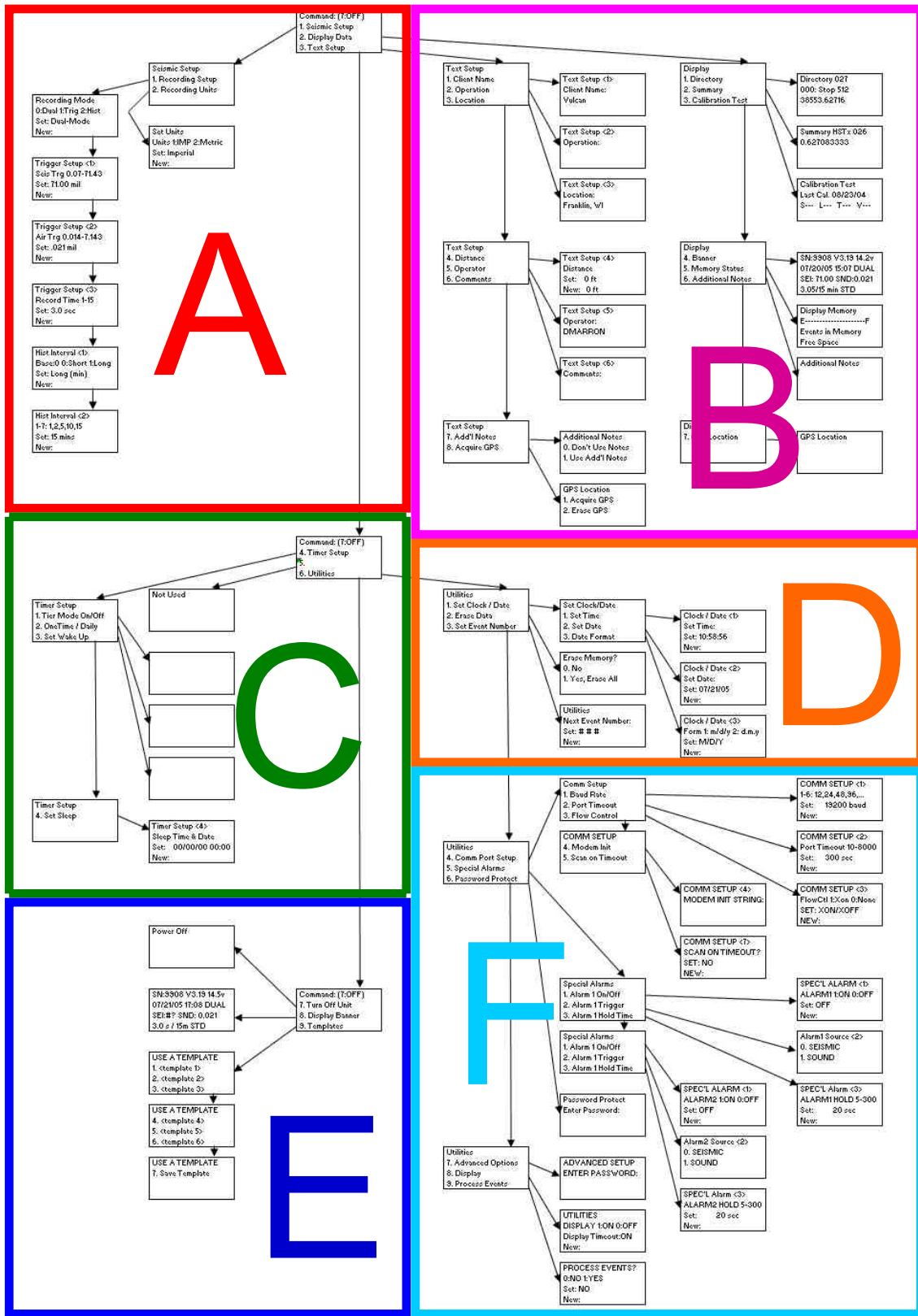


Figure 2.7 System TTY mode layout for programming.

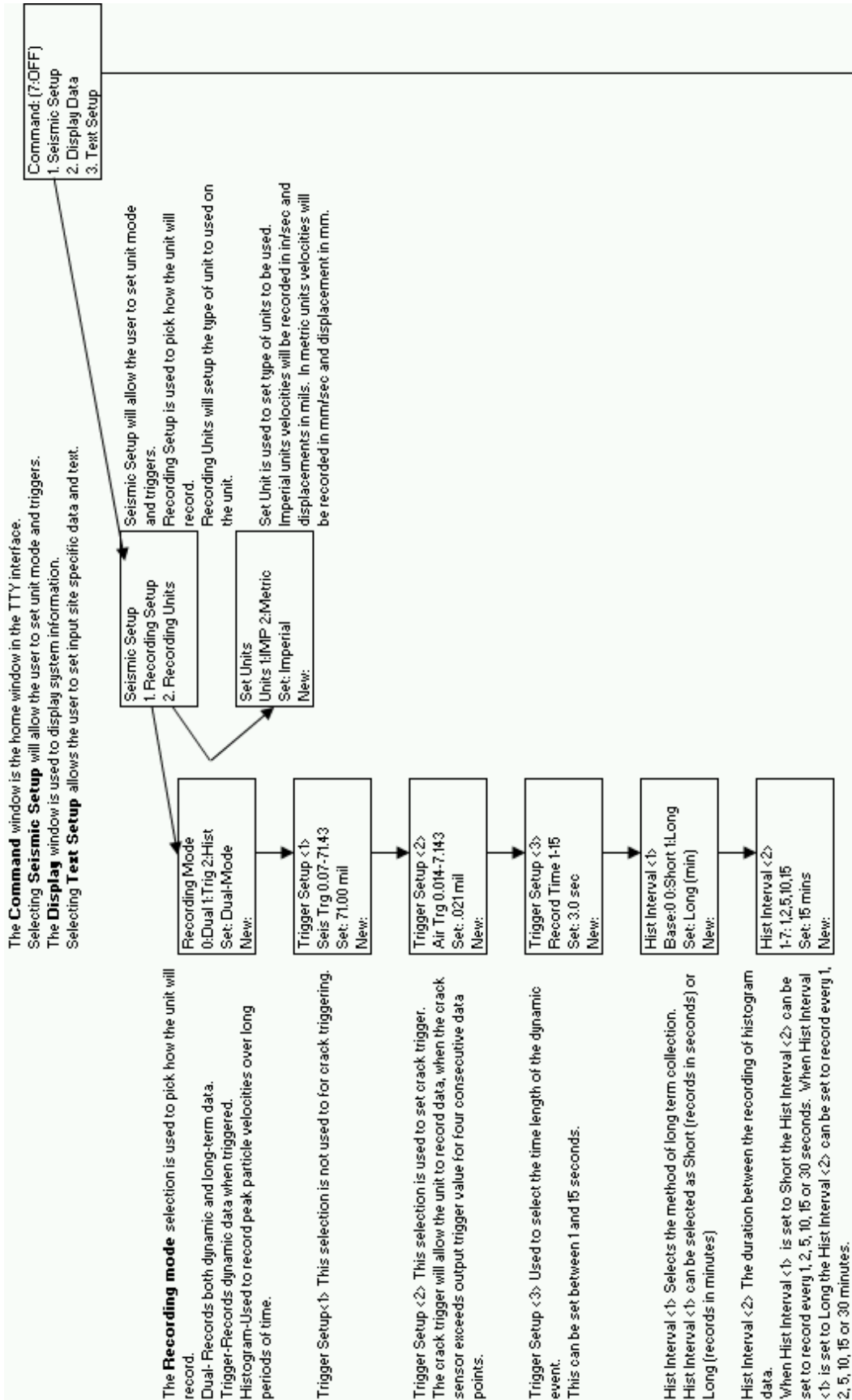


Figure 2.8 Detailed description of the trigger settings for system X.

Data Analysis Software

Once the monitoring has been completed, or during regular intervals data collected by system X can be removed and processed. Two software packages are employed to analyze the data collected during monitoring. The first software package is called “Event Manager” and is used to view the file summaries and export dynamic data files. Figure 2.9 is a typical screenshot from the Event Manager software main menu, that allows review of the file summary which includes date, time and peak recorded values.

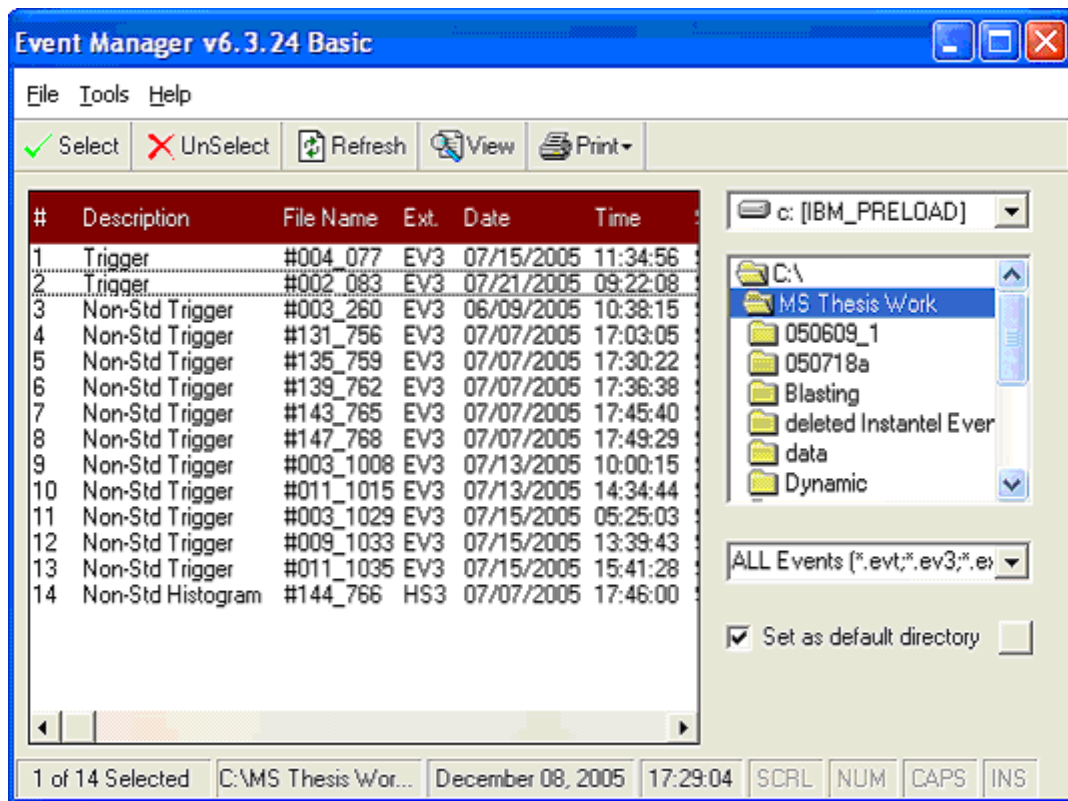


Figure 2.9 System X, Event Manager Software interface

The second software package for analyzing and processing the data is called “Seismic Analysis.” The original intended use of the Seismic Analysis software package was for processing and viewing ground motion time histories. This software package

enables the user to view and print the time histories of both ground motion and crack motion captured by the geophone and crack sensor, respectively. The software was also capable of creating event reports, which described the key points of an event and frequency content analysis. Figure 2.10 shows a typical screenshot from the Seismic Analysis software when creating a crack time history. When reviewing a crack or ground motion time history, any areas of interest can be isolated and enlarged for further review. An ACM specific software application or adaptation of the Seismic Analysis software is currently unavailable.

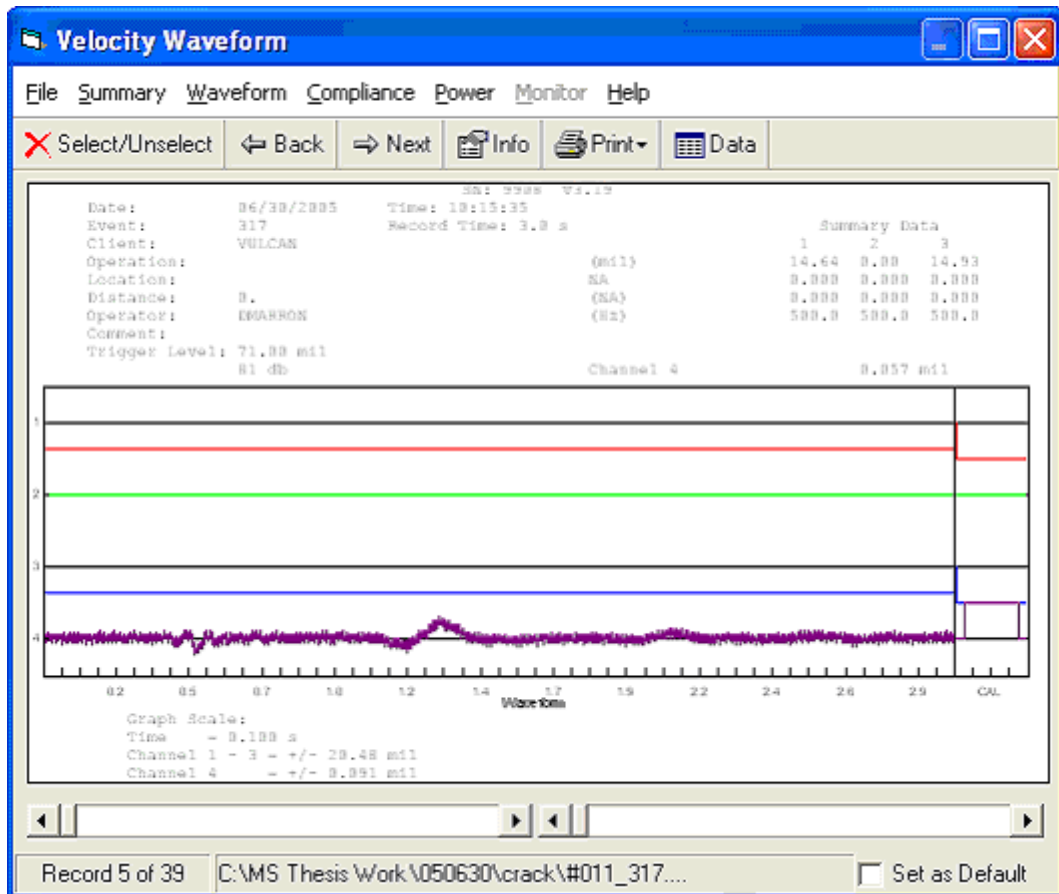


Figure 2.10 Seismic Analysis Software screenshot when creating a crack time history

Literature and Manuals

The literature and manuals supplied with an ACM system should include thorough documentation to allow a new user to install and operate the system independently.

Without the proper manuals, setup and operation of an ACM system would be very difficult. System X was supplied with three core documents. These documents included an operator's manual for the Seismic Analysis software, 3000 series seismographs and a beta version of the crack monitor installation guide. Additionally, system X was supplied with a quick start card, located in the case of the crack monitor, for on-site programming.

Study of the manual entitled "Basic Compliance Software" was necessary to learn more about the Seismic Analysis software package prior to its use. Files removed from both the crack and ground motion monitor could be processed and viewed with this software. The first section of the manual details the requirements to operate Seismic Analysis, the layout and keys used in the software package. The second section of the manual describes how to handle files. Both dynamic or triggered and static or histogram events are reviewed. Methods for plotting the events and creating reports are shown.

The manual entitled "Safeguard Seismic Unit" was used to learn about the operation and programming of the series 3000 seismograph. This manual describes the methods for installing a seismograph and step by step key-pad programming. Key-pad programming was reviewed in the Computer Interface and Programming section. The manual also reviews typical system capacities, operation durations & limitations and capacities.

ACM specific literature supplied with system X, included the quick start card and the manual entitled "Additional Resources for Portable Crack Response Monitor." This

manual reviews installation methods and programming steps for ACM system. The first section of the manual included recommended installation methods for the crack sensors and geophone. This includes detailed instruction for attaching and centering the LVDTs. The second section of the manual described the methods for programming the unit. The quick start card, located in the crack monitor case top, included a brief review of the setup information included in the manual. The card also included instructions for setting the triggers. This included triggering off both the crack and seismograph.

Chapter 3

Laboratory Qualification of Crack Monitoring System X

This chapter presents the qualification evaluation of system X. System X was first operated in the laboratory to ensure proper operation and then in the field to evaluate the system's ability to collect valid data under real field conditions. Laboratory operation was undertaken to verify that the displacement of the crack monitoring system operated within the acceptable standards established with the benchmark sensors. Performance was evaluated for both static and dynamic response.

Long Term or Static Response

Long term response was evaluated to verify the proper operation of the sensors when used in a field environment. Previous work by (Petrina 2004) had been completed to determine that the system X sensors operate correctly in terms of sampling rate, linearity, noise and resolution. Prior to the evaluation of system X as a complete crack monitoring system, the sensors were tested statically. To verifying the linearity of the sensor output, they were first calibrated. Calibration was needed to determine the conversion equations used to change the sensor voltage output into displacement. Calibration results can then be used to verify that the existing equations are correct and within acceptable tolerances.

Qualification of a sensor to measure micrometer crack opening and closing due to long term environmental influences should be completed in a similar manner in which the

sensor is expected to perform in the field. In order to determine if the sensor will respond linearly during cyclic use, the sensors were tested under cyclic loading when attached to a plate of known thermal properties. The sensors were attached to a plastic plate and then exposed to varying temperatures to allow the plate and the sensor to expand and contract. The expansion and contraction of the plate allowed the sensor to record changes in displacement of the sensor core to the housing. During testing the sensors were attached to a plastic plate made of Ultra-High Molecular Weight Polyethylene (UHMW-P). This material was used previously by (Petrina 2004) and provides a large thermal response that approximates a cracked wall's thermal behavior. The coefficient of thermal expansion (CTE), α for UHMW-P is $\alpha=198.0 \mu\text{m}/\text{m}/^\circ\text{C}$. The CTE for the sensors made of steel is $\alpha=13.0 \mu\text{m}/\text{m}/^\circ\text{C}$ and approximately 15 times smaller than UHMW-P plastic. During this study since the CTE of steel is an order of magnitude lower than that of the UHMW-P, the expansion of the sensor was ignored. Since the expansion and contraction of the actual sensor components were ignored, the accuracy attained in this calibration is limited by this effect.

Calibration

Prior to long term testing, each sensor was calibrated to determine its voltage to displacement relationship. The relationship between voltage and displacement for the tested Transtek LVDT is a linear relationship. The system X crack monitor has an internal setup file that can be factory adjusted for the calibration of the sensors. A Kaman metric calibration fixture, with a sensitivity of 0.01 millimeters was used to calibrate the sensors. Figure 3.1 shows the Kaman calibration fixture used to determine displacement and a voltmeter for displaying the corresponding sensor voltage output.

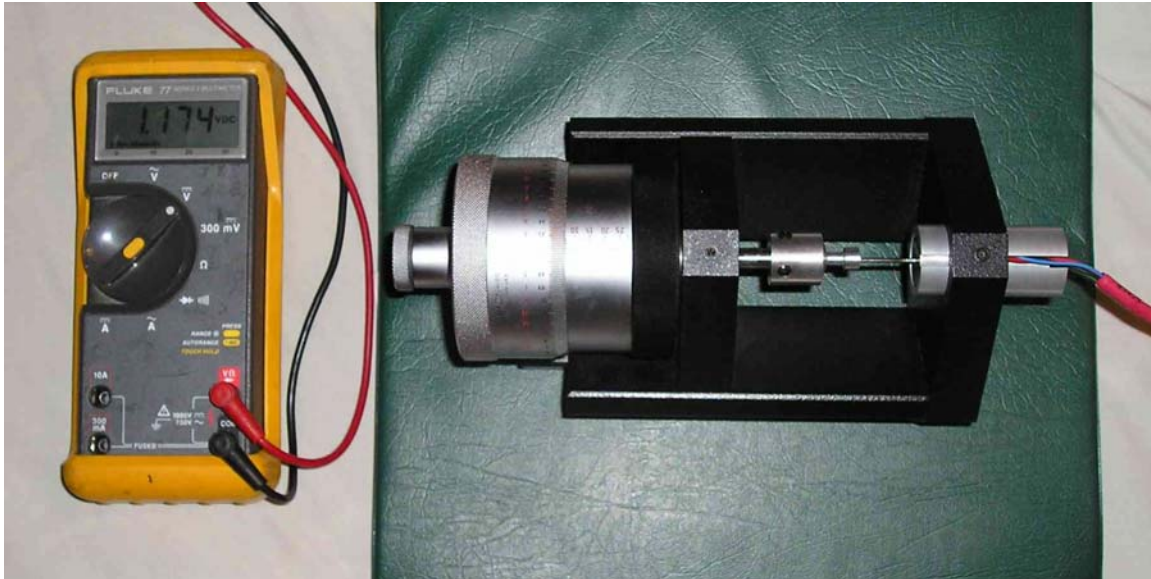


Figure 3.1 Kaman calibration equipment setup used to test the system X LVDT's.

Before calibrating a sensor, the manufacturer specifications should be reviewed to determine the expected working range. In the case of the Transtek LVDT, the voltage output range was found in the sensor coil and core literature to be ± 1.5 volts. Next the LVDTs, were mounted in the calibration fixture and locked it into place. A voltmeter was then attached to the test points of the system X data logger to determine the LVDT voltage output during testing. The displacement of the core is then increased incrementally with the calibration fixture and the corresponding voltage is recorded. During calibration, the displacement was increased at 0.05 mm per each reading. The calibration process was completed three times to insure repeatability.

Once the calibration process was completed three times for each sensor, the data collected were entered into a computer and plotted to determine a best fit line for the data. Figure 3.2 shows the plotted voltage versus displacement data collected during calibration. It can be seen in Figure 3.2 that both LVDTs tested have a linear fit, as would be expected.

Sensor calibration showed that the LVDTs had a displacement range of approximately 3mm, which corresponds to the working voltage range of ± 1.5 volts.

Statistical analysis can be completed on the data collected during sensor calibration to gauge the consistency of the sensors during repeated use. Additionally, an equation or slope can be found to convert the voltage output to displacement. Table 3.1 shows a summary of the data and statistics found during the calibration process. The first LVDT tested, called the null gauge, was found to have an average slope of 0.985 V/mm. The crack gauge or second LVDT tested, showed similar results to the null gauge. The average slope found for the crack gauge was 0.991 V/mm. During the three rounds of testing the standard deviation for the null and crack LVDTs was minimal and found to be 0.0006 and .0052 respectively. Furthermore, the R^2 values recorded for the linear best fit line for each sensor were very close to a unity value. The worst R^2 case found during evaluation was 0.999957.

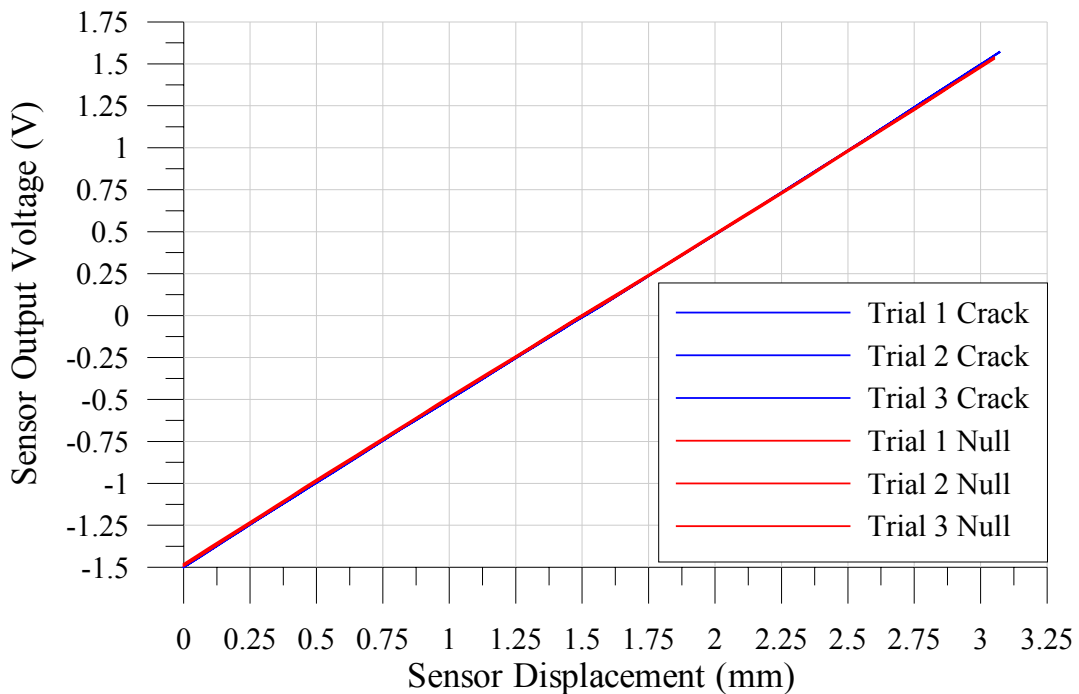


Figure 3.2 Voltage vs. displacement for calibration of the Transtek LVDTs

Trial	Null		Crack	
	Slope	R ²	Slope	R ²
1	0.9853451	0.999972	0.99424109	0.999957
2	0.9842311	0.999975	0.99425171	0.999960
3	0.9852917	0.999976	0.98529173	0.999976
Average	0.9849560		0.99126151	
Standard Deviation	0.0006284		0.00516998	

Table 3.1 Calibration test summary data, equation slope, average slope, R² and standard deviation.

Long Term or Static Testing Equipment Setup

Once the sensors have been calibrated to ensure that system X has a proper conversion factor from output voltage to displacement, the sensor can be subjected to typical environmentally induced wall displacements and temperatures to determine the hysteresis loops and drift (Patrina 2004, Baillot 2004). The LVDTs were mounted on a flat piece of UHMW-P, approximately 400 mm square. During the mounting process, the relatively smooth surface of the UHMW-P was roughened with sandpaper to allow a proper bond between the epoxy and the UHMW-P. Each sensor was mounted at least 30 cm apart from another LVDT to limit sensor to sensor interference. Evaluation of system X was completed outdoors to take advantage of the natural temperature swings similar to those found during field operation. To prevent any possibility of water damage and direct contact with the sun, all equipment was placed in a weather resistant enclosure. Figure 3.3 shows the equipment setup used during the static testing.

System X does not have the ability to measure temperature changes along with crack displacement. Temperature and humidity were monitored with a SUPCO data logger, which

was set to record the temperature once per minute. The humidity readings recorded during testing were ignored because UHMW-P does not respond to changes in humidity as do construction material such as wood or drywall.

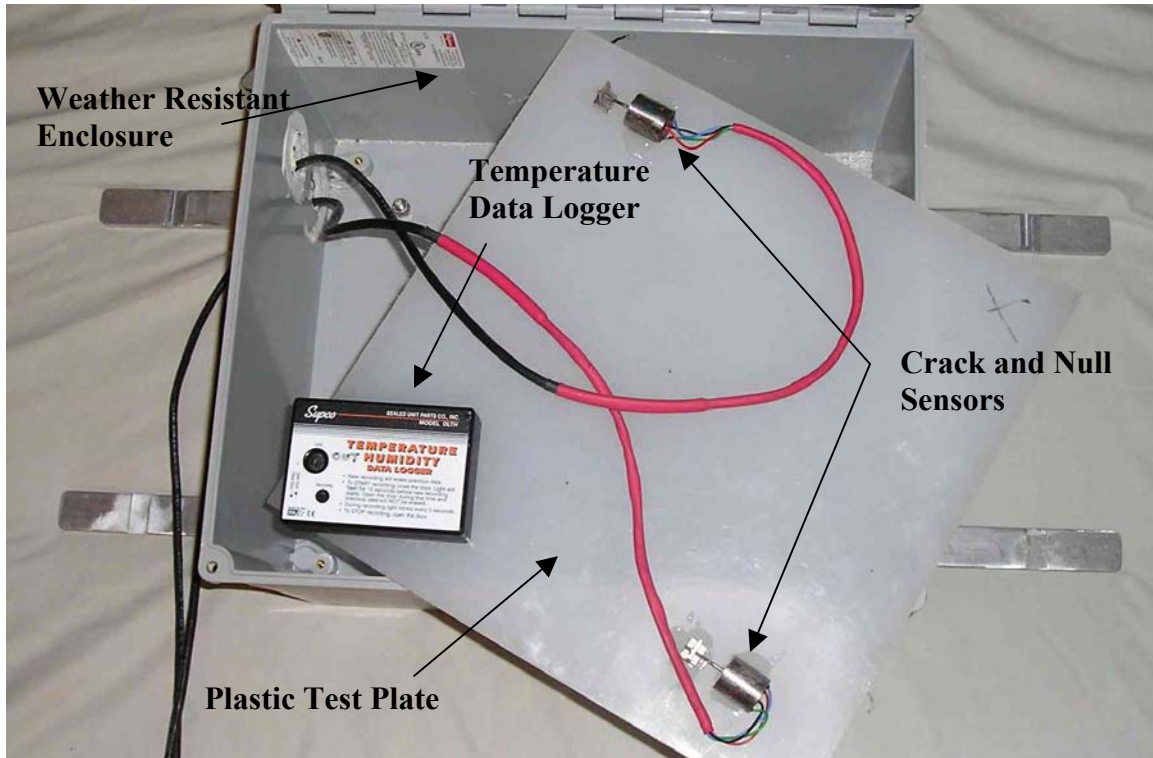


Figure 3.3 Static response qualification equipment layout.

To measure long term response of system X LVDTs, a simple procedure was followed. First, the system was assembled as described previously. The internal clocks in both the system X data logger and the SUPCO temperature data logger were synched to the local computer clock. The sampling rate for system X and the SUPCO temperature data logger were set to record the sensor displacement once per minute. Early testing of both system X and the SUPCO logger were helpful in determining a reasonable sampling rate for operation during testing. Early tests showed that system X and the SUPCO logger were able to return a value with four significant Figures. Because of the limited ability to record data at

a higher precision, collecting data at higher sample rates would not be meaningful and only increase file sizes and reduce the length of time at which the equipment could record. Once both data loggers were programmed, they were then activated to start the data collection process. The weather resistant enclosure was then sealed and the entire unit was allowed to operate outdoors for approximately three to four days. During this period of evaluation, the UHMW-P plate with the attached sensors endured daily temperature swings from 17°C to 33°C.

Long Term or Static Response Results

At the completion of the testing period, the recorded data were removed from the individual data loggers to be processed and merged into one time history. Prior to merging the data collected, individual time histories can be plotted for each displacement sensor and temperature with respect to time; this can be seen in Figure 3.4. From the time histories shown in Figure 3.4 it can be seen that peak temperatures recorded correspond to peak in sensor displacement. It is expected that during peak temperatures, the UHMW-P plate would expand and cause larger LVDT displacements. During the static testing, as expected, the highest temperatures occurred during the early afternoon and the lowest during the early morning.

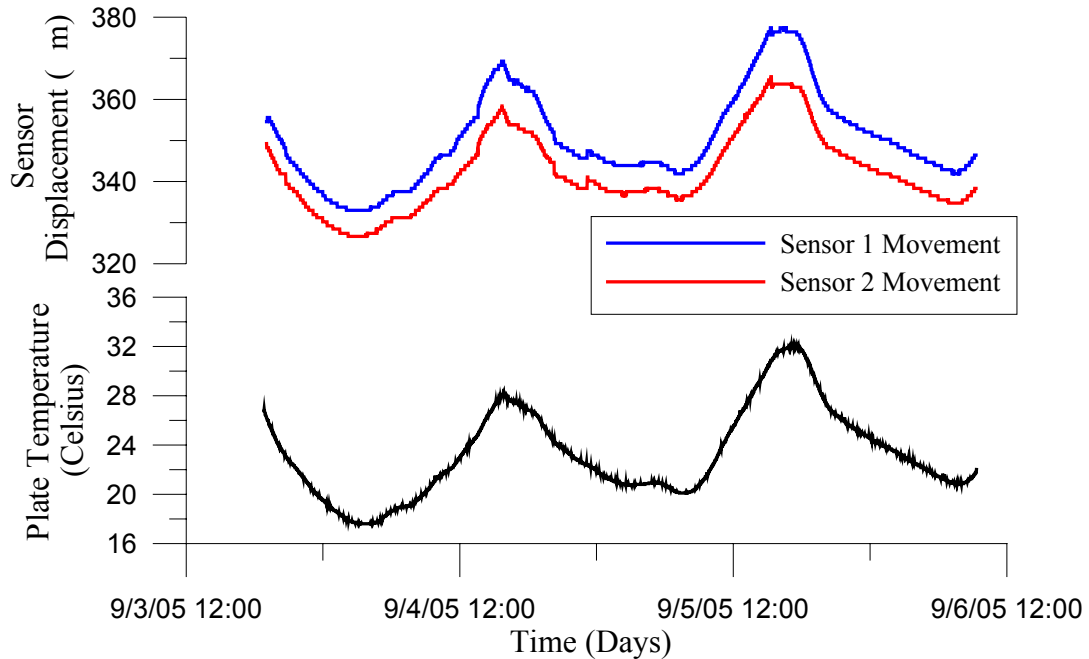


Figure 3.4 Independent temperature and displacement recorded during static testing.

To determine graphically the effect of temperature on the cyclic expansion and contraction of the system X sensors, the collected data needed to be merged as shown in Figure 3.5. Figure 3.5 illustrates the relationship between temperature and displacement. Additionally, the theoretical expansion of the plate can be plotted along with experimental results to validate the process. The calculated displacement can be found based on the materials CTE and the initial gap measurement between LVDT housing and core bracket. The measured sensor displacement that was collected during the static evaluation of system X, was found to be in good agreement with both the theoretical calculations and temperature data collected during testing. Additionally, the hysteresis loops created by the sensors during testing were small and within the limits of previously tested sensors (Petrina 2004 & Balliot 2004).

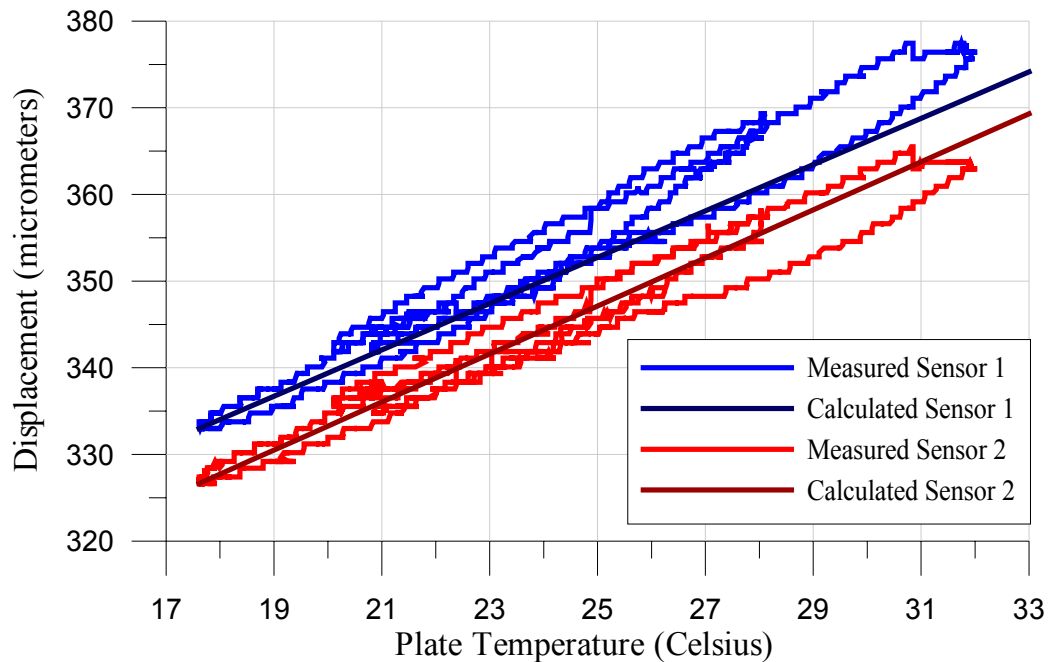


Figure 3.5 Measured and calculated displacement vs. temperature for sensor 1 and 2.

Short Term or Dynamic Response

This section describes the dynamic qualification of system X to verify the system’s ability to capture dynamic activity in the lab prior to its placement in a field environment. Previous work in dynamic testing by (Ozer 2005) had been completed on other types of sensors. Testing methods by (Ozer 2005) were used as a foundation for further development of an apparatus for validating ACM sensors dynamically. Validation of system X was assessed in two categories; frequency and amplitude.

During a dynamic event, the displacement sensor must record a transient waveform. Because this event will only occur in limited numbers or only once during the monitoring period it is important for an ACM system to sample the waveform at an adequate sampling rate. The structural response frequency of most buildings measured in the field is normally

in the range of 10 to 15 Hz. (Dowding 1996). This frequency range required the ACM system to sample at 1000 Hz to define the dynamic response of the crack. During dynamic testing, the testing apparatus was vibrated at frequencies up to 100 Hz, this allowed at least ten data points per excitation cycle. In addition to the ability to capture events with high frequencies, ACM systems must be able to capture events with small amplitudes. Field testing has shown that interior cracks in residential structures can respond with displacements between 2 to 5 μm zero to peak during a dynamic event. During the dynamic testing of system X, the sensors were driven at amplitudes ranging from approximately 2 to 15 μm zero to peak.

Dynamic Testing Equipment Setup

Ozer, (2005) verified the potentiometer as an ACM displacement sensor by measuring the response of two aluminum blocks stacked upon each other to a drop weight. The blocks were separated by a thin rubber sheet which modeled an interior crack. The control Kaman sensor was then mounted on one side of the blocks and the sensor to be tested on the other. A small weight could then be dropped at varying heights on the upper block. Varying the height of the drop varied the amplitude of the crack movement. The resulting movement of the upper aluminum block with respect to the lower block was then record by both systems and compared.

As shown in Figure 3.6, the system was modified in order to accommodate larger sensors and increase the controllability of excitation frequency and amplitude. The initial testing device was adapted to include larger aluminum blocks and a small electric motor with an eccentric weight. The addition of the electric motor allowed for the frequency of the upper block to vary with the angular velocity of the motor. The amplitude was varied with

an eccentric weight attached to the electric motor. During dynamic testing, small amounts of putty were attached to a cardboard wheel which served as an eccentric weight. Excitation was completed in seven intervals, reducing the eccentric weight from approximately 0.60 to 0.20 grams.

Dynamic response of system X was compared to that of the Kaman eddy current displacement sensor and the Edaq mobile field computer and data logger as described in Ozer (2005). The Kaman eddy current sensor has been used for experimental crack monitoring projects for years and are accepted to be the most reliable and sensitive sensors available.

Considerations taken during dynamic testing included limiting electromagnetic noise, preventing movement of the lower block and ensuring the proper adjustment of the sensors/upper block combination before each test. Any excess equipment in the laboratory that may induce electromagnetic noise during testing was turned off or moved away from the devices. To limit the movement of the lower block during dynamic excitation, it was attached to the edge of the more massive lab table. During test runs 3 through 7, the electric motor was run prior to the test to ensure the aluminum blocks were adequately seated upon each other and any slack in the system was removed. During test runs 1 and 2 this pre-running of the electric motor prior to testing was not completed which resulted in a baseline offset in the recorded waveforms.

Dynamic testing of system X was accomplished by following a simplified procedure. First, the aluminum blocks were assembled with a small foam spacer between them. Guide plates were then installed on the lower block to limit horizontal translation of the upper block. A front and right view of the modified testing apparatus can be seen in Figure 3.6.

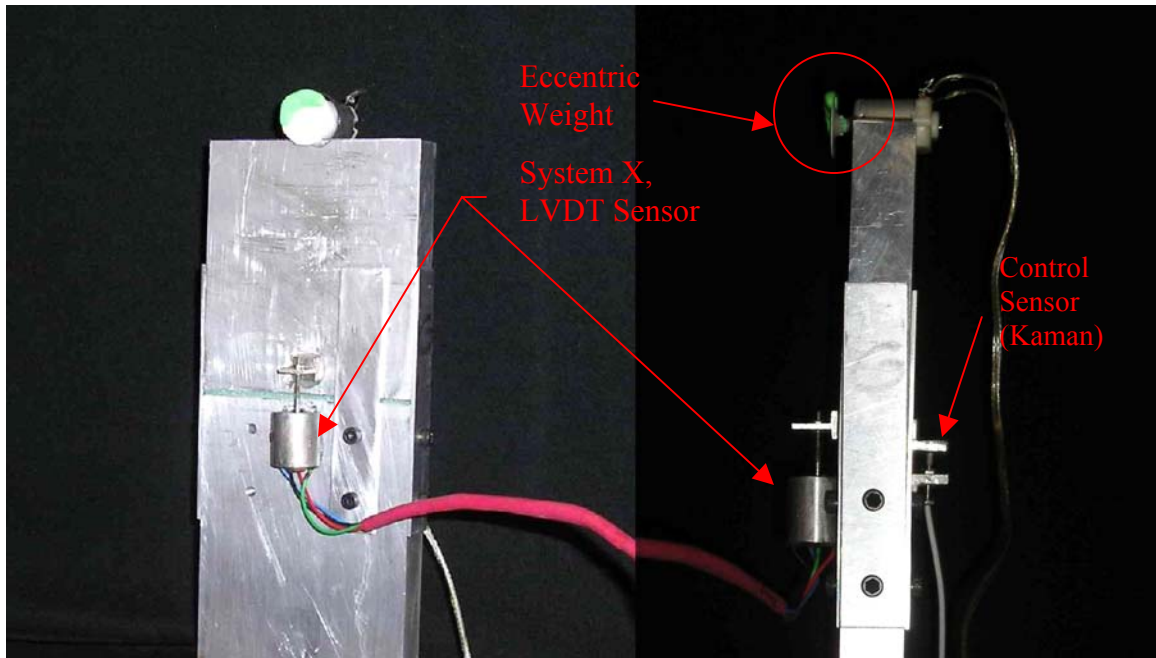


Figure 3.6 Modified dynamic testing apparatus.

The sensor to be tested and the control Kaman sensor were each attached to opposite sides of the block assembly. Both systems were set to record dynamic data for a three second time period. The electric motor was activated by a 1.5 volt source to vibrate the upper block. The corresponding dynamic crack movement was then recorded by each system. The first attempt at dynamic testing was done with the largest eccentric weight. Sequential tests were run after the removal of small amounts of the eccentric weight until a crack amplitude of 2 μm was reached.

During testing, differences in the dynamic response of the control sensor and test sensor were found. Differences in the sensor responses such as non-uniform displacements and phase shifts could be attributed to limitations in the testing equipment, including equipment alignment, connection and size effects. Uniform displacement of the upper block with respect to the lower block was anticipated. However, lack of horizontal support or difficulty in the alignment of the eccentric motor to the center of gravity of the upper block

was encountered. This eccentricity caused a small rocking motion of the upper block and non-uniform displacements at the face of the upper block. Any slight deviations in the alignment affected the magnitudes of the displacements measured by the sensors. This misalignment of the eccentric motor was found to cause a phase shift in the waveform. When the eccentric weight oscillates, it functions as a vibrator and creates a net upward and downward force. This changing force causes the upper block to move relative to the lower block and simulates crack movement. However, the eccentric movement of the eccentric weight produced a rocking motion which produced a 180° phase shift between the two transducers, as shown in Figure 3.7.

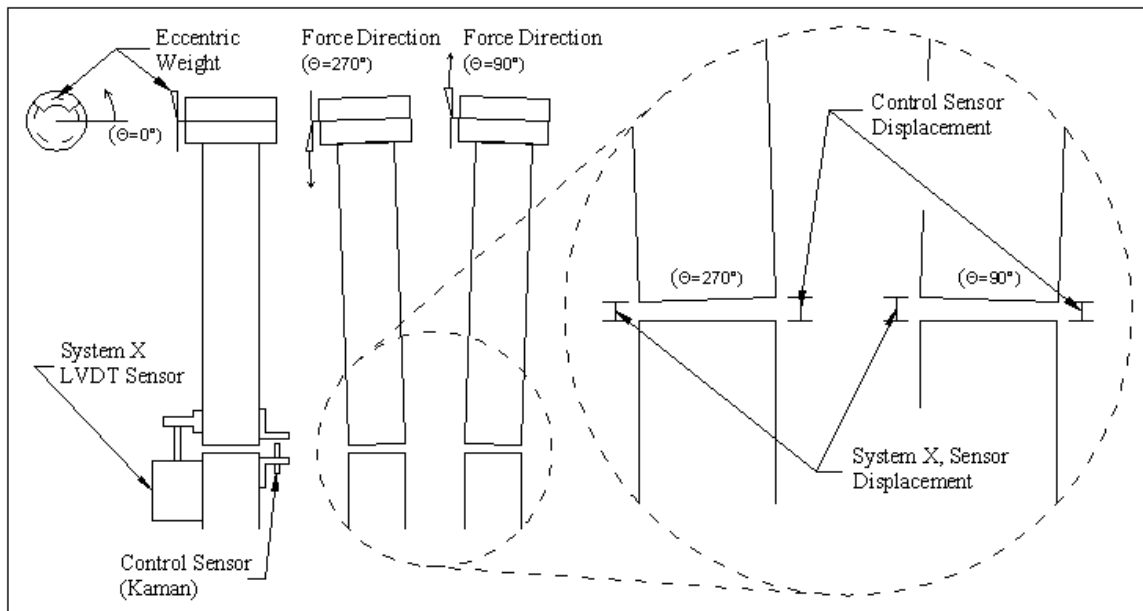


Figure 3.7 Description of how a phase shift was created in the waveforms, during dynamic testing.

In addition to equipment alignment, sensor size and type of connection could affect the amplitude of the recorded waveform. The Kaman control sensor is advantageous for crack monitoring because it does not require a cross crack connection between the sensor tip

and target. However, because Kaman sensors have limited durability, it is recommended for only research use. The inertia of the wall is orders of magnitude greater than that of the sensors, so that the sensor differences are irrelevant across a crack. The connection of the LVDT core to the core housing can dampen the response of the system when out-of-plane movement occurs. During dynamic testing, because of the slight rocking motion that occurs from the eccentric weight, the LVDT core can bind in the core house, creating frictional losses. Any binding that would occur during testing should reduce the amplitude of the waveform recorded by system X.

Dynamic Qualification Results – Amplitude Comparison

Dynamic responses of the LVDT from system X, were compared to that of the control system in terms of both frequency and amplitude. Figure 3.8 shows a typical waveform captured by both the control system and system X. This Figure shows both the DC coupled channel 3 used for waveforms with baseline shifts and the AC coupled channel 4 used for waveforms without baseline shifts. Table 3.2 summarizes a comparison of the maximum amplitudes collected during the dynamic tests completed on system X. During dynamic tests, when a baseline shift did not occur, the amplitude of the AC coupled channel was used to compare to the control waveform.

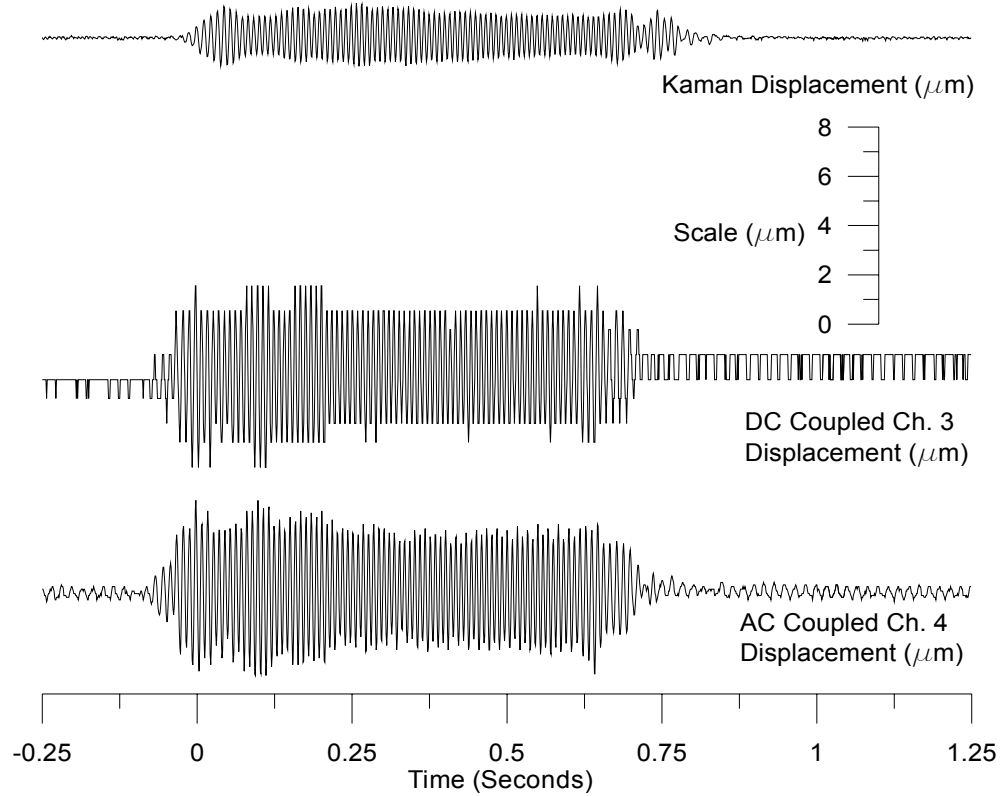


Figure 3.8 Typical waveform recording during the dynamic testing of system X.

Event #	Eccentric Weight (g)	System X Trigger Level (μm)	Kaman Max Amp. (μm)	CH.3 Max Amp. (μm)	CH.4 Max Amp. (μm)	Amp. Ratio Ch3/Kaman (Floating Center)	Amp. Ratio Ch4/Kaman (Zero Centered)	Notes
1	0.60	3.175	4.2	14	11.5	3.3	2.7	Offset
2	0.46	3.175	2.5	8.7	8	3.5	3.2	Offset
3	0.46	3.175	2.7	9	8.4	3.3	3.1	
4	0.39	1.905	2	5.5	4.8	2.8	2.4	
5	0.30	1.905	1.4	4	3.7	2.9	2.6	
6	0.21	0.635	0.6	2	1.3	3.3	2.2	Late Trigger
7	0.29	0.635	1.1	2.8	2.5	2.5	2.3	
Standard Deviation All Data						0.4	0.4	
Average Ratio During an Offset Event							3.0	
Average Ratio During Non-Offset Event						2.9		

Table 3.2 Summary of the dynamic tests completed for system X.

An average ratio of the maximum amplitude of the system X to the control was 2.9 with a standard deviation of 0.4. During dynamic excitation when a baseline shift did occur, the amplitude of the DC coupled channel was compared to the control waveform. Testing determined that the average ratio of the maximum amplitude of system X to the control was 3.0, with a standard deviation of 0.4. Testing showed that on average, the system X LVDT recorded three times more crack displacement than the control sensor. The ratio of the maximum crack displacement was found to be relatively constant throughout a wide range of amplitudes tested. The large difference in crack movement collected by system X was compared to the control and attributed to the testing apparatus and not the sensor. The larger crack responses are most likely due to the location of the eccentric weight, in comparison to the center of gravity of the blocks. Field testing in Chapter 4 shows that across the same crack the two systems responded similarly. This observation has also been made by (Mckenna, 2002)

Dynamic Qualification Results – Frequency Comparison

Measured response frequency of system X was compared to the Kaman standard. During testing, the apparatus was operated at a frequency of approximately 100 Hz, this is well above the 10 – 50 Hz range that the equipment will be exposed to in the field. Equipment that can capture waveforms accurately at a high frequency can readily capture waveforms at lower frequencies. Thus lower frequency excitation was not necessary to capture the same frequency as the Kaman standard as shown in Figure 3.9. During the start-up of the eccentric weight, the frequencies that were encountered by the sensors were lower

than during constant operation. During both start-up and at a constant angular velocity, the frequency of system X was comparable to the control system.

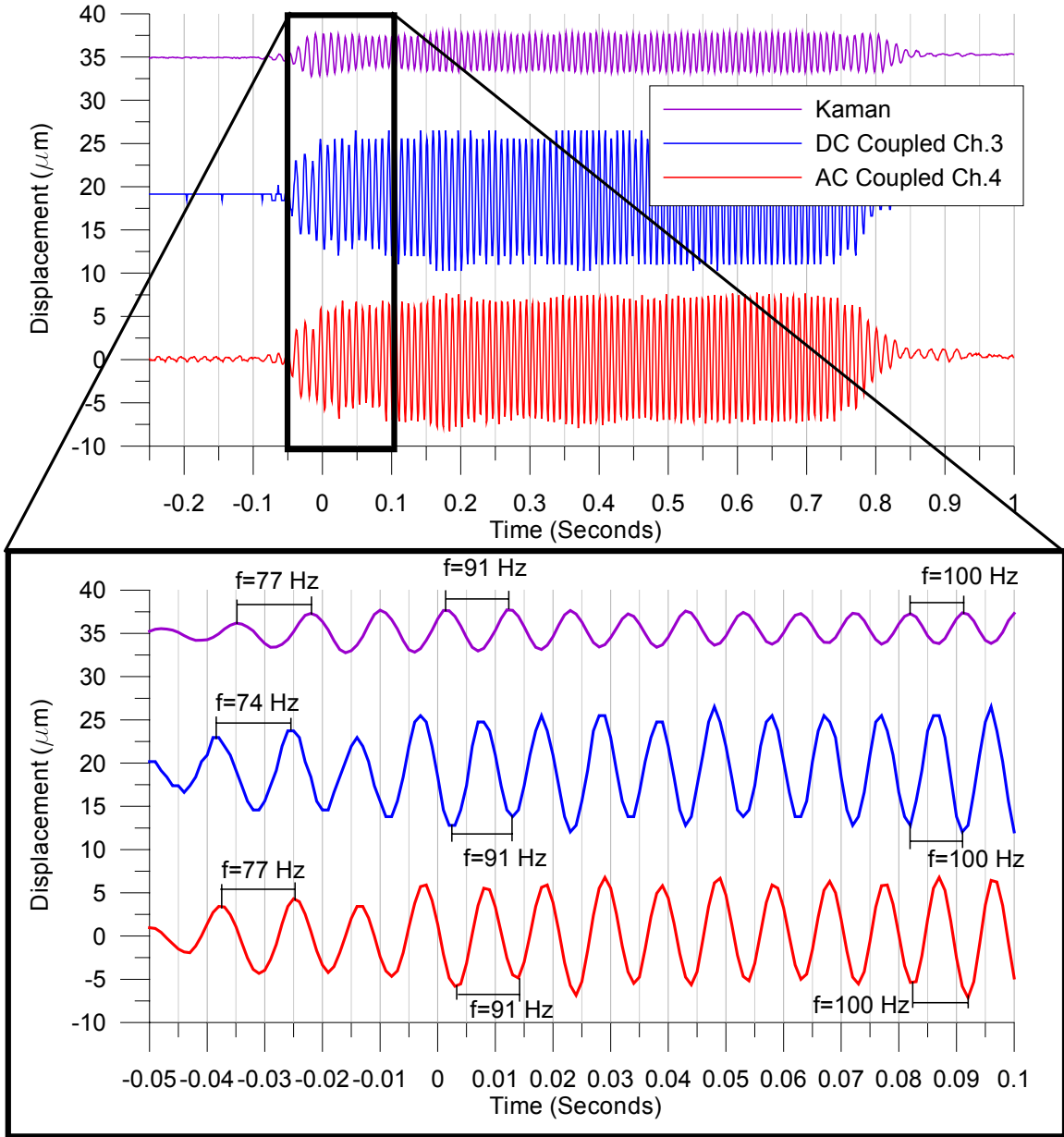


Figure 3.9 Frequency comparison of system X to the control system.

Dynamic Qualification Results – Offsets

Baseline shifts or temporary offsets of a crack during a dynamic event occur from time to time. Use of the AC coupled response of system X eliminates this temporary response as shown in Figure 3.10. The waveform of the DC coupled channel on system X was able to capture the same crack offsets reported by the Kaman sensor. Data presented in Chapter 4, shows that the LVDT has tendency for temporary baseline shifts, whereas the Kaman has less of a tendency. As described in Patrino, (2004) and McKanna, (2002), the LVDT shifts may be due to misalignment between the core and coil.

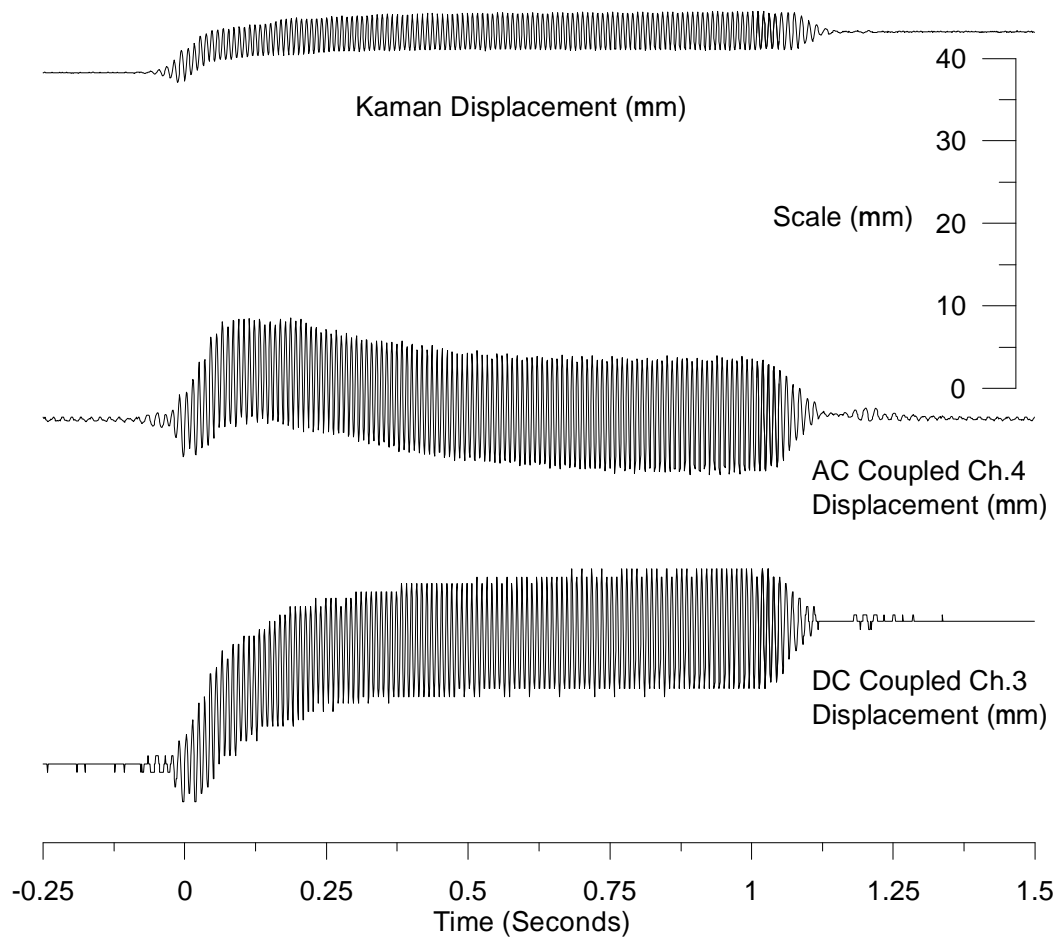


Figure 3.10 Typical waveform time history of the control system and system X during a baseline shift.

Chapter 4

Field Testing of Crack Monitoring System X

This chapter describes the field testing of Autonomous Crack Monitoring (ACM) system X. Field performance of the system was evaluated in three modes of monitoring operation or levels of trigger operation; 1) every hour to measure long term crack movement; 2) upon exceeding a preset intensity of ground motion; and 3) upon exceeding a preset change in crack width. System X's field installation was across a crack in a house located near an active limestone quarry. All procedures were reviewed to ensure that the system was easy to use by the average field technician.

Field Trial Blast Vibrations

System X was evaluated in a real blasting environment. The system was installed in a house near an active limestone quarry where blasting occurred approximately once per week during the blasting season. During testing, system X was operated as a level I, II and III system. A level I system records only long term crack response, which can be compared to long term changes in temperature and humidity. A level II system records both long term and dynamic crack response during blasting. A level II system directly measures the magnitude of the crack movement during blasting. A level III system records long term data, as well as dynamic response during blasting and dynamic data produce by other forms of

excitation. A level III system records all forms of crack excitations including blasting, occupant and weather (wind) induced.

Level I Operation

System X was first evaluated for level I operation by Petrina (2004). According to Petrina, the system was found to be adequate for long-term data collection. Level I systems record peak micrometer changes in crack width at selected time intervals. System X has 13 different time intervals to choose from when programming. Different time intervals allow data to be collected from every second to every hour, depending upon the need. Long term patterns of crack response to environmental effects can be compared to determine if dynamic excitation has caused permanent changes. Level I system operation does not include measurement of dynamic crack response. During level I operation and testing the system was verified and compared to the results collected by Petrina, (2004).

Level I Equipment Setup

In order to continue the evaluation of system X as a level I system, the unit was installed in the Milwaukee test house to monitor long-term crack movement. The Northwestern University (NU) system was used to monitor the same crack concurrently with system X to directly compare response. System X was setup to record level I as described in Chapter 3. The histogram function on the unit was set to record the peak crack displacement every 15 minutes.

Level I Data Collection

Level I data were collected from January to July of 2005, which allowed the units functionality to be evaluated during the extreme changes in temperature and humidity observable during both heating and cooling seasons. During the winter months low temperature and humidity were observed. During the spring and summer months the system was operated at higher temperatures with varying levels of humidity. Varying levels humidity could be expected when windows are opened in the spring.

During monitoring the inside temperature and humidity were maintained within a cyclically small range, which is normal for homes with a furnace and air conditioner. Both the indoor and outdoor temperature and humidity were recorded for comparison. Figure 4.1 shows the indoor and outdoor temperature and humidity readings collected during the monitoring period between January 1, 2005 and March 12, 2005. The grey lines in Figure 4.1 depict the raw data that was collected every 15 minutes. The black line shown in Figure 4.1 is a 24 hour average of the data. The data collected every 15 minutes illustrates the large daily variations in temperature and humidity that were encountered.

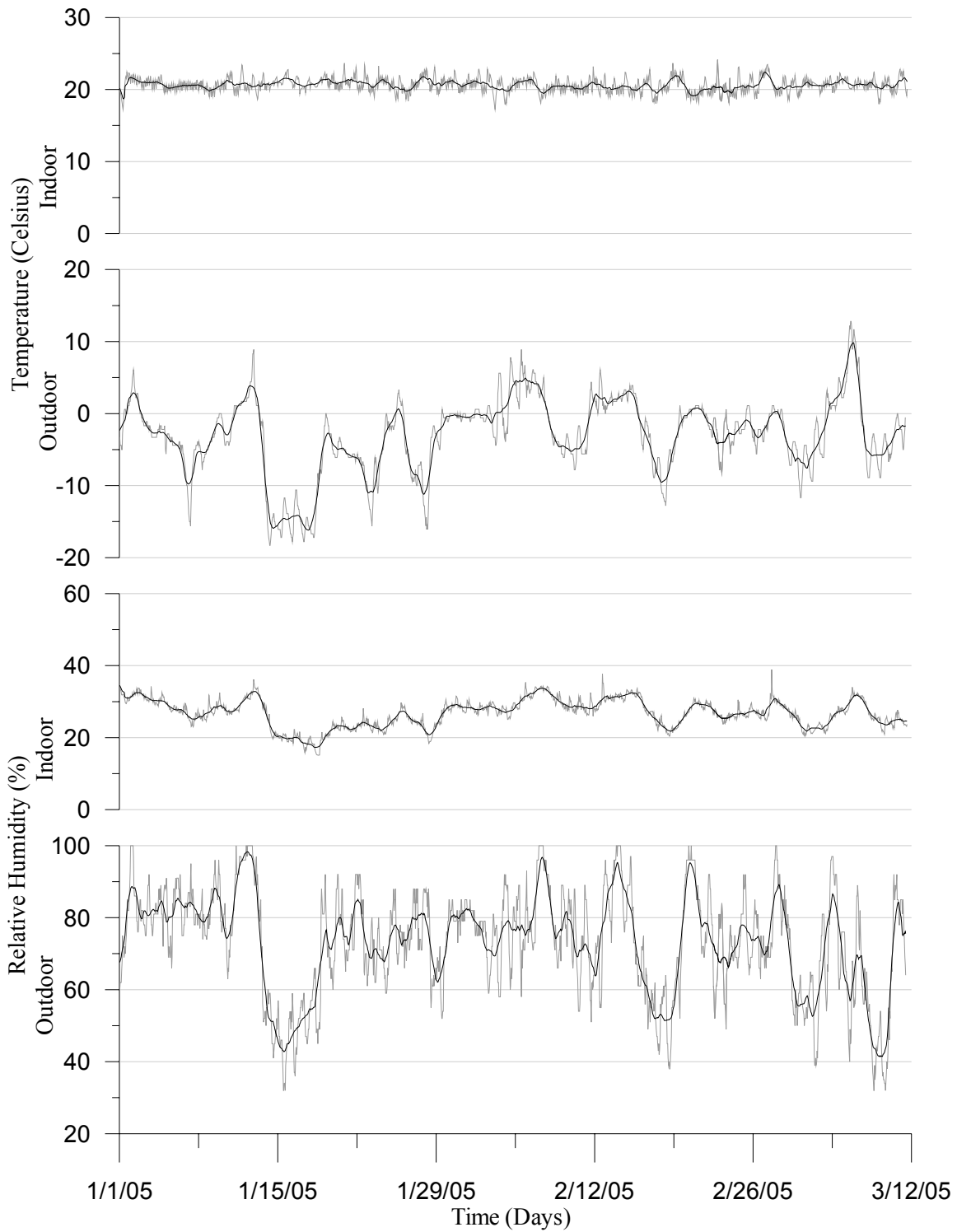


Figure 4.1 Environmental data from a three-month monitoring period. Gray jagged lines are a one-hour rolling average while the black lines are 24-hour rolling average.

The 24-hour average removes the extreme hourly fluctuations and produces a long-term representation of the weather trends. The patterns in humidity and temperature are similar for both outdoor and indoor results. From the temperature plots it can be shown that the indoor and outdoor temperatures are much more comparable than those for humidity. On average the home was maintained at a temperature of 20°C and a relative humidity of 30%.

To compare with data collected from system X, data were also obtained from the NU LVDT. Figure 4.2 compares the crack displacements recorded by the NU LVDT and system X LVDT to the indoor temperature during monitoring. Any thermal expansion effects experienced by the ceiling crack would be expected to be heavily influenced by the change in indoor temperature. In Figure 4.2 peak displacements in the NU LVDT and system X LVDT occur at approximately the same times. Maximum peaks in displacement also occur at the same time at minimum indoor temperatures. When comparing the 15 minute data it can be shown that the magnitude of the system X peaks and valleys were only slightly smaller than those of the NU LVDT. The shape of the 15 minute graph shown in grey for system X LVDT does not appear as sharp, in comparison to the NU LVDT. The peaks in the 24 hour averaged data tend to be similar in magnitude for both LVDTs. The following example comparison of 24 hour averaged crack response can be made. On 2/19/05 a minimum value of 35µm and 20µm were recorded on the NU and System X LVDTs, respectively. On 2/20/05 a maximum value 58µm and 43µm were recorded on the NU and System X LVDTs, respectively. Net change in crack width on both systems was similarly found as approximately 23µm. Similar trends and magnitudes in data of system X compared to the NU LVDT indicate comparable responses.

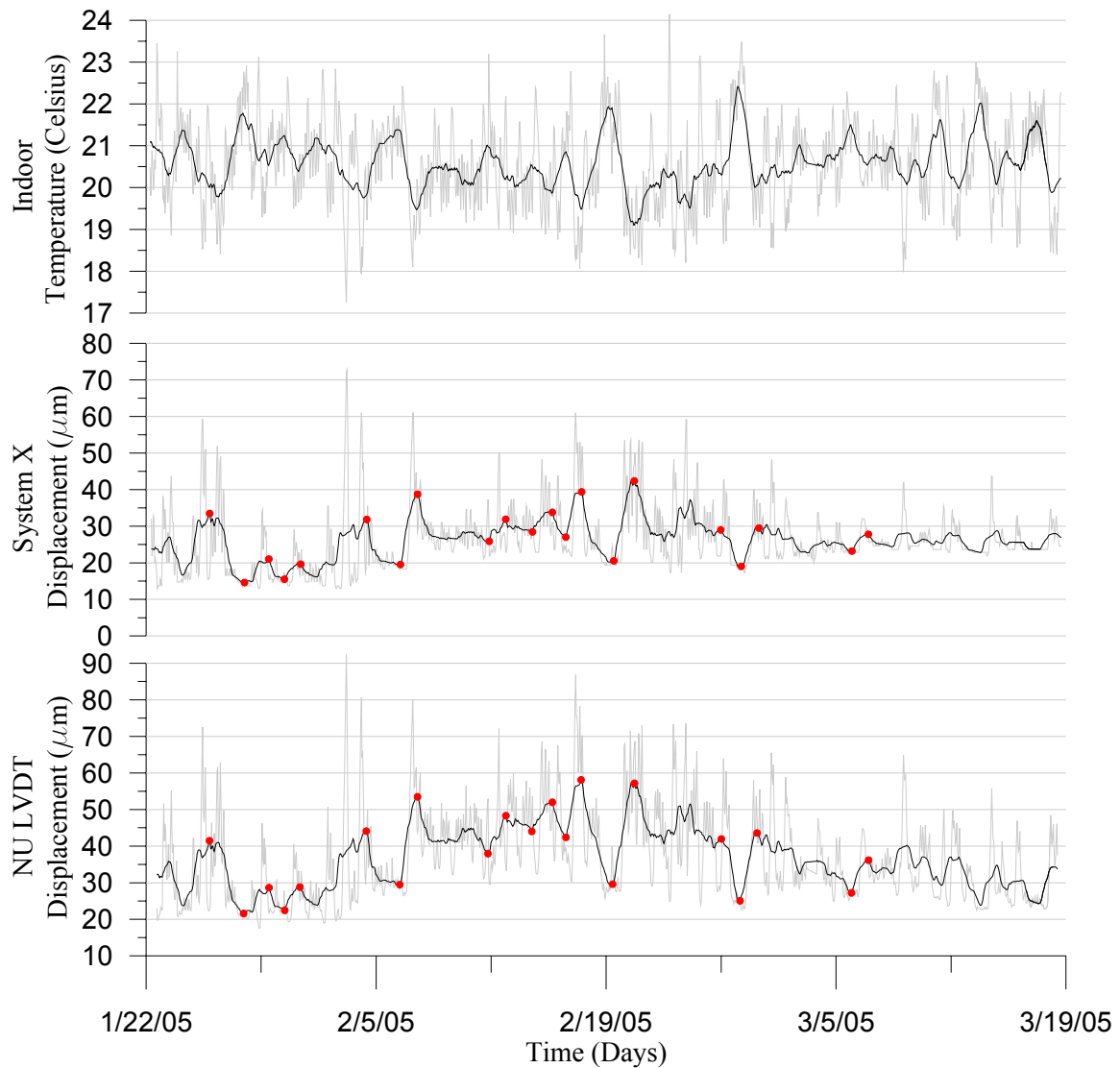
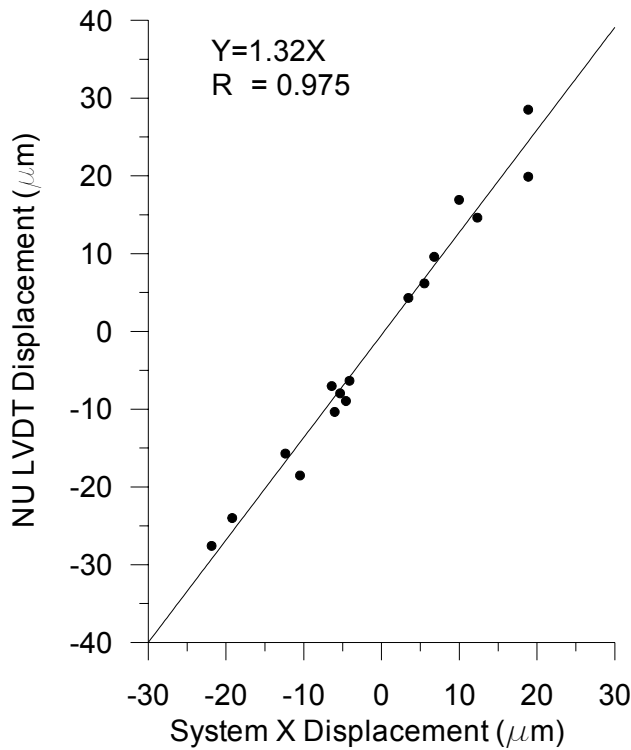


Figure 4.2 Comparison of the displacement time histories for the NU LVDT, System X LVDT crack gauge and indoor temperature. Gray jagged lines are a 1 hour rolling average; and the black lines are a 24-hour rolling average. (red dots indicate points used to calculate the long term static ratio.)

During operation, an ACM system must be able to maintain a constant ratio or long term to dynamic movement. A constant ratio is needed to directly compare dynamic crack excitation to long term crack movement to determine the significance of dynamic events. During level I or long term data collection, the ratio of the NU LVDT to the system X sensor

was found. The peak data points collected, denoted with (red dots), in Figure 4.2 are presented in Table 4.1 and graphically in Figure 4.3. The NU LVDT has been used previously in ACM applications and has been tested for compliance therefore used as baseline for comparison. The NU LVDT to system X ratio was found to be 1.32 during long term operation.



NU LVDT ΔDisplacement (µm)	System X ΔDisplacement (µm)	Ratio NU/X
19.89	18.87	1.05
-7.03	-6.41	1.10
6.17	5.51	1.12
-6.35	-4.13	1.54
14.62	12.32	1.19
-24.00	-19.21	1.25
-10.36	-6.03	1.72
4.30	3.45	1.25
-7.97	-5.33	1.50
9.59	6.77	1.42
-15.71	-12.38	1.27
28.51	18.86	1.51
-27.58	-21.86	1.26
16.91	9.97	1.70
-18.53	-10.49	1.77
-8.95	-4.58	1.95
Average		1.41
Slope linear best line		1.32

Figure 4.3 Long term system X versus NU LVDT data used to determine the system X long term or static ratio

Table 4.1 System X and NU LVDT calculated changes in displacement from the data collected in Figure 4.2.

To determine if the thermal expansion of the ceiling material or the crack was causing the recorded results on system X, the null gauge must be compared to the crack gauge.

Figure 4.4 is a comparison of the displacements recorded by the crack and null gauge in the same environment. The System X null gauge was mounted on an uncracked section of

ceiling. As expected the null gauge showed little to no response during testing. Any small spikes in data could be attributed to electronic noise. The displacement of the intact portion of the ceiling was found to be a fraction of the displacements of the crack and insignificant. Since the readings of the null gauge were so low, it was confirmed that the crack sensor was measuring the displacement of the crack, not the displacement of the ceiling material or temperature response of the sensor.

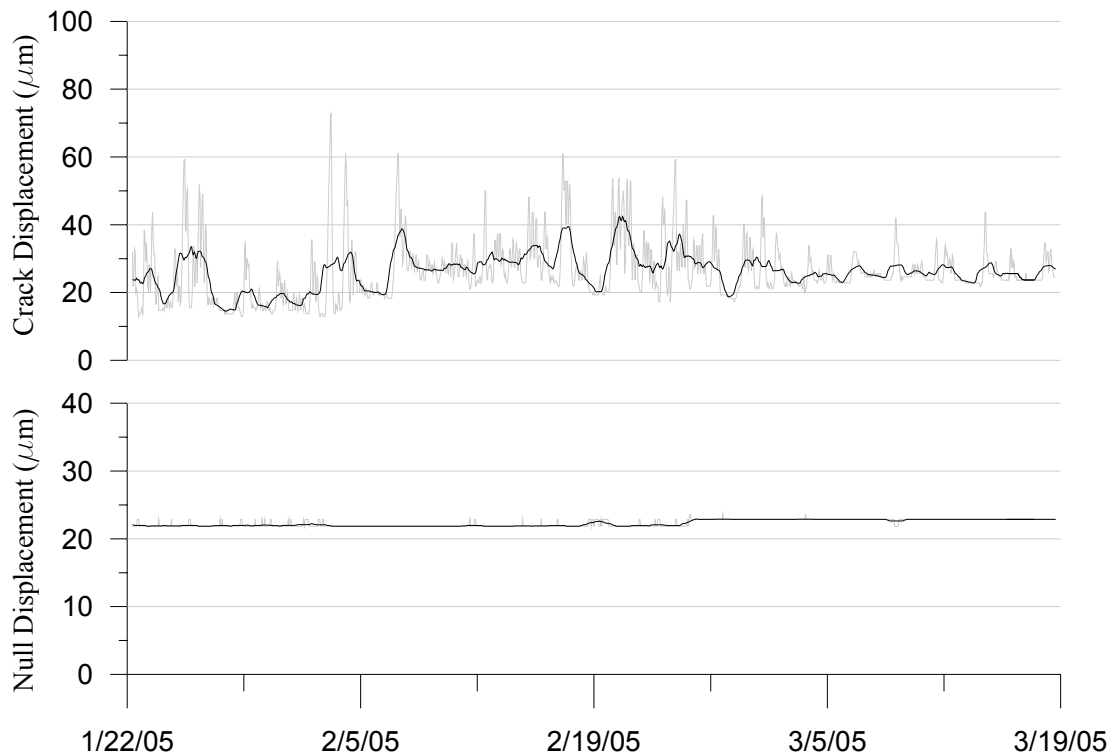


Figure 4.4 Comparison of the System X Crack and Null gauges over two-month duration of testing

For materials that are considered non-homogeneous and nonlinear, such as sheetrock nailed to wood, the crack behavior was expected to be influenced by many factors. Figure 4.5 compares the indoor temperature to crack displacement for system X data collected from Patrino, (2004) and this study. Also shown in Figure 4.5 is a straight line representing the

theoretical displacement for the thermal expansion for an uncracked portion of gypsum drywall. (Gypsum drywall CTE, United States Gypsum USG) Data from this study and Patrino, (2004) had similar relative crack movement with respect to temperature. Historical data such as Figure 4.5 shows that the crack movement is cyclical and occurs in a constant displacement zone over the two year period. The relative crack movements of both data sets were also found to be greater than theoretical thermal expansion. This difference is no doubt heavily influenced by the effect of humidity on the wood wall frame.

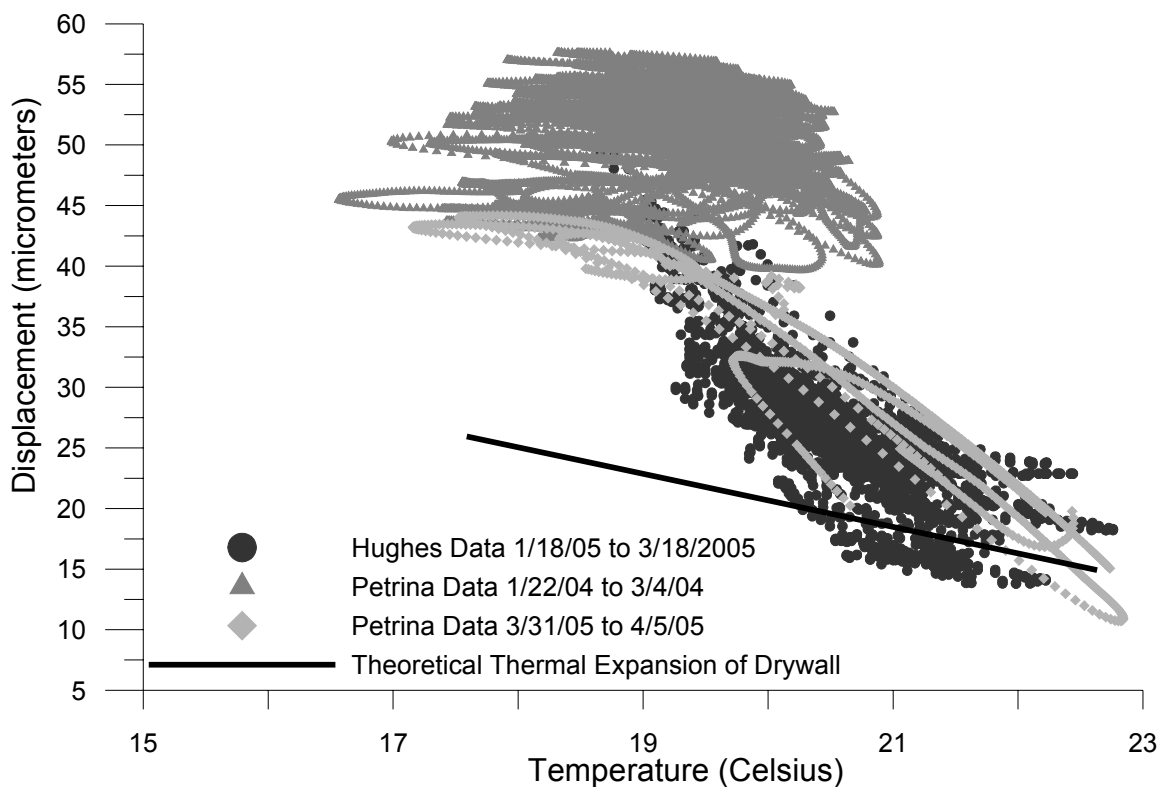


Figure 4.5 Temperature versus crack displacement data compared to the theoretical thermal expansion of gypsum, the main component of drywall.

Level II Operation

Level II systems normally are triggered by ground motions, which in turn initiate the recording of the crack response. Crack responses are measured as micrometer changes in

crack width at high sampling rates (normally 1000 Hz). Long term crack width is also recorded at regular time intervals ranging from every 15 minutes to once an hour for comparison with the long term environmental and dynamic effects. Collection of the long term data is also accomplished with the operation of a Level I system.

Level II evaluation was conducted in a quarry blasting environment in Milwaukee, WI by comparing system X response with that of the NU system. During simultaneous operation of system X and the NU system, it was found that the NU system introduced higher noise levels to system X. As a result system X was operated both with the NU system and independently. Data collected during the operation of system X was only compared to the historical data collected from the NU system.

Level II Equipment Setup

To evaluate operation of system X at level II, it was installed to record data as described in Chapter 3. Level I operation was also enabled by setting the histogram function to record the peak crack displacement every 15 minutes. The geophone data logger was set to record ground motion and trigger the crack monitor data logger when ground motion exceeded 1.02 mm/sec (0.04 in/sec).

Level II Data Collection

Level II data were collected over six months of operation from January to June of 2005. During the winter months of operation, blasts occurred approximately once every few weeks; during spring and summer, blasts occurred about once a week. On days when blasting did occur, two or three individual blasts would be observed within approximately an

hour. As shown in Table 4.2, 37 blasts were recorded during Level II evaluation of system X. The ground motion measured during monitoring ranged in PPV from 1.09 to 6.60 mm/sec with an average PPV of 1.81 mm/sec. The largest and smallest blasts recorded during monitoring occurred on the same date, May 19, 2005. During the largest event the system X geophone, spaced farthest from the blast, recorded a PPV of 6.60 mm/sec. The closer NU geophone position outside of the test house, recorded a PPV of 8.20 mm/sec and the even closer quarry geophone recorded a PPV of 9.73 mm/sec. The smallest blast recorded during monitoring resulted in a PPV of 1.09, 1.40 and 1.96 for the system X, NU, and quarry geophones, respectively. In both cases of the smallest and largest blasts, it was found that PPV attenuated as ground motion approached the test house. Since the design of system X is considered as known and trusted for capturing ground motion, measurement of ground motion will not be reviewed.

Records obtained from the quarry indicated 49 blasts occurred during the months of evaluation of system X. Approximately 75% of blasts were large enough to trigger system X. Any blast that did not trigger system X during testing had attenuated below the trigger value of 1.02 mm/sec by the time the ground motion reached the test house basement.

During the level II testing of system X, the unit was operated in two electronic noise environments while in the same blasting environment. The first noise environment occurred when the NU equipment was operating and the noise levels averaged 2.3 μm . Any data collected when the NU equipment was operating required frequency filtering before it could be analyzed. When the nearby NU equipment was deactivated, the noise level decreased to 0.8 μm .

Date	Longitudinal		Transverse		Vertical		Max PPV		Crack Displacement Zero to Peak (μm)	
	PPV (mm/sec)	Freq. (Hz.)	PPV (mm/sec)	Freq. (Hz.)	PPV (mm/sec)	Freq. (Hz.)	PPV (mm/sec)	Freq. (Hz.)	Ground Motion	Air Blast
1/20/2005	1.60	17.2	1.60	16.7	1.35	14.7	1.60	17.2	1.4	1.2
1/20/2005	1.27	31.3	1.09	35.7	1.02	31.9	1.27	31.3	1.4	1.1
1/20/2005	1.91	16.1	1.35	11.1	1.02	8.3	1.91	16.1	1.9	1.0
1/28/2005	1.91	13.9	1.47	16.7	1.02	15.2	1.91	13.9	1.6	0.8
1/28/2005	1.14	41.7	1.35	12.8	0.97	41.7	1.35	12.8	0.3	1.8
1/28/2005	1.65	15.6	1.40	12.2	1.02	38.5	1.65	15.6	1.0	1.2
1/28/2005	1.47	139.0	1.27	13.9	1.14	16.7	1.47	139.0	1.5	0.9
3/30/2005	1.35	13.9	1.09	13.5	0.51	29.4	1.35	13.9	0.6	1.1
3/30/2005	1.35	20.8	1.14	13.5	1.02	10.4	1.35	20.8	1.1	1.2
3/30/2005	2.62	16.7	1.85	17.9	1.60	14.7	2.62	16.7	0.8	1.7
4/8/2005	1.27	16.7	1.02	18.5	1.27	20.0	1.27	16.7	0.5	1.5
4/8/2005	1.52	11.4	0.89	8.8	0.97	8.6	1.52	11.4	0.3	1.8
4/8/2005	1.65	11.6	0.97	13.2	0.97	12.2	1.65	11.6	0.5	2.0
4/13/2005	1.78	13.9	1.02	13.9	1.47	21.7	1.78	13.9	0.8	1.4
4/13/2005	1.35	29.4	1.22	29.4	0.84	38.5	1.35	29.4	0.8	1.5
4/13/2005	1.09	11.1	1.14	13.9	0.64	25.0	1.14	13.9	0.8	1.3
4/18/2005	3.89	13.9	3.05	11.1	5.21	31.3	5.21	31.3	0.8	1.1
4/18/2005	1.40	8.2	1.73	5.9	1.35	7.2	1.73	5.9	1.2	1.5
4/26/2005	1.09	11.1	1.22	7.7	1.02	31.3	1.22	7.7	0.6	0.7
4/26/2005	1.14	11.6	0.84	33.3	0.58	16.1	1.14	11.6	0.3	1.8
4/26/2005	1.14	13.2	1.02	16.1	0.64	11.1	1.14	13.2	1.1	1.4
5/4/2005	1.14	16.7	1.40	17.2	0.89	33.3	1.40	17.2	0.6	1.4
5/4/2005	1.14	13.5	0.97	29.4	0.97	25.0	1.14	13.5	0.4	1.4
5/19/2005	4.27	41.7	2.36	19.2	6.60	33.3	6.60	33.3	1.1	1.1
5/19/2005	1.22	11.6	1.27	4.7	1.35	29.4	1.35	29.4	0.6	0.9
5/19/2005	1.09	26.3	0.89	15.2	0.58	17.2	1.09	26.3	0.6	0.9
5/27/2005	1.27	33.3	1.02	35.7	0.84	22.7	1.27	33.3	0.5	0.6
5/27/2005	1.02	10.9	0.97	14.7	1.14	11.4	1.14	11.4	0.8	1.0
5/27/2005	1.91	13.2	1.02	14.7	1.47	11.6	1.91	13.2	1.0	1.1
5/27/2005	3.12	15.6	1.91	35.7	4.78	38.5	4.78	38.5	0.6	0.9
6/2/2005	1.52	12.8	1.27	15.6	1.60	12.8	1.60	12.8	0.6	2.0
6/2/2005	1.02	13.5	1.14	27.8	1.02	25.0	1.14	27.8	0.6	1.5
6/2/2005	1.35	31.3	1.27	23.8	0.97	41.7	1.35	31.3	0.4	1.2
6/9/2005	1.78	23.8	1.09	8.6	2.62	26.3	2.62	26.3	1.0*	0.9*
6/20/2005	1.14	12.2	1.27	27.8	0.84	26.3	1.27	27.8	0.6*	1.6*
6/20/2005	0.89	17.2	0.97	21.7	1.22	27.8	1.22	27.8	0.8*	0.9*
6/20/2005	1.02	10.4	0.84	10.4	1.35	7.8	1.35	7.8	2.1*	2.0*

Table 4.2 Summary of blast data collected during Level II testing of system X. *Denotes events that did not require noise filtering. (NU system inactive)

Level II Performance

The peak crack displacements measured by the system X LVDT were compared to the NU LVDT and Kaman sensor. The evaluation of the sensors included a direct comparison of the shape and amplitudes of the waveforms. Figure 4.6 compares the NU LVDT sensor to the system X LVDT. To create a direct level II comparison of system X to the NU system, system X waveform was filtered to remove frequencies above 50 Hz. The shape of the waveform captured in Figure 4.6 by system X, was similar to the waveform captured by the NU LVDT. Both waveforms showed a peak crack vibration 0.5 seconds. Additionally, both waveforms have a large low frequency peak at approximately 1.75 seconds from the air overpressure wave of the blast event. The system X waveform displayed a lower peak crack displacement after filtering.

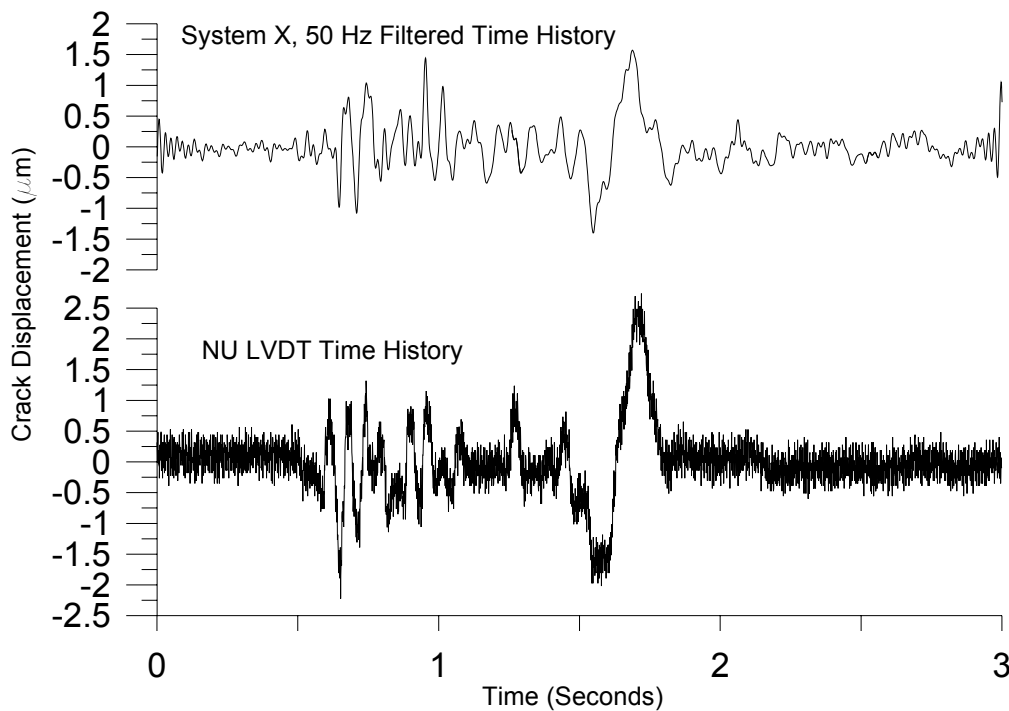


Figure 4.6 Direct comparison of crack time histories for system X, and NU LVDT, blast April 18, 2005. System X, data filtered to remove all content greater than 50 Hz.

During evaluation, all waveforms captured by system X were of smaller amplitude than those captured by the NU system. While system X and the NU system were installed on the same crack, they were spaced approximately 16 inches apart from each other and their responses should have similar ratios of long term to dynamic displacement. Figure 4.7 compares time correlated significant dynamic responses to ground motion and air over pressure recorded by both the NU LVDT and AC coupled channel on system X during five different blasts. This comparison was made with eight different blasts that occurred between March and May of 2005. During all eight blasts reviewed the NU LVDT was active, and the NU Kaman gauge was only active for two blasts, due to equipment constraints.

Interpretation of ratios of the NU LVDT to system X response is complicated. For instance, the ratio for long term effects (shown in Figure 4.3 as 1.32), is 25% of the ratio of dynamic effects (shown in Figure 4.7 to be 1.75). While these ratios could be used to adjust the dynamic response to be comparable to the long term response, it may not be the proper adjustment because of filtering and the difference in noise compared to signal for dynamic and long term response. Unfortunately, to obtain a comparison requires simultaneous operation of the NU system, which induces high noise levels.

The required filtering of the system X waveforms to reduce the effects of noise reduces the amplitude of the signal. Thus, had filtering not been required, the resulting waveforms would have had larger system X crack response amplitudes and thus, a smaller dynamic ratio of the NU LVDT to system X. In other words, the 1.75 dynamic ratio of the NU LVDT to system X would have been smaller and thus closer to the 1.32 long term ratio.

The noise level of system X while the NU system was operational was much larger than the dynamic crack response amplitude but small with respect to the long term

crack response amplitudes. For example during a blast event with a ground motion of 0.1 PPV there was only 1 μm of crack displacement (zero to peak) while the noise with the NU system operational was 1.1 μm (zero to peak) or a 110 % of the signal. This high noise level shown in Figure 2.5 of Chapter 2 required filtering to obtain any signal relating to crack displacement, which complicates the comparison as discussed above. On the other hand the noise level is only 3% of the signal for a typical long term, weather induced crack response shown in Figure 4.2.

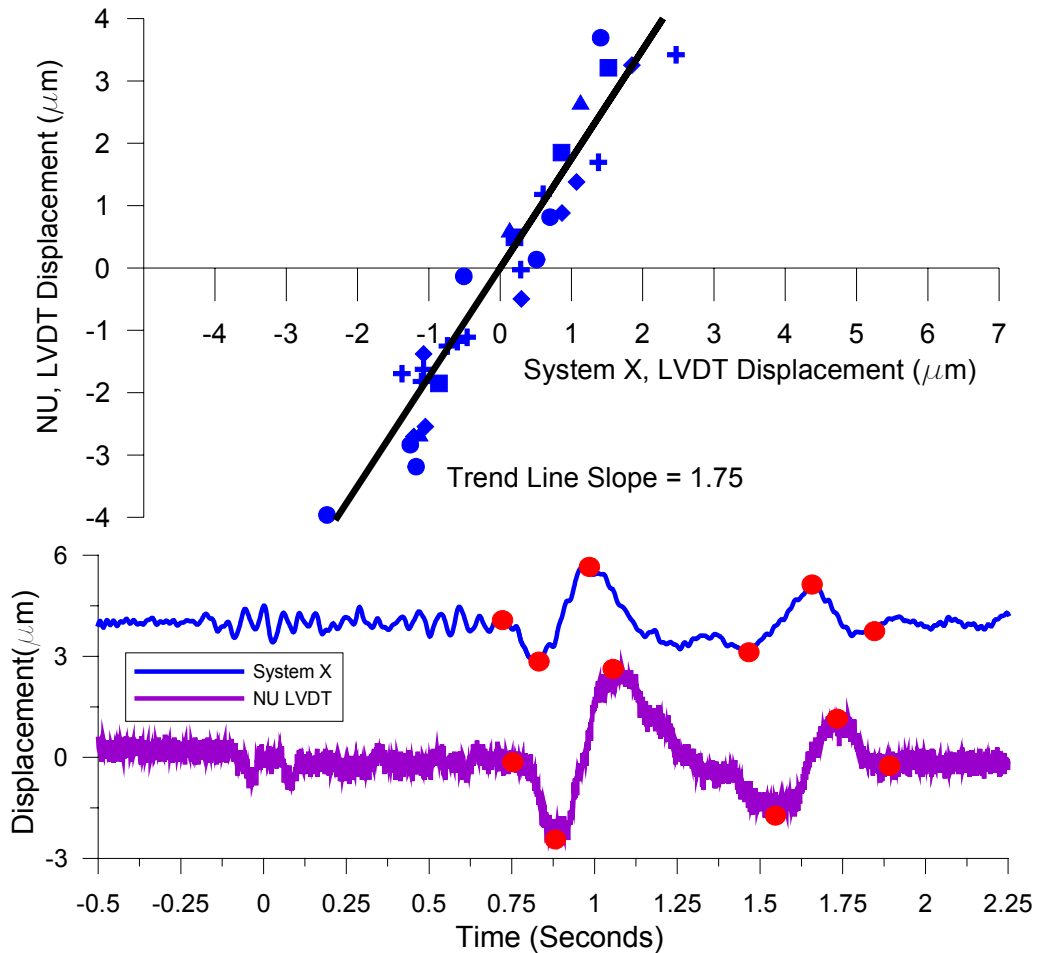


Figure 4.7 (Top) Comparison of the displacements of system X to the NU LVDT sensor during dynamic recording. (Five individual blasts denoted by symbols.) (Bottom) Example of how the dynamic ratio was selected for a given filtered waveform.

To determine the overall effectiveness of the system's ability in capturing level II data as an independent system, two different types of data captured by the system, an AC and DC coupled response, are reviewed. Consider the event shown in Figure 4.8, which is a blast event that occurred on June 9, 2005 with a PPV of 2.62 mm/sec on the vertical channel. The corresponding crack displacement produced by the ground motion was less than 2 μ m, peak to peak. Crack responses captured on the DC coupled channel 3 differ with those from the AC coupled channel 4 of system X. As described in chapter 2, the AC coupled channel 4 waveform is more highly resolved and is zero centered during a blast. One disadvantage of a zero centering sensor is that a temporary shift would not be visible in the time history, as is seen in the DC coupled waveform, which displays a temporary offset of 2 μ m.

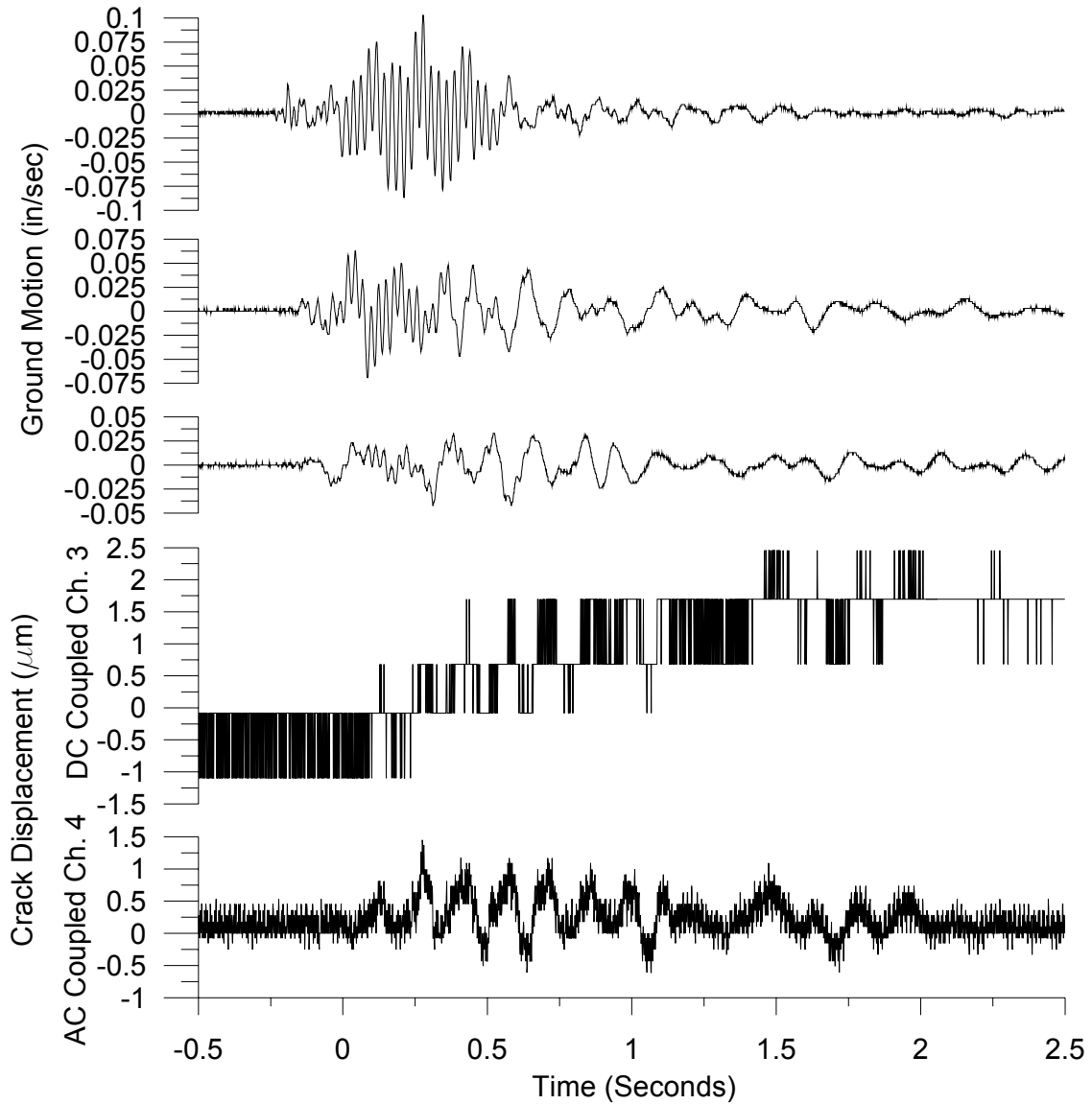


Figure 4.8 System X, recorded crack displacement from a blast occurring June 9, 2005 were a temporary offset occurred.

The importance of the temporary offset in figure 4.8, can be assessed by comparing with the long term response shown in figure 4.9. The 2 μm offset, while seeming significant in figure 4.8, is seen in figure 4.9 to be small compared to the large swings in crack displacement. In addition, this event does not change long term crack response pattern.

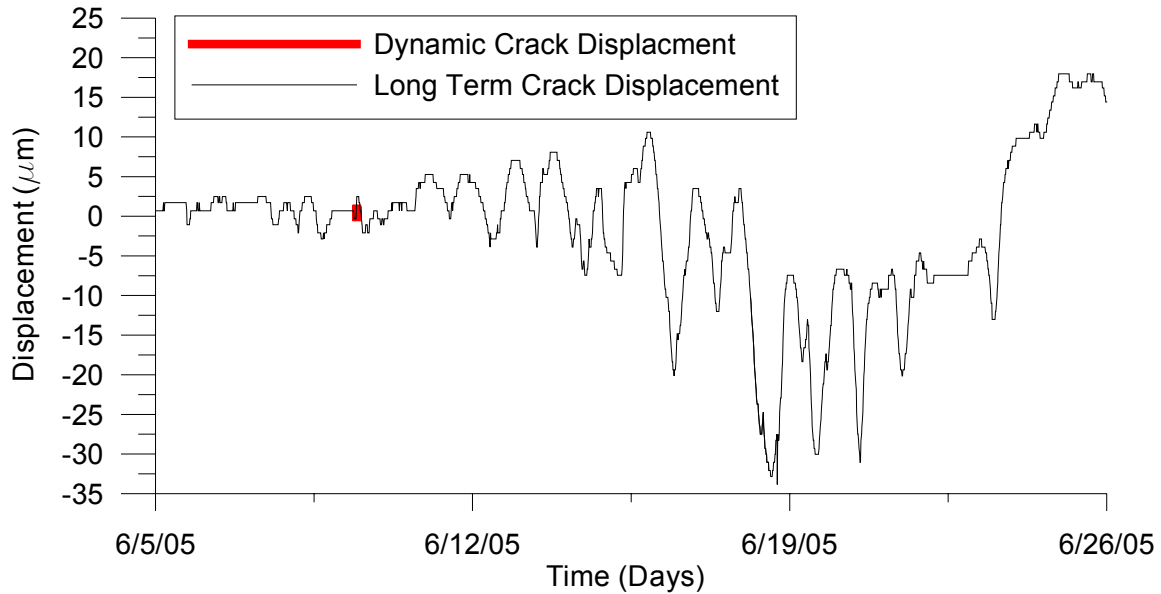


Figure 4.9 Comparison of the crack displacement captured by system X dynamically during blasting on June 9, 2005 and long term crack displacement during three weeks of the month of June.

System X's ability to capture air pressure response is shown in Figure 4.10. This blast event was recorded with system X, on June 20, 2005 and is more typical of the blasts seen during monitoring. The system X geophone recorded a PPV of 1.27 mm/sec on the vertical channel of the geophone. This blast has a smaller peak crack displacement due to the blast vibration compared to the June 9th blast, but a larger low frequency crack displacement due to the air overpressure wave associated to the blast event. Like the June 9th blast, a small temporary crack offset could be noticed on the DC coupled channel 3 of Figure 4.10. Also, similar to the June 9th event, this event's temporary offset is overwhelmed by the environmentally induced crack response.

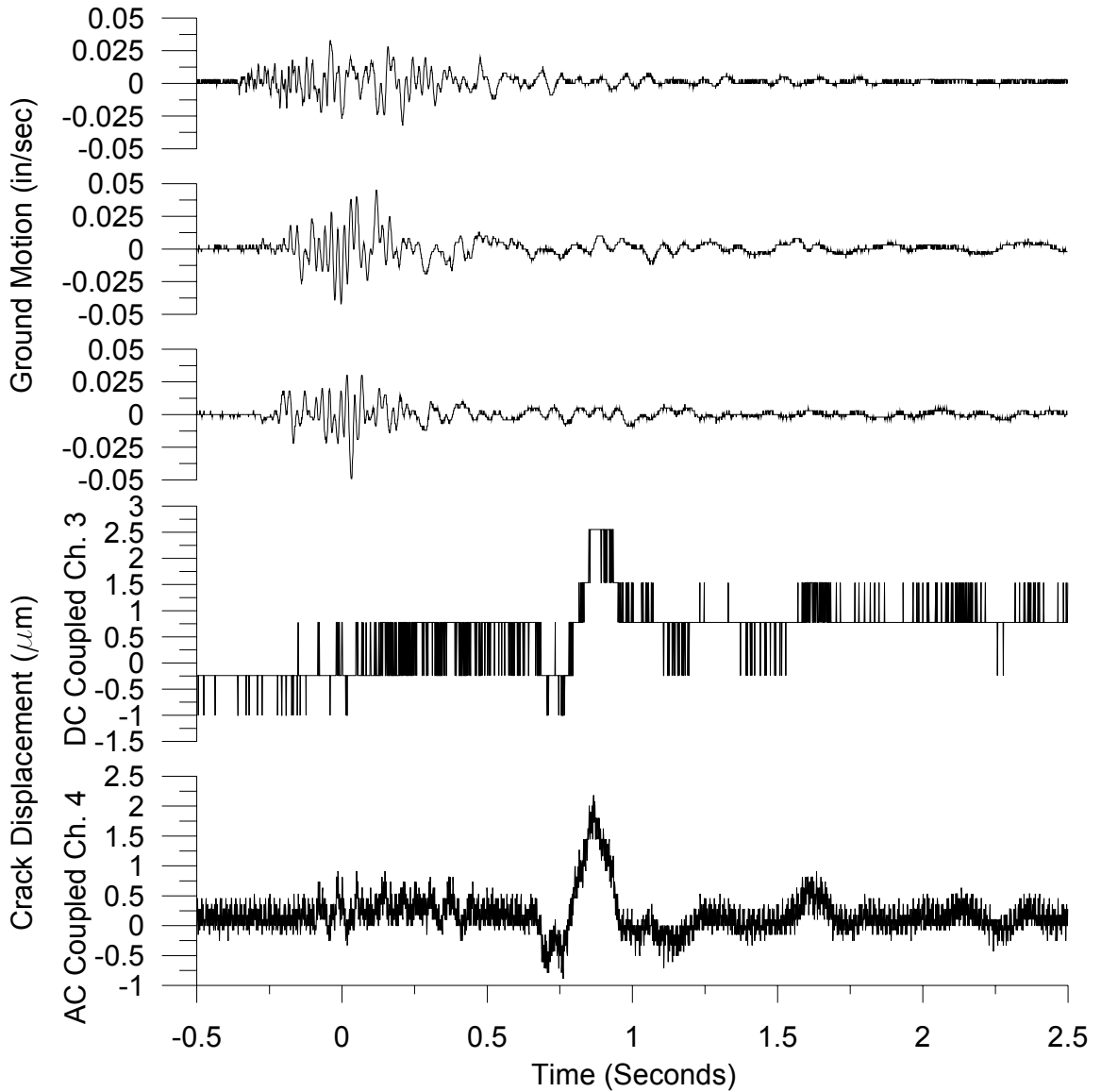


Figure 4.10 System X, recorded crack displacement from a blast occurring June 20, 2005 during which the crack responded to primarily to the air blast.

Level III Operation

System X was evaluated for level III operation by triggering the unit off the crack movement. The unit was set to trigger off the crack when the crack displacement exceeded a threshold value more than four times in a row. An example of the triggering logic of system X is shown in Figure 4.11. Crack triggering operation is very similar to level II operation

when the unit is triggered off the ground motion. Unlike ground motion the zero point or trigger reference shifts on the AC coupled channel with long term crack response. The “zero” for the AC coupled channel is taken as to the mid scale of the signal A/D range. The system triggers when the AC coupled channel displacement exceeds the current zero by a user defined amount for four consecutive samples. Once the trigger level is exceeded, the dynamic crack response is recorded at a frequency of 1000 Hz.

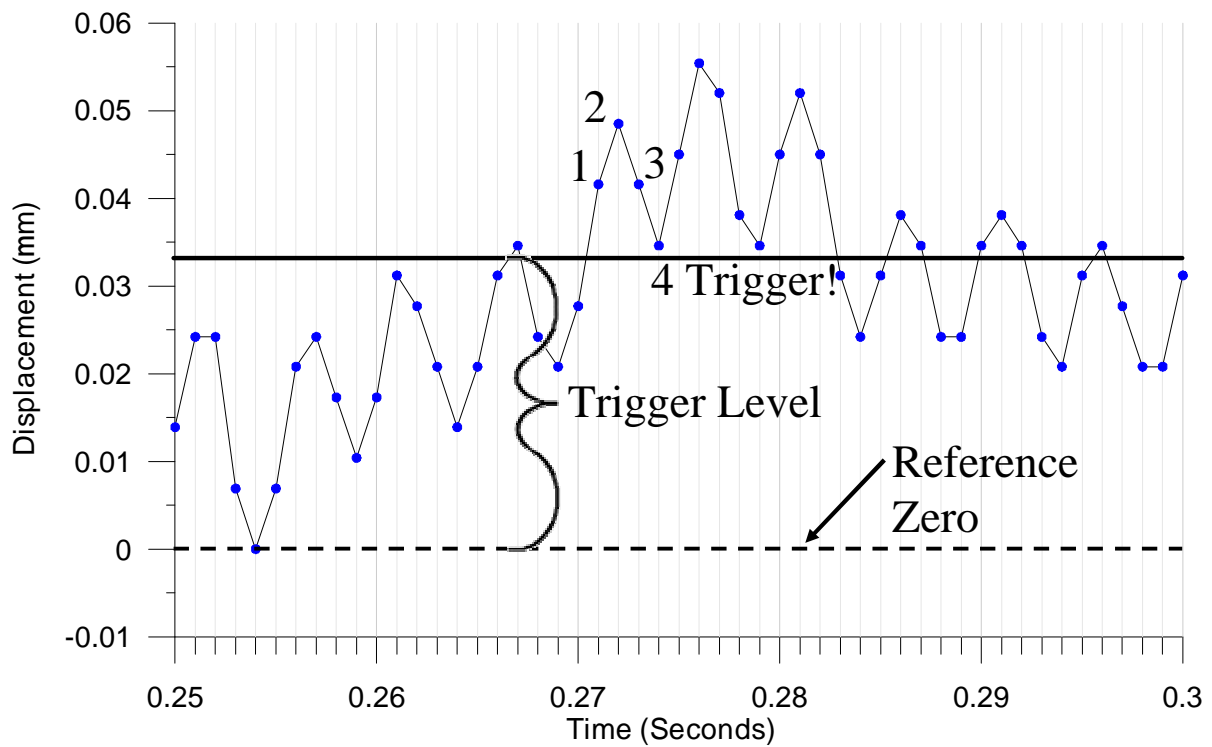


Figure 4.11 Example of the crack triggering logic for system X, when operating as level III system.

Level III ACM operation can be implemented by triggering of the crack (without the geophone) to record both blast and occupancy-triggered events. Occupancy-triggered data included events caused by door slams, dropped objects and high winds, which can cause the crack to respond. The prime advantage of being able to measure crack movement from

occupancy events was the ability to compare blast to occupancy-induced crack movements that occur at unforeseen times. In level III operation crack width was also recorded at intervals of 15 minutes to one hour for comparison with long term environmental effects obtained during the level I and II operation.

Level III Equipment Setup

In order to evaluate system X during level III operation, the crack data logger was installed as described in Chapter 3. The histogram function was set to record the peak crack displacement every 15 minutes. The geophone data logger was set to record the ground motion when it exceeded 1.02 mm/sec. If desired, system X could be operated at level III without the geophone data logger and record only data from the crack. The geophone trigger function on the crack monitor data logger was allowed to remain active.

When both trigger mechanisms are activated each response will be recorded regardless of the type of excitation. The only time when an event would not be recorded during level III monitoring would be if the unit triggers twice within a 20 – 30 second period. System X, requires a short period of time between dynamic events to reinitialize, before another event can be recorded. If an occupant induced event occurs within the 20 – 30 second period before a blast event, there is a possibility that the crack monitor will not be prepared to record dynamic data during the event, and the crack will be lost. However, when the crack trigger has been properly set the potential for losing data can be minimized by reducing the number of crack triggered events to only those which are significant.

During testing, the crack trigger level was varied between 0.36 to 0.75 μm of movement, zero to peak. The lower the trigger value was set, the more events the unit

recorded. When reviewing crack triggered events on system X, the waveform recorded on the AC coupled channel 4 was used for analysis. The waveform captured on the DC couple channel 3, was only used when a baseline shift in the time history was assumed.

Level III Data Collection

System X was operated as a level III system for approximately three weeks, from late June through the end of July 2005. During the 20 days of testing as a level III unit, system X recorded almost 300 crack triggered events. As shown in Figure 4.12 the number of events recorded per day plotted as a function of the crack trigger level. The more sensitive the crack trigger was set, the more events were recorded. To determine the optimal trigger level shown in Figure 4.12, an algorithm was run on the data collected over a two day period when the trigger was set to 0.014 mils or 0.36 μm . A trigger level of 0.014 mils is the lowest possible trigger level for system X and not recommended for during a standard installation. Trigger levels below this would fall below the system's noise level. The test algorithm determined the number of events the system would have recorded had the trigger level been set higher.

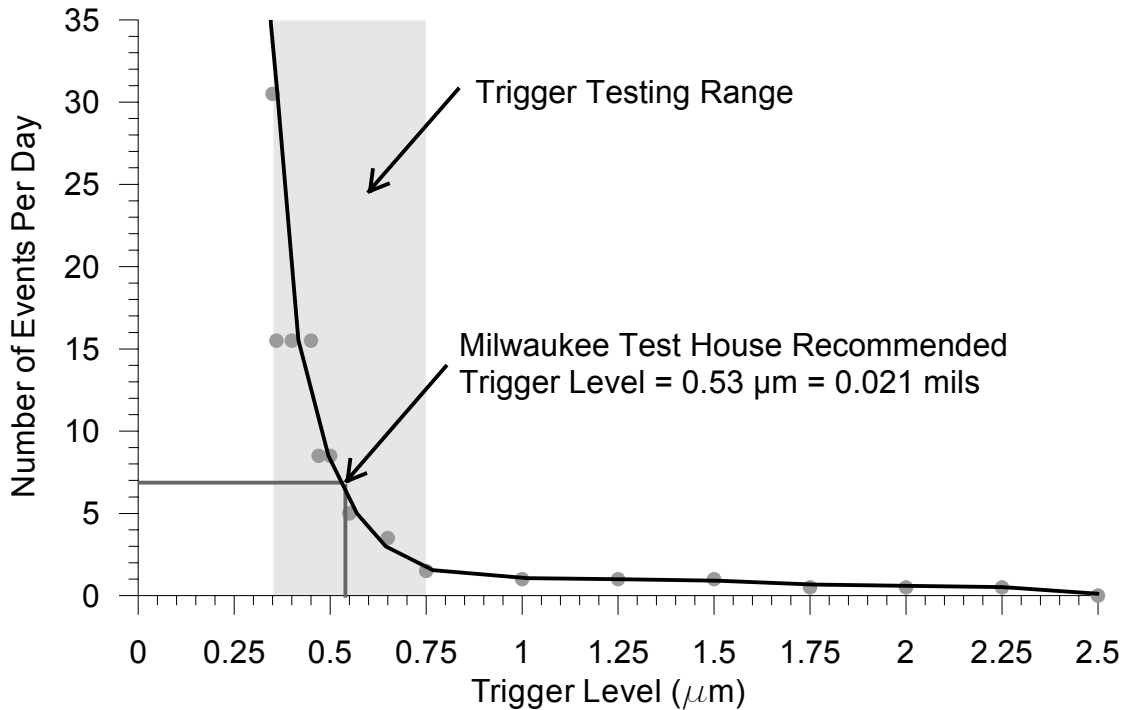


Figure 4.12 Number of events recorded by system X as function of the trigger level. Specific to the Milwaukee test house, data collected on July 8-9, 2005, with a trigger level of 0.36 μm .

Trigger data shown in Figure 4.12 shows a few interesting trends. A vertical asymptote occurred at a trigger level of 0.36 μm and a horizontal asymptote of one event per day began at a trigger level of 0.75 μm . The system was therefore able to capture most events when the trigger level was set between 0.36 μm and 0.75 μm . During these two days of testing, no events triggered at a level greater than 2.50 μm . Trends in the data show that as the trigger level approaches 0.36 μm , the number of events approaches infinity. This trend means that the crack is beginning to trigger off the system's noise, rather than actual events. The average noise level of system X was previously found in Chapter 2 to be approximately 0.40 μm , zero to peak. As shown in Figure 4.13, when the trigger level was set to 0.36 μm , any noise fluctuations in the waveform greater than 0.04 μm would cause the unit to trigger. This very small trigger level could be exceeded easily by environmental noise.

During testing, the optimal trigger level was found to be 0.53 μm . At this trigger level, most of the noise spikes and insignificant events were eliminated. When the trigger level is less than the optimal trigger level of 0.53 μm , the number of events collected per day increases quickly. To identify legitimate events, when the trigger is set to a low value becomes labor intensive and may not be the most efficient method of monitoring.

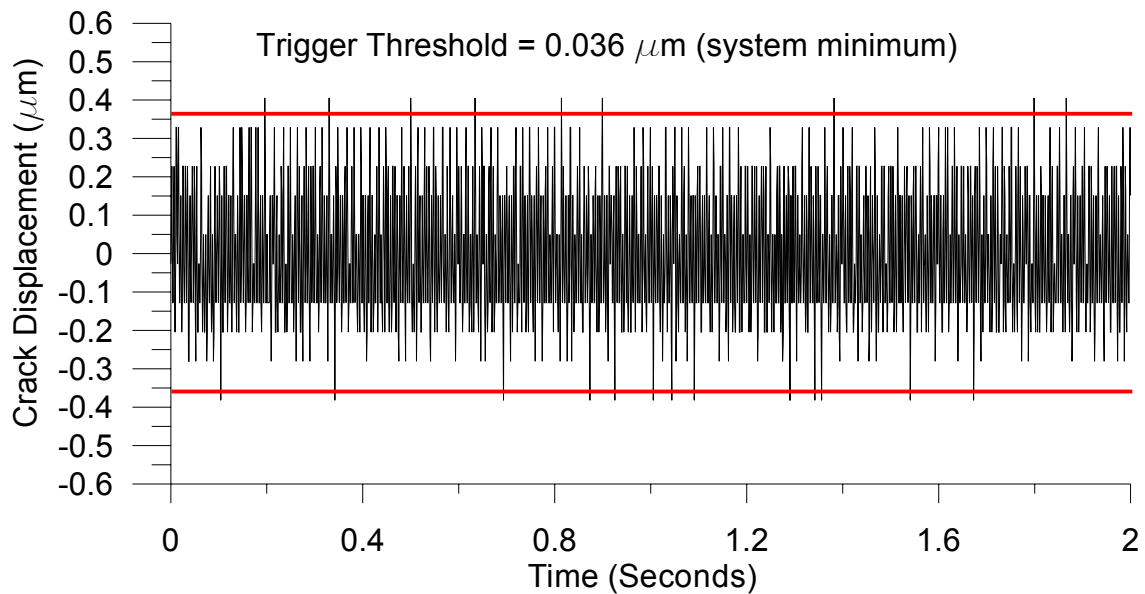


Figure 4.13 Example of the typical system X noise during monitoring in comparison to the smallest crack trigger level. Trigger level of 0.036 μm shown in red.

Level III Performance

Many different types of crack responses can occur during dynamic excitation. Occupant events can vary both in frequency and magnitude. Figure 4.14 shows a variety of deliberately induced occupant events at the monitored house, in Milwaukee, WI (Waldron, 2006). The first event, labeled A, was created by quickly closing the kitchen door of the house. This event has a high frequency and was small in amplitude. The second event, B

resulted from pushing on the ceiling near the crack. This event shows large amplitude and low frequency with periods as long as a second. The third event labeled event C, was proved by lightly striking the ceiling near the crack. This event has a large frequency and small amplitude and is comparable to the size and shape of the event recorded when the kitchen door was being closed. Examples of occupancy events with known causes, such as those found in Figure 4.14, are useful in determining the significance of a blast induced response.

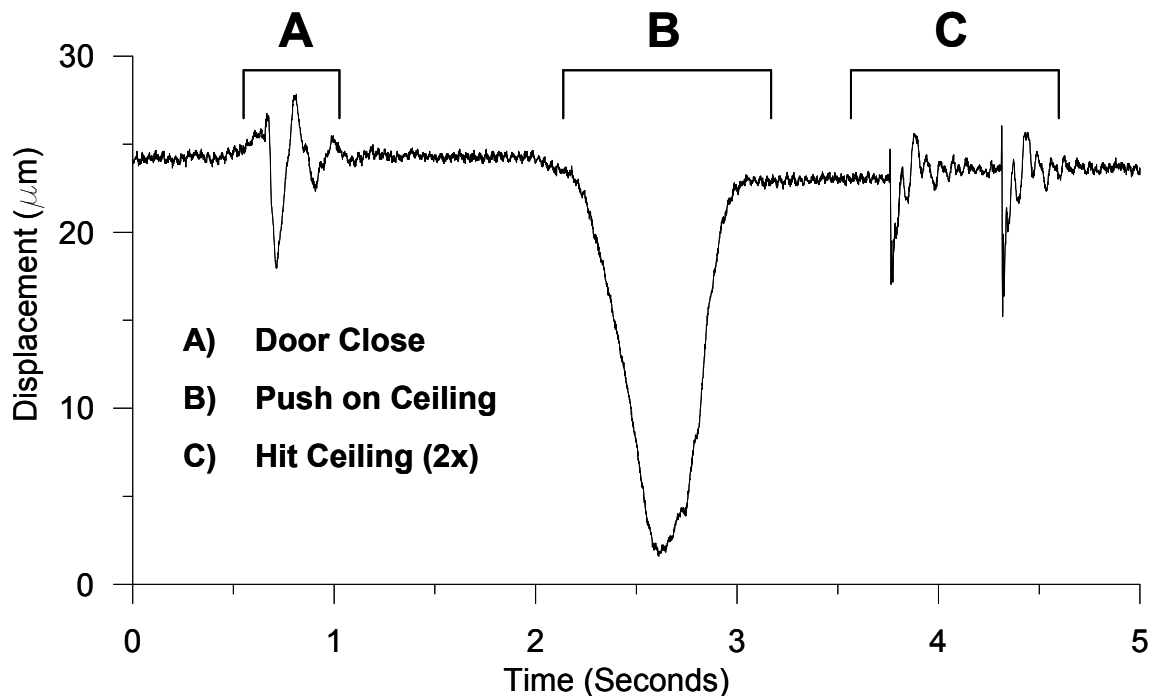


Figure 4.14 Examples of created occupancy activity recorded on the NU system, for comparison of the actual events from system X. (Waldron 2006)

Most of the crack triggered response collected during level III evaluation of system X could be classified as either high or low frequency events. Low frequency events were classified as having a frequency lower than 4 Hz. Shown in Figure 4.15 are two examples of low frequency waveforms collected by system X. These events have a single peak in crack displacement. The crack displacement waveform rises and falls slowly as the crack opens

and closes. In most cases the crack returned to its original position within approximately half a second.

Natural wind gusts exert dynamic air overpressure forces on structures. It was hoped that this type of response would be detectable during crack triggered events with high winds. Wind gusts of 20 mph were observed on the 15th and 20th of July at nearby Mitchell airport as shown in Figure 4.16 (NOAA, 2005). In Figure 4.16 the constant line indicates the average hourly wind speed while the red dots depict the 5 second peak wind speed during gusts. Wind gust data can be compared to crack responses like those in Figure 4.16 to determine the magnitude of the wind response.

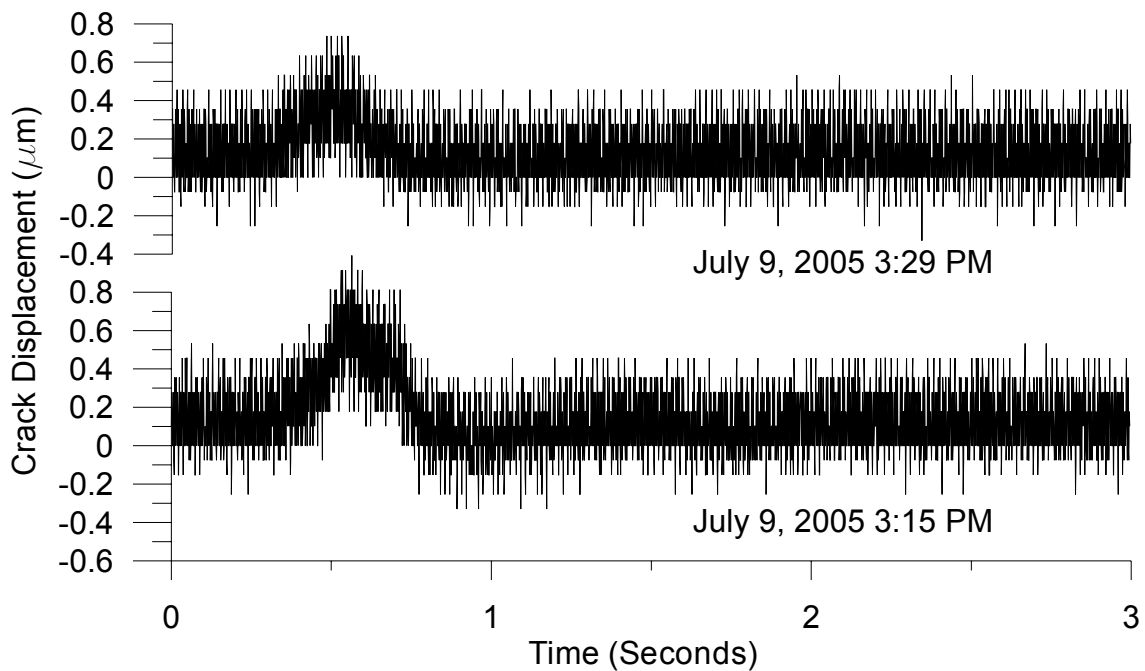


Figure 4.15 Low frequency (4 Hz or less) crack triggered movement recorded during system X, monitoring in Milwaukee, WI.

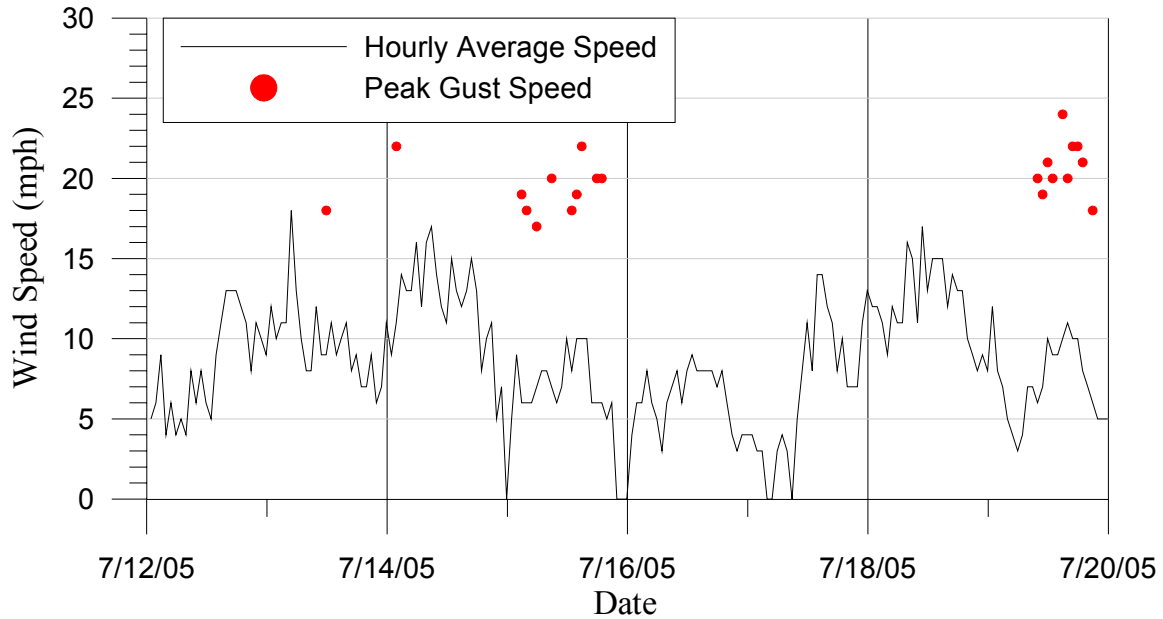


Figure 4.16 Average hourly and gust wind speed data collect from the Mitchell Airport weather station, Milwaukee, WI.

The natural wind gust data collected from the nearby Mitchell airport (NOAA) can be compared to the crack triggered events to determine the effect that the wind has on the crack displacement. Wind induced response is compared to the wind gust speed on the 15th and 20th of July, 2005 in Figure 4.17. A similar study was conducted by Aimone-Martin (2005) in Henderson, NV, and her data are shown in this graph for comparison. In both the Henderson, NV study and in this study, it was found that the crack displacement increased with an increase in wind gust speed. Additionally, in both cases the crack displacement provided by wind gusts was larger than the average displacement from local blasting. Due to the differing types of structures, varying wind directions, the individual building response to the wind is expected to vary.

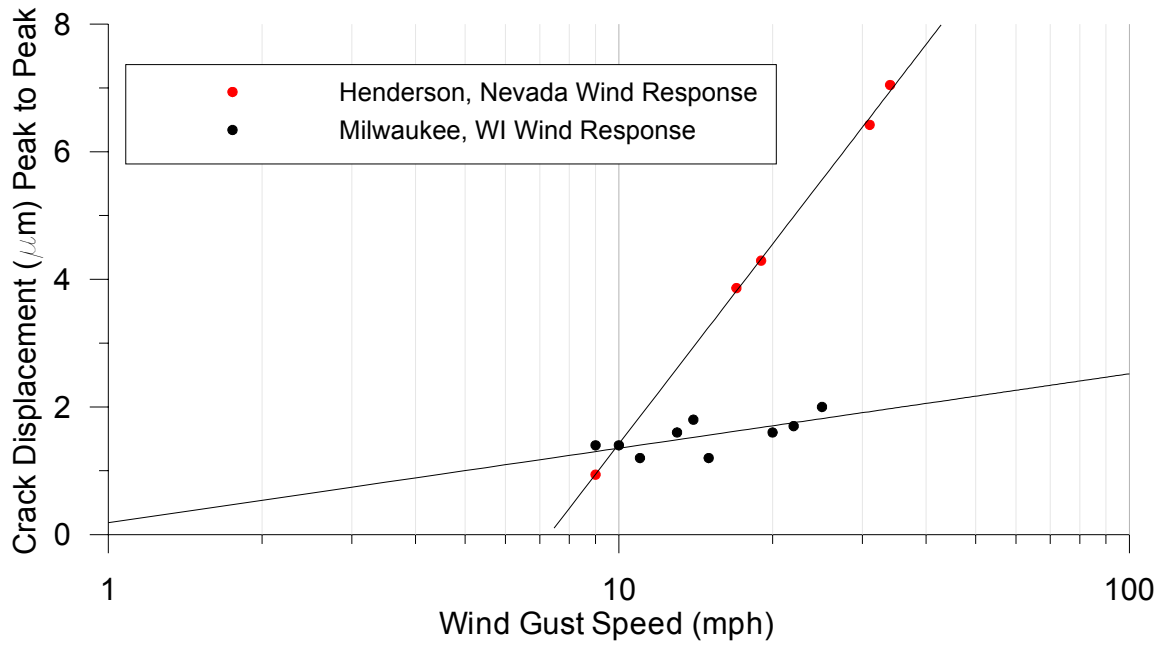


Figure 4.17 Peak to peak crack displacement as function of wind speed for data collected by Aimone-Martin in Henderson NV, and during this study.

High frequency crack movement was classified as crack responses with a frequency greater than 4 Hz. Two examples of high frequency crack time histories recorded during system X level III monitoring are shown in Figure 4.18. When high frequency waveforms are encountered, at least 3 to 4 cycles of opening and closing occurred before the waveform returns to its original baseline. The higher frequency waveforms shown in Figure 4.18 are comparable to the door closing and striking the ceiling shown in Figure 4.14.

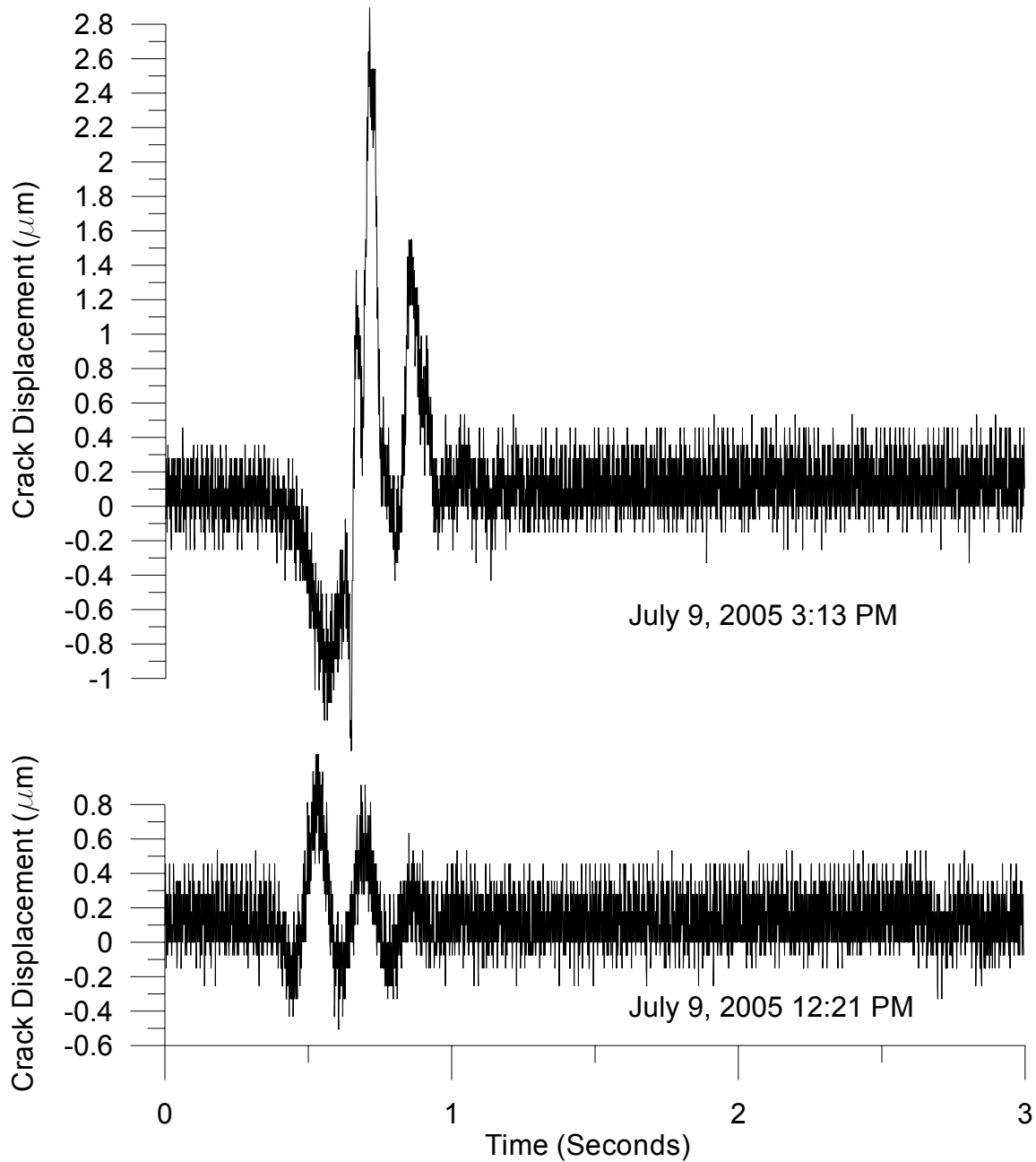


Figure 4.18 High frequency crack triggered movement recorded during system X monitoring in Milwaukee, WI.

Crack triggered events can be used to determine time dependent trends in the data.

Figure 4.19 represents the frequency of occurrence of crack triggered data. These data were collected for 12 consecutive days of monitoring with the crack trigger level set to $0.36 \mu\text{m}$.

Time dependant data like Figure 4.19 is a valuable tool for correlating the relationship between triggered events and the actions of the building's occupants. When reviewing the plot of the 12 consecutive days it could be noticed that a peak in the number of events occurred at 5 am and then again from 9 am to 6 pm at night. These events appeared to correlate well with the time of day in which most people are active in their homes. Late in the evening and during the middle of the night, few crack triggered events occurred.

To further determine the cause the events, the data were divided into seven working and five weekend days. The plot of working days shown in Figure 4.19, indicated that a large number of events occurred at approximately 5 am and at 2 pm. This could be attributed to the comings and goings of the building's occupants. The plot of the weekend days shown in Figure 4.19 indicated that a large number of crack triggered events occurred from 9 am to 6 pm. Interestingly, on the weekends, early morning events are eliminated and more activity occurred in the late morning.

One possible scenario for these trends in the data could be attributed as follows:

On weekdays: Occupant A leaves the building for work at approximately 5 am each morning. Occupant B leaves the building at approximately 9 am and returns at 2 pm. The building remained active from 2 pm until 9 pm when the occupants went to bed.

On weekends: The building's occupants wake between eight and nine in the morning. They were active in the house throughout day, with peaks at 12 noon and 5 pm. Activity reduced throughout the evening until the occupants went to bed at approximately 10pm.

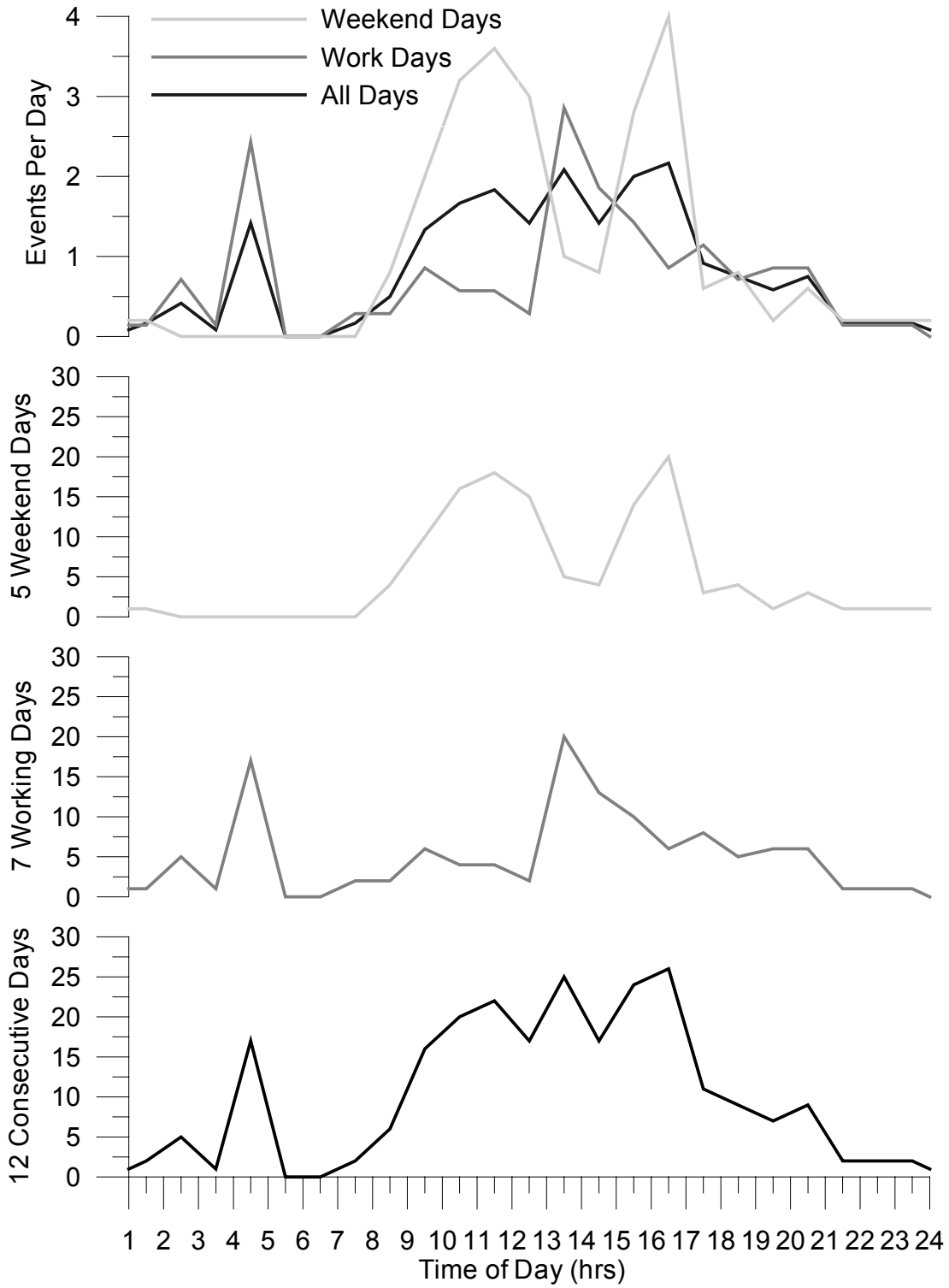


Figure 4.19 Number of events occurring in the Milwaukee test house as function of time of day. Data collected from June 30 to July 11, 2005.

Chapter 5

Installation, Software and Literature of Crack Monitoring System Y

In this chapter, the installation, software and literature of a commercial Autonomous Crack Monitoring (ACM) system, hence called system Y, are reviewed and summarized. Specifically, the software and manuals of system Y were reviewed to ensure their ease of use by the average field technician. Additionally, the effects of electromagnetic noise interference on system Y were measured. Methods for reducing and removing electromagnetic noise were also evaluated for system Y.

Installation

The general installation methods that were followed for installation of system Y in both the laboratory and the field are described in this section. The physical installation of system Y in a residential structure can be completed in approximately one day. Figure 5.1 shows the general wiring diagram and equipment location for the complete system Y crack monitor as it was installed in the test house. During this specific installation the geophone was mounted in the basement of the house and the crack sensors placed across a crack on the ground floor ceiling.

During monitoring the ACM system Y was capable of measuring ground motion, air overpressure and crack response. For this installation air overpressure was not monitored.

The central components of system Y were contained within the monitor enclosure and included a micro processor, a data logger, battery and display screen. The crack and ground motion sensors were then attached to the monitor. System Y included a geophone, which monitored ground motion and then triggered the system to record crack displacement and ground velocity time histories when the system was programmed to operate as a level II system.

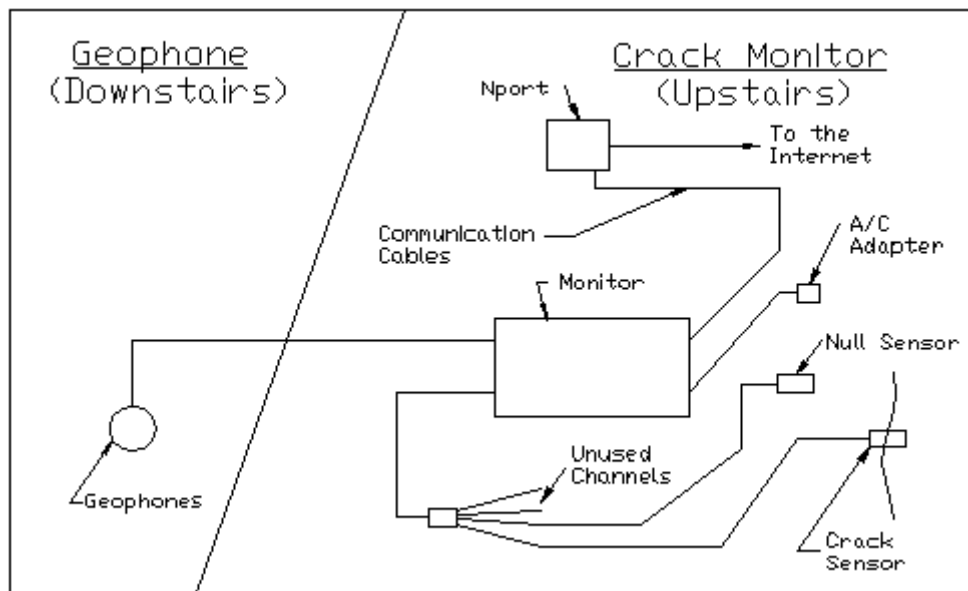


Figure 5.1 System Y wiring diagram

Geophone

The first step in the installation of system Y was to install the geophone in the basement of the test house. A storage area under the basement entry stairway was chosen, due to its remoteness. Normally, the geophone would be installed by burying, anchoring, sandbagging or spiking in the earth outdoors. The best location for the geophone is to place it between the structure being monitored and the blast. In this installation, since it was not

employed to ensure regulatory compliance it was adhered to the existing concrete slab. A plaster coating on the bottom of the geophone block. Figure 5.2 shows the completed installation of the geophone adhered to the basement slab. Plaster was found to be advantageous when compared to other types of mounting because, after the testing was completed, the remaining plaster could be scraped away without leaving any residue or mounting holes. Once the plaster cured, the geophone cable was then connected to the geophone port on the side of the system Y monitor.



Figure 5.2 Installation of the geophone in the downstairs of the test house.

Crack Monitor

The second step of the installation of system Y was to attach the crack sensors across the drywall crack. Two linear potentiometers sensors supplied with the system, shown in figure 5.3, were mounted across the crack using a 90 second quick setting epoxy. The sensors were placed 30 centimeters apart. The first sensor was mounted directly across the crack to measure crack movement. The second sensor was mounted on a nearby uncracked

section of the drywall to measure environmental effects. System Y uses linear potentiometers to measure crack displacement.

To install the crack sensors, the first sensor was connected to the crack monitor and the monitor was turned on. The linear potentiometer was manually placed at the center of its range of displacement. The lock screw located on the side of the sensor was tightened to prevent the slider from moving. The crack monitor was turned on and a sensor test was run. A sensor test verified the sensor was connected properly. Following the sensor test, an autozero was performed by pressing the “option” and “start monitor” buttons at the same time. The autozero function made the current position of the sensor equal to zero and allowed maximum travel of the sensor during operation in both directions. To verify the current position of the linear potentiometer from the main screen on system Y, the “option” and “start monitor” buttons were pressed to review the current position of the sensor. If the sensor had been properly zeroed, the current reading should be approximately zero.

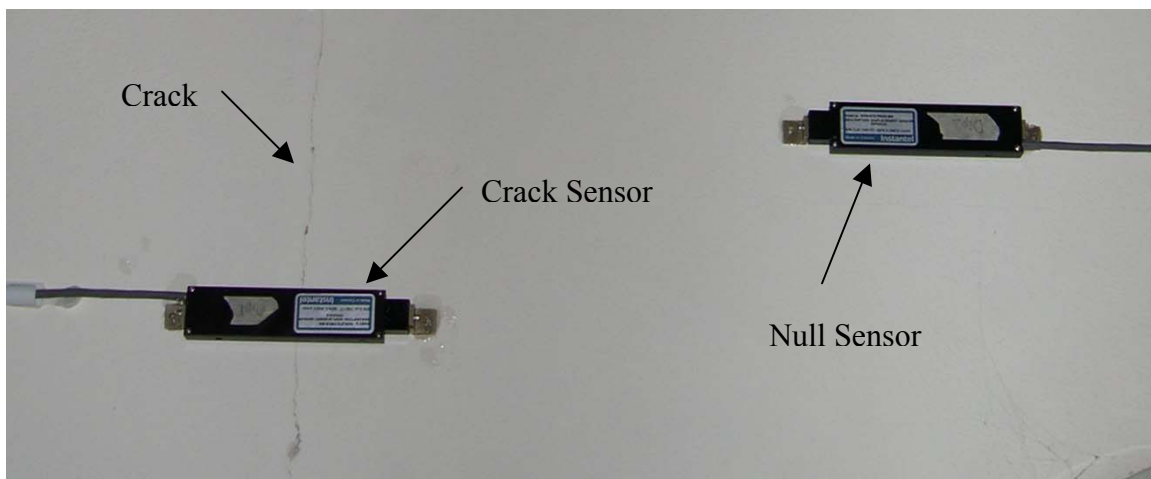


Figure 5.3 Installation of the system Y crack and null linear potentiometers on the cracked and uncracked drywall.

Depending upon the expected range of motion the linear potentiometer would encounter in the field, it could be set to record displacement in the normal or sensitive mode. In normal mode, the system Y sensor will have a range of ± 5.22 mm and a resolution of 2.61 μm . When operating in sensitive mode, the range is reduced to ± 0.653 mm and the resolution becomes 0.33 μm . If system Y is installed in an environment where only long term crack information was needed, as in level I operation, the unit should be programmed in normal mode to take advantage of the larger range. If the unit is intended to record both long term and dynamic crack data, the unit should always be operated in sensitive mode to take advantage of the higher resolution. A higher resolution enables the system to define the crack displacement during a dynamic event more closely.

In the test house, the displacement sensors were mounted over a crack in a drywall ceiling using a 90 second quick-set epoxy. With linear potentiometers locked in position, they were installed with quick-set epoxy across the crack. Figure 5.3 illustrates the mounting of the linear potentiometers across the crack and on the drywall ceiling. After the epoxy had set, the setscrews were released to allow the sensors to move and record displacement.

The crack and null displacement sensors were connected to the system Y monitor and placed in a small closet. The system Y equipment was placed on the bottom shelf of the nearby closet and the crack sensor cables were then routed through a small hole in the wall and connected to the unit. The crack monitor was powered by both an internal battery and A/C adapter. During this installation, the unit was powered by the A/C adapter since electrical outlets were available and the internal battery was only used during a power outage. The auxiliary port on the crack monitor was connected to a standard serial cable that was then connected with the Nport for internet communication as shown in figure 5.1.

Sensors

System Y crack monitors employed linear potentiometers to measure micrometer opening and closing of the crack and geophones to measure the particle velocity of the ground motion. The linear potentiometer displacement sensors were evaluated in the laboratory both statically and dynamically to validate their performance and to compare it to the previously calibrated sensors. Laboratory evaluation of the system Y sensors is described in Chapter 6. External SUPCO temperature and humidity sensors were used to monitor the environmental effects during selected testing. Future ACM systems should include integrated temperature and humidity sensors.

Geophone Sensors

Geophones measure ground motion in terms of particle velocity. Since there are three principal directions: longitudinal, transversal and vertical, three geophones are necessary. In this case all three components are housed in a single geophone block. During a dynamic event, a geophone records the time history of the ground motion for a preset duration of 3 seconds. During normal monitoring, the geophone is programmed to monitor ground motion constantly. When the ground motion exceeds a user defined trigger value, the geophone then records. In addition to recording the particle velocity-time history after triggering, the geophone monitor also records time histories prior to triggering, called the pretrigger. A pretrigger setting of 0.25 seconds and a particle velocity trigger level of 1.02 mm/sec were used for all measurements. When the unit records ground motion a sampling frequency of 1024 samples per second is used for both the preset pre and post trigger record time. For blast monitoring, the recorded time length for an event is normally three seconds. Figure 5.4

compares the three components typical of a particle velocity time history during a blast.

During this blast, the geophone was triggered on the vertical channel and the maximum peak particle velocity (PPV) was 6.73 mm/second.

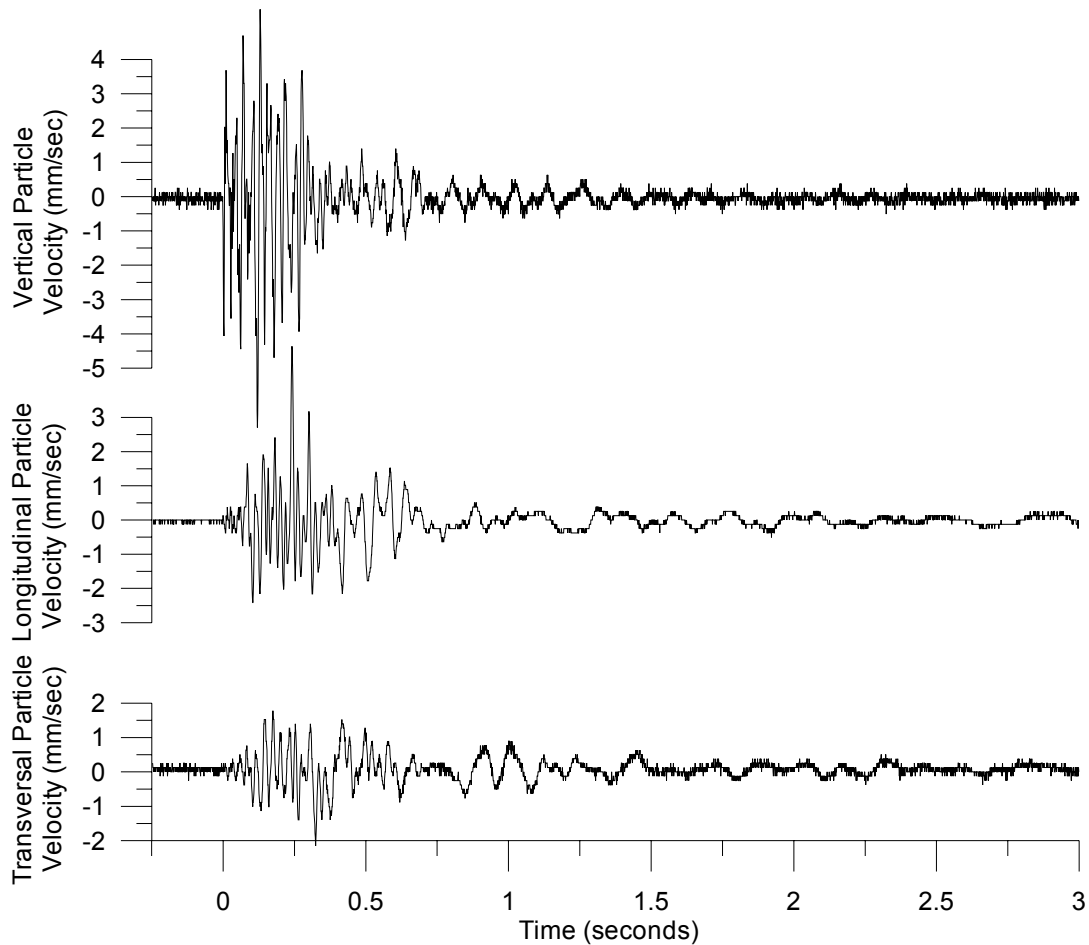


Figure 5.4 Typical ground motion record by the system Y geophone. Blast occurred on May 19, 2005.

Crack Sensors

The opening and closing of a crack during a blast event is very small and often only a few micrometers of displacement will be recorded. System Y was qualified with StructureMetrix SMG035A linear potentiometers. These sensors were used to measure crack displacement. Since the displacements measured by an ACM system are very small, the

displacement sensors used must have a small range and a high resolution. When the gain setting is set to 8 or ‘sensitive’, the range of the StructureMetrix sensor at $\pm 653 \mu\text{m}$ was approximately 1.3 times that of the benchmark Kaman sensor. When the gain is set to 1 or ‘normal’ the range of the sensor was $\pm 5220 \mu\text{m}$ or 10.4 times that of the Kaman sensor. A direct comparison of the specifications of StructureMetrix linear potentiometers to the Kaman eddy current sensor is shown in Table 5.1 The StructureMetrix linear potentiometers were easy to install, however they were much larger in size compared to other any sensors tested. StructureMetrix linear potentiometers were qualified both dynamically and statically to compare their response to the Kaman sensors, which are discussed in Chapter 6.

Manufacturer	StructureMetrix		Kaman
Model	SMG035A		SMU-9000-2U
Type of Sensor	Linear Potentiometer		Eddy Current
Input, (Volts DC)	7.2 max, 5.5 min		30 max, 7.5 min
Input, (Current mA)	200 max		15mA
Output, full Scale (DC)	± 1.65		0 to 5
Scale factor (V/μm)	0.0003085		0.01
Gain Setting	1x (normal)	8x (sensitive)	N/A
Range (μm)	± 5220	± 653	± 500
Resolution (μm)	2.61	0.33	0.045

Table 5.1 Specification comparison for the StructureMetrix linear potentiometer to the Kaman eddy current sensor.

Noise Levels and Electromagnetic Interference (EMI)

Electromagnetic Interference (EMI) can be produced by all types of electronics and equipment and can mask the signal from a sensor measuring crack displacement in an Autonomous Crack Monitoring (ACM) system. EMI induces voltage fluctuations, which are superimposed over the sensor output. ACM systems employ highly sensitive sensors that produce a voltage change proportional to changes in displacement. These small crack movements resulted in small voltage changes which can be masked by normal EMI. Any introduction of EMI during these measurements may result in significant voltage spikes. EMI on the crack displacement channel during a transient event can obscure the crack time history by noise. EMI is emitted from most electronic devices and therefore measuring equipment should be designed to operate in environments with moderate levels of noise. Most EMI encountered during testing occurred at the 60 Hz frequency, common for AC power in residential and commercial buildings.

System Y was initially qualified in the test house with the experimental Northwestern University (NU) system operating at the same time. With the NU system operating, system Y recorded an average noise level of 5.3 μm peak to peak. It was found that during testing the high noise levels were directly related to EMI production by the NU system. For this reason, testing was completed on system Y with and without the concurrent operation of the NU system. Table 5.2 shows the noise levels of the system with and without the operation of the NU system. System Y was found to operate at a noise level of 1.3 μm peak to peak in a standard residential environment. The most significant reduction of the noise levels of system Y was attained when the NU System was deactivated. While the cause of noise in this testing environment was easy to pinpoint and eliminate, in some field environments this

may not be possible. Figure 5.5 demonstrates the noise levels before and after the NU equipment was disabled.

System Y Historical Noise Levels			
Date	Noise Level (μm)	Gain	Notes
5/4/2005	5.3	1	Blast Triggered Event NU System running.
6/4/2005	1.3	8	Blast Triggered, NU System Off.

Table 5.2 Historic noise levels for system Y during testing.

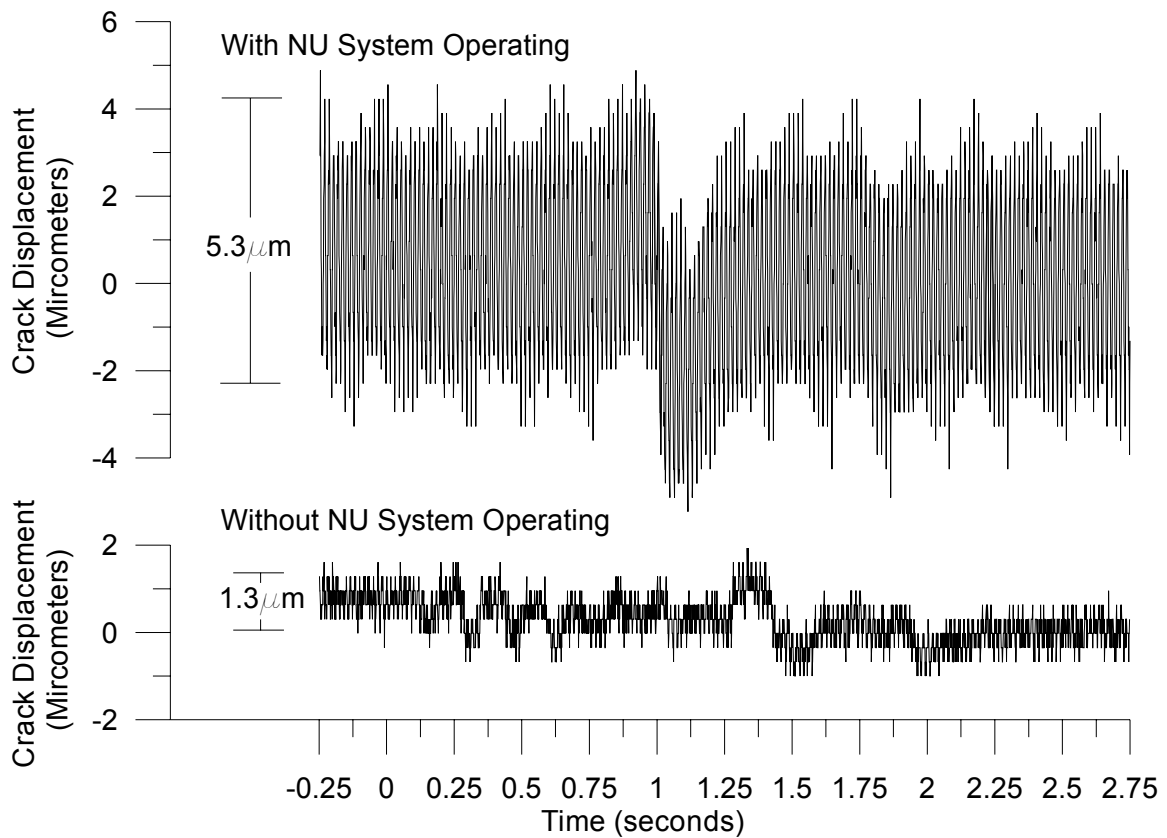


Figure 5.5 Typical system Y noise level visible in the crack velocity-time history with and without NU system in operation.

Computer Interface and Software

In this section, the computer interface and software supplied with system Y are evaluated to determine the adequacy and ease of use. Once the long-term and dynamic data have been collected by an ACM system, it must be displayed properly to allow for review and comparison. The primary function of the computer interface and software for the equipment was to allow the operator to organize, sort, store, remove and process the data. A well designed ACM system should include quality software, which aids in automating typical data processing tasks and reduces the amount of time spent working with data by the operator. One advantage of system Y was that ground velocity and crack displacement time histories for a blast were stored in a single file. Poorly designed or insufficient software would cause the operator of a system to spend extra time and expense processing the data.

System Y Programming & Connection

System Y can be programmed both on-site and remotely. This system uses a serial port to connect for sending and receiving data from the unit. On-site, the unit could be programmed with the external keys and LCD screen or with a computer connected to the serial port. With the key pad and LCD screen, menus can be cycled through and changes made to the system such as switching monitoring modes and trigger levels. In Figure 5.6 the external keys on the crack monitor are shown. The system could also be programmed on-site with a computer connected to the serial port. During evaluation the majority of the on-site programming was done using the software and a laptop computer.

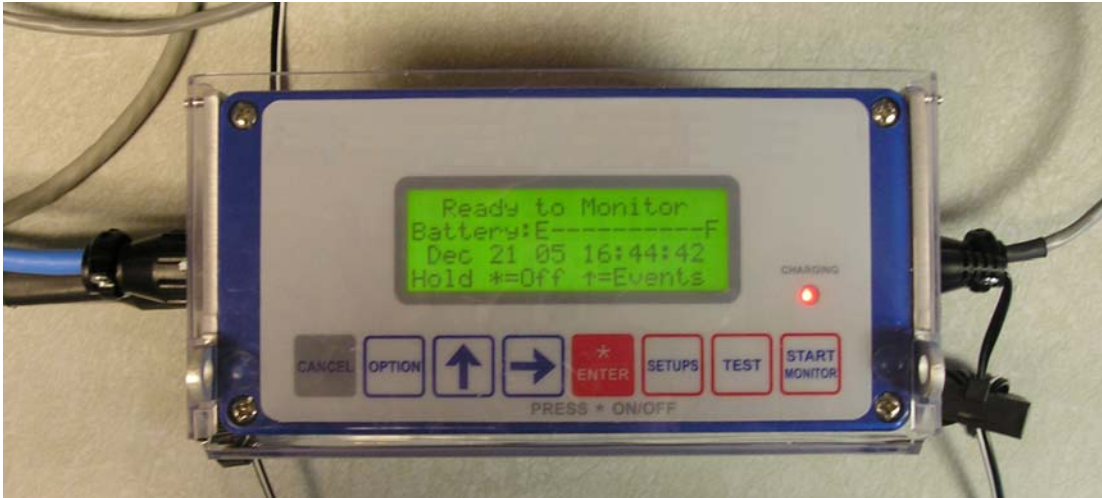


Figure 5.6 External key pad for on-site programming of the system Y crack monitor.

Remote communication with system Y can be accomplished over the internet or by modem. During evaluation, modem communication was only lab tested, and is therefore not discussed. This method was not implemented in the field since it was considered standard practice for system Y. During the field evaluation, data were retrieved from the unit over the internet. The serial cable from the unit was connected to an Nport(Moxa), to allow access over the internet. The Nport creates a virtual serial port for the unit over the internet. Once connected to the unit over the internet, the software can be used as it would have been on site. The only drawback to off-site programming was very slow data transfer rates. However, in almost all situations slow remote data transfers were preferred to site visits.

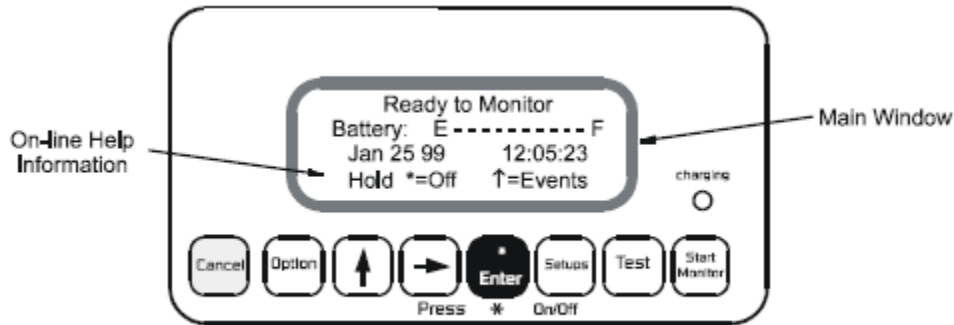
System Y is capable of recording up to eight waveforms during a dynamic event. This greater flexibility allows for the addition of other sensors to the unit for monitoring. As an ACM system, system Y was capable of monitoring two cracks with a single unit. However, due to the limited number of available sensors, this feature was not used during evaluation. The only side effect of monitoring multiple channels was that the more channels recorded during a dynamic event, the less number of events that can be recorded during a

monitoring period. Once the maximum number of events had been reached, the unit needed to be reset before it could continue monitoring for dynamic events. Table 5.3 describes the relationship between the number of channels recorded and the number of events the unit could record per monitoring period. During evaluation, only five channels were used to maximize the number of dynamic events recorded during a day. This was done since the unit is only capable of being automatically reset once per day. A typical crack monitoring project would use six channels recording ground motion, air overpressure, crack and null movement. During evaluation the equipment setup did not include an air overpressure transducer.

Number of Channels	Maximum Events Recorded	Notes/Typical Setup
3	16	3 Channel Geophone
4	12	Geophone/Air Overpressure
5	9	Geophone/Air Overpressure/Crack
6	8	Geophone/Air Overpressure/Crack/Null
7	6	
8	6	
* All calculations are based on a 3 second recording		

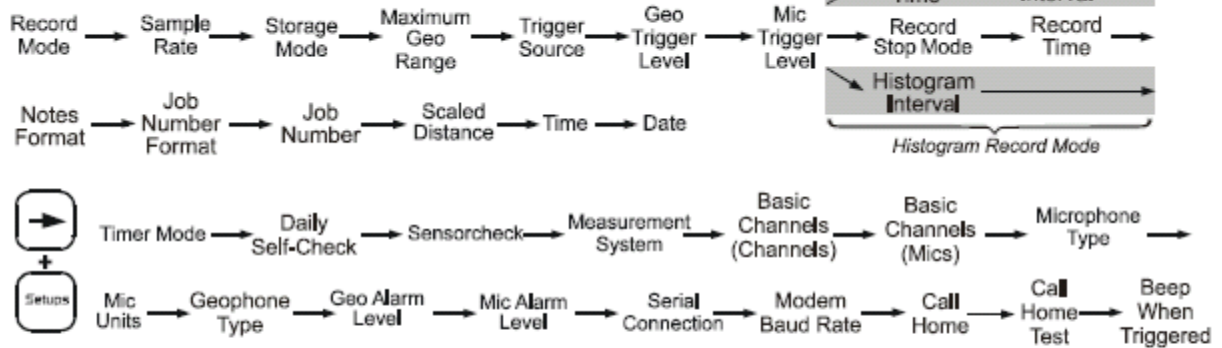
Table 5.3 System Y relationship between the number of channels recorded and the number of events the unit can record per monitoring period.

The software can also be used to start, stop and retrieve data from system Y. The software also allows an operator to collect data from the unit remotely and limit costly site visits. During field testing, data were manually downloaded remotely on a weekly basis and only when blast events were least likely to occur. The layout and display of the command settings allowed easy access to the different settings while using the key pad on site. Figure 5.7 shows the layout of the command windows an operator would see during programming.

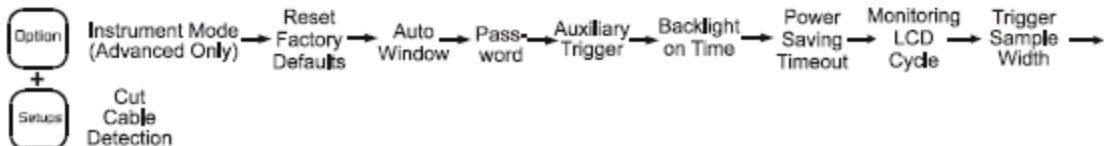


- Enter** (with a dot)
 - turns monitor on or off.
 - chooses menu options and saves choices.
 - enter password to exit monitor mode.
- Start Monitor**
 - enters monitor mode.

- Setup**
 - displays menus to setup the monitor for event recording including:



- Up Arrow**
 - moves you through event menu choices. Provides the following functions from the Main Window:



- Test**
 - performs Sensorcheck.
- Option + Test**
 - Review Setups.
- Option + Up Arrow**
 - down arrow function.
- Left Arrow**
 - moves through menu choices and moves the cursor.
- Cancel**
 - returns to previous menu.
- Option + Enter (with a dot)**
 - On-Line Help.
- Option + Left Arrow**
 - left arrow function.
- Option + Cancel**
 - turn backlight on or off.

Figure 5.7 System Y command layout when programming with the keypad. (Company Y Operator Manual)

Data Analysis Software

Once the monitoring had been completed or during regular intervals, the data collected by system Y was removed and processed. To analyze the data collected during monitoring, system Y used the manufacturer supplied software. Figure 5.8 is a typical screenshot from the software main menu that allows review of the files. The files can then be managed and sorted from this screen.

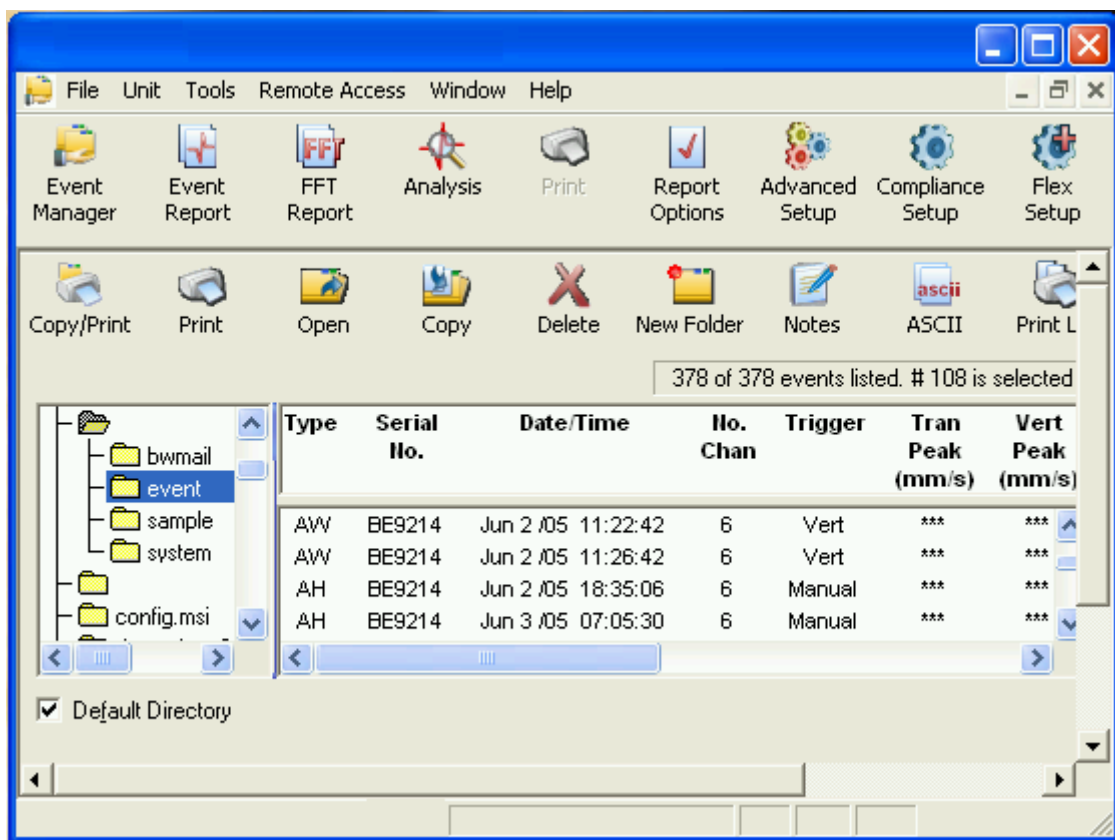


Figure 5.8 System Y, Event Management software interface

The software can also be used for analyzing and processing the data collected on system Y. The original intended use of the software was for processing and viewing ground motion time histories. This software package enables the user to view and print the time histories of ground and crack motion captured by the crack monitor. The software is also

capable of creating event reports, which describes the key points of an event and frequency content analysis. Figure 5.9 shows a typical screenshot from the software when creating a crack time history. One significant advantage of the software is that ground motion and crack displacement time histories are included in one file. When reviewing a crack and ground motion time history, any areas of interest can be isolated and enlarged on for further review. An ACM specific software application or further adaptation of the software is not available.

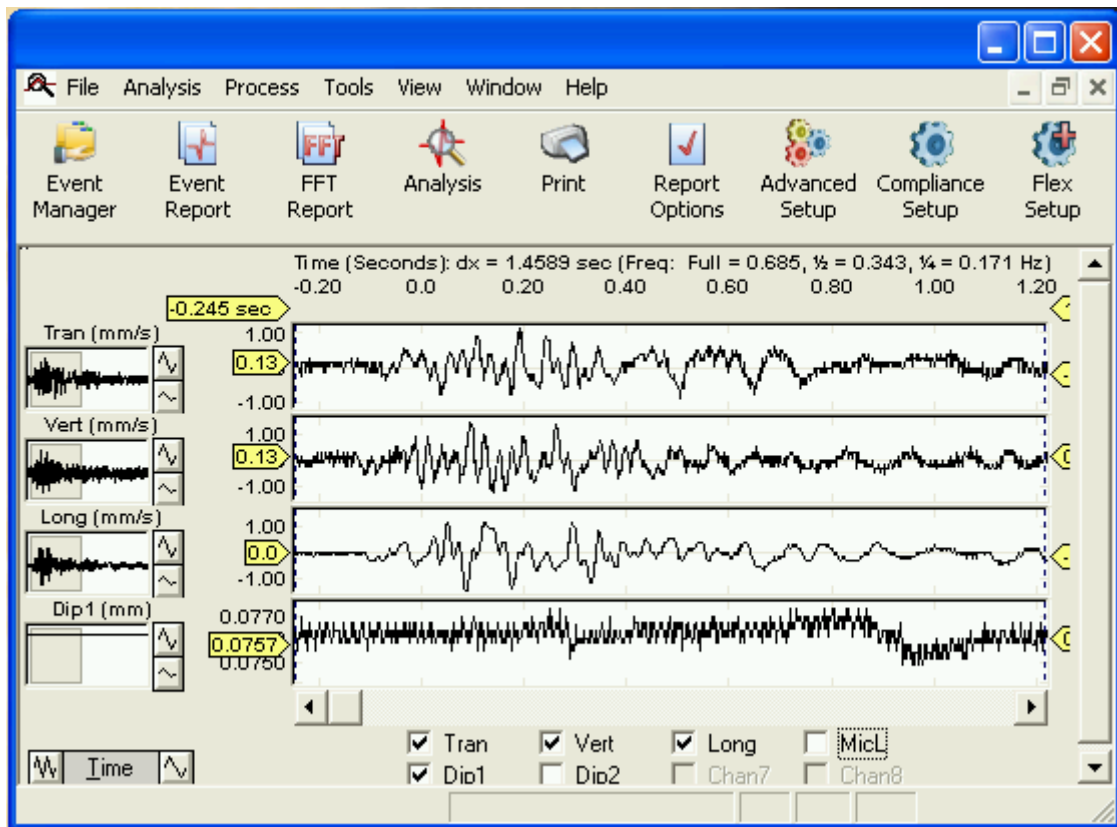


Figure 5.9 Software screenshot of a ground motion and a crack time history

Literature and Manuals

The literature and manuals supplied with an ACM system should include thorough documentation to allow a new user to install and operate the system independently. Without

the proper manuals, setup and operation of an ACM system would be very difficult and confusing. System Y was supplied with multiple documents to aid in the installation. The primary documents included an operator's manual for the software and System Y seismographs. Additionally, system Y was supplied with a quick start card, located on the side of the case of the crack monitor, for on-site programming.

Review of the manual entitled "Operator Manual" was required to learn more about the software package prior to its use. The manual describes the process to remove files from the crack monitor. Once removed from the unit they can be processed and viewed with the software. The first section of the manual describes a basic tutorial of how to use the software. The second section of the manual describes the layout and keys used in the software package and how to handle files.

The manual entitled "System Y Operator Manual" was used to learn about the operation and programming. This manual describes the methods for properly installing a seismograph and step by step programming prior to monitoring. The system can be programmed in three modes; compliance, advanced and flex. For crack monitoring, flex programming was used. From the flex setup window the sensor specific information could be entered and sent to the unit. Key-pad programming was reviewed earlier in Chapter 5 in the section on computer interface and programming. The manual also reviews typical system capacities, operation durations and limitations and capacities. The quick start card located on the side of system Y shows the condensed instructions for operating system Y. The quick start card is useful for on-site programming when the manuals are not available.

Chapter 6

Laboratory Qualification of Crack Monitoring System Y

The laboratory qualification evaluation completed on Autonomous Crack Monitoring (ACM) system Y is presented in this chapter. It was important to first operate System Y in the laboratory to ensure proper operation prior to field deployment. This step was undertaken to verify the system's ability to collect valid data under field conditions. Laboratory operation was undertaken to verify that the displacement of the crack monitoring system operated within the acceptable standards established with the benchmark LVDT and Kaman sensors used by the Northwestern University (NU) system. Performance of the system Y sensors was evaluated for both static and dynamic response. Laboratory testing of system Y, was also evaluated to ensure that the system was easy to use by the average field technician.

Long Term or Static Response

Long term or static evaluation was completed on system Y to verify the proper operation of the sensors when used in a field environment. Prior to the evaluation of system Y as a complete crack monitoring system, the sensors were tested statically.

Qualification of a sensor to measure micrometer crack opening and closing due to long term environmental influences should be completed in a similar manner in which the sensor is expected to perform in the field. This requires the sensors and system to be tested

together so that the complete system can be evaluated. To determine if the sensor will respond linearly during cyclic use, the sensors were plate tested under cyclically changing temperature loading. The sensors were attached to a plate with known material properties and then exposed to varying temperatures to allow the plate and sensors to expand and contract. The expansion and contraction of the plate allowed the sensor to record cyclic changes in displacement. During testing the sensors were attached to a plastic plate made of Ultra-High Molecular Weight Polyethylene (UHMW-P). This material provides a large thermal response that approximates a cracked wall response. The coefficient of thermal expansion (CTE), α , for UHMW-P is $\alpha=198.0 \mu\text{m}/\text{m}/^\circ\text{C}$. The sensor body is expected to expand slightly during testing. However, the CTE for the sensors made of steel is $\alpha=13.0 \mu\text{m}/\text{m}/^\circ\text{C}$ and was approximately 15 times smaller than the CTE for UHMW-P plastic. Therefore the effects from the expansion and contraction of the actual sensor components are an order of magnitude lower and were ignored.

Long Term Testing Equipment Setup

The sensors can be evaluated over long time periods (level I operation) to determine the size of the hysteresis loops. The larger the hysteresis loops, the less responsive the sensor is to small changes in displacements. To test the sensors in a level I operation, the linear potentiometer was mounted on a flat piece of UHMW-P, approximately 400 mm square. During the mounting process, the smooth surface of the UHMW-P plate needed to be roughened with sandpaper to allow a sufficient bond between the epoxy and the UHMW-P plate. While testing system Y, the sensors were placed outdoors in a protected enclosure to take advantage of the natural temperature swings. These temperatures changes are similar to what would be found during actual field operation. To prevent any possibility of water

damage and direct contact with the sun, all equipment was placed in a weather resistant enclosure. Had the sun been allowed to shine on the plate directly, the sensor displacement would have also been a function of the cloud cover. Figure 6.1 shows the equipment setup used during the static testing.

System Y as supplied does not have the ability to measure temperature and humidity changes along with crack displacement. Temperature and humidity were monitored with a SUPCO data logger. The SUPCO temperature and humidity data logger was set to record the temperature once per minute. The humidity readings recorded during testing were ignored because UHMW-P does not respond to changes in humidity like more susceptible construction materials such as wood or drywall.

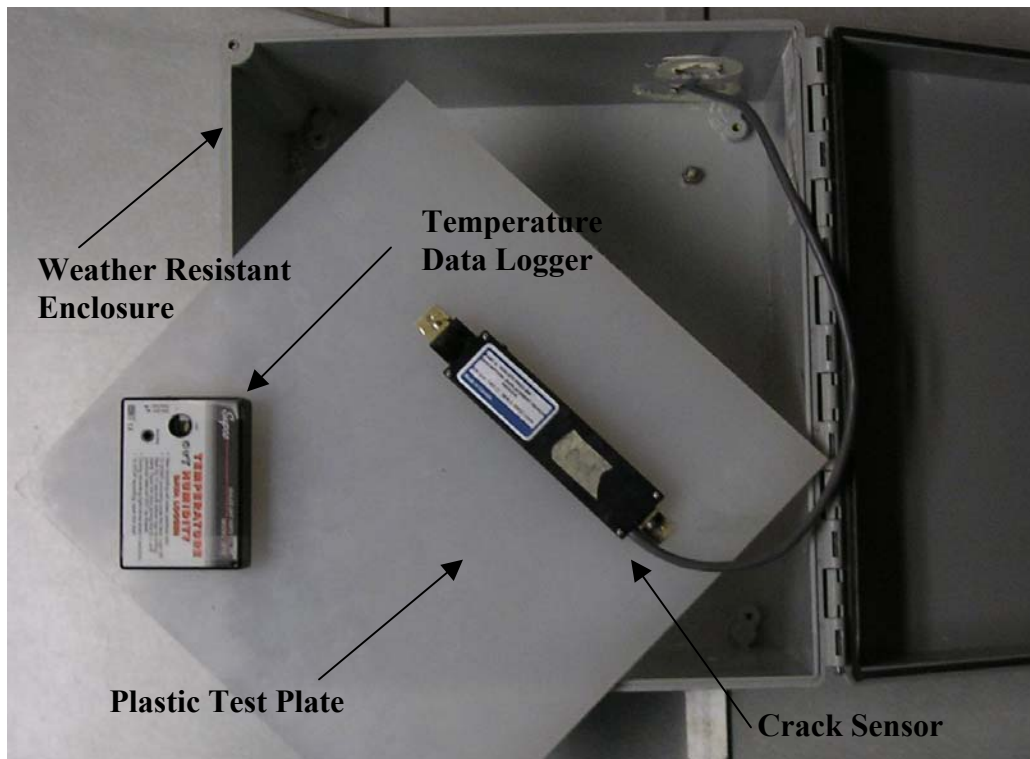


Figure 6.1 Static testing equipment layout for system Y

A simple procedure was followed to measure the long term, level I response of the system Y linear potentiometer. First, the system was assembled as described previously in Chapter 5. The internal clocks in both system Y and the SUPCO temperature data logger were synched to the local computer clock. The sampling rate for system Y and the SUPCO temperature data logger were set to record the sensor displacement and temperature at least once per minute. Once both the systems were programmed, they were activated to start the data collection process. The weather resistant enclosure was then sealed and the entire unit was allowed to operate in the outdoor temperatures for approximately three days. During this period of evaluation, the UHMW-P plate with the attached sensor endured daily temperature swings from 18°C to 32°C.

Long Term Response Results

At the completion of the testing period, the recorded data were removed from the individual systems to be processed and merged into one time history. Prior to merging the collected data, individual time histories can be plotted for the displacement sensor and temperature with respect to time, as shown in Figure 6.2. During the static testing, as expected, the highest temperatures occurred during the early afternoon and the lowest during the early morning. From the time histories shown in Figure 6.2 it is visible that the peak temperatures recorded correspond to peak in sensor displacement. It was expected that during the peak temperatures recorded, the UHMW-P plate would expand and cause a larger displacements of the linear potentiometer.

The linear potentiometer was found to record larger changes in displacement because of the span of the gauge at 140 mm was rather large. This relatively large span is at least ten

times larger than any other ACM sensor tested. The smaller the span of the gauge the less material effects are included in monitoring.

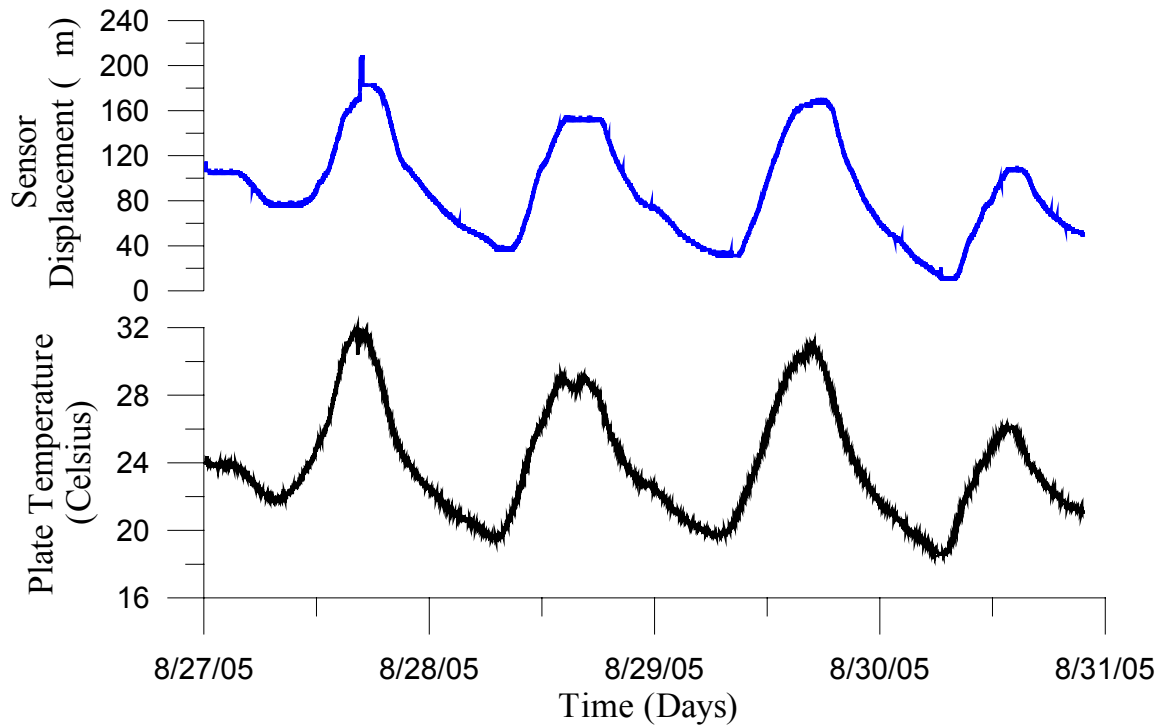


Figure 6.2 Correlation showing the comparison of the temperature and displacement recorded during static testing.

To determine the effect of temperature on the cyclic expansion and contraction of the system Y sensors, displacement was compared to temperature in Figure 6.3. While hysteresis loops are visible they do not drift, but oscillate about a common mean response. This cyclic response is compared to the theoretical expansion of the plate shown as the solid inclined line. The theoretical displacement was calculated by multiplying the coefficient of thermal expansion or (CTE) by the temperature change and initial gap measurement between the brackets of the linear potentiometer. The slope of the calculated displacement was found to be approximately two times larger than the measured value. The sensor was able to

consistently record displacements with approximately half the magnitude compared to the control sensor. The hysteresis loops created by the sensors during testing were slightly larger than those of previously tested sensors such as the LVDT and Kaman sensor (Balliot 2004).

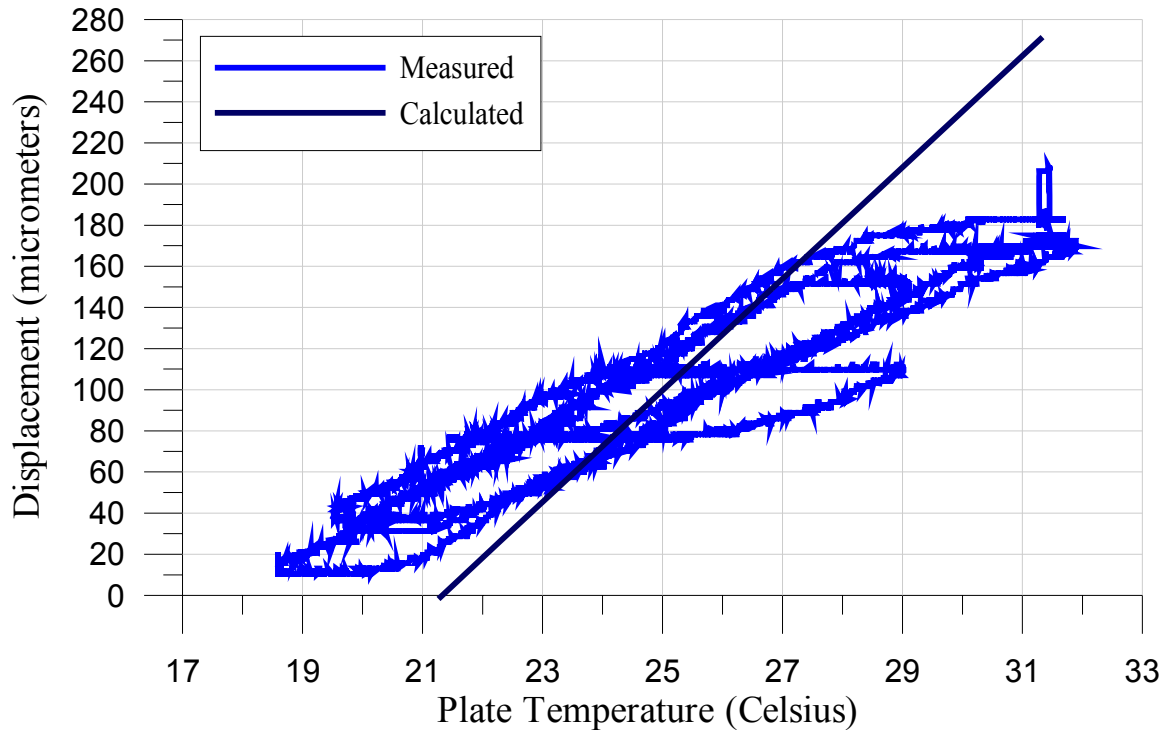


Figure 6.3 Measured and calculated displacement vs. temperature for system Y.

Short Term or Dynamic Testing

Dynamic qualification was undertaken to verify the system's ability to capture dynamic activity in the laboratory prior to its placement in a field environment. Previous work in dynamic testing by (Ozer 2005) had been completed on string potentiometers and served as a basis for development of an apparatus to validate the dynamic response of system Y.

During a dynamic event, the displacement sensor is responsible for capturing a transient waveform. Because this event will only occur once during the monitoring period it

is important for an ACM system to sample the waveform at a high sampling rate. The structural response frequency of most buildings measured in the field is normally in the range of 10 to 15 Hz. This frequency range required the ACM system to sample at 1000 Hz to define the dynamic response of the crack. The standard sampling rate for control system was 1000 Hz and for system Y was 1024 Hz. During dynamic testing, the testing apparatus was vibrated at frequencies up to 100 Hz so that 10 samples were obtained per excitation cycle. In addition to the ability to capture events with large frequencies, ACM systems must be able to capture events with small amplitudes. Field testing has shown that interior cracks in residential structures can respond with displacements between 2 and 5 μm zero to peak during a dynamic event.

Ozer (2005) verified the string potentiometer as an ACM displacement sensor by measuring the response of two aluminum blocks stacked upon each other and vibrated by a drop weight. The blocks were separated by a thin rubber sheet which modeled an interior crack. The control Kaman sensor was then mounted on one side of the blocks and the sensor to be tested on the other. A small weight could then be dropped at varying heights on the upper block. Varying the height of the drop varied the amplitude of the movement between the upper and lower block.

Dynamic Testing Equipment Setup

As shown in Figure 6.4 the system was modified in order to accommodate larger system Y sensors and increase the control of the variability of the system's frequency and amplitude. Larger aluminum blocks than Ozer's were employed to accommodate the larger sensors. A small electric motor with an eccentric weight was employed to control the excitation frequency. Changing the arm and mass of the eccentric weight allowed the

amplitude of the excitation to be controlled. During dynamic qualification, a copper wheel weighing 5.1 grams served as an eccentric weight. When the eccentric weight oscillates, it functions as a vibrator and creates a net upward and downward force. This changing force caused the upper block to move relative to the lower block and simulated crack movement.

Dynamic response of system Y was compared to the NU system Kaman eddy current displacement sensor and the Edaq mobile field computer and data logger. The Kaman eddy current sensor has been used for experimental crack monitoring projects for years with which there is a great deal of experience.

Considerations taken during dynamic testing included; limiting electromagnetic noise, preventing movement of the lower block and ensuring the proper adjustment of the sensors/upper block combination before each test. Any excess equipment in the laboratory that may induce electromagnetic noise during testing was turned off or moved away from the devices. To further limit electromagnetic noise, it was found that all cable runs for system Y needed to be wrapped in aluminum foil in the laboratory to reduce the noise levels within expectable ranges. To limit the movement of the lower block during dynamic excitation, it was attached to the edge of the more massive table to limit its movement.

Dynamic testing of system Y was accomplished by following a simplified procedure. First, the aluminum blocks were assembled with a small foam spacer between them. Guide plates were then installed on the lower block to limit horizontal translation of the upper block. A front and right view of the modified testing apparatus can be seen in Figure 6.4.

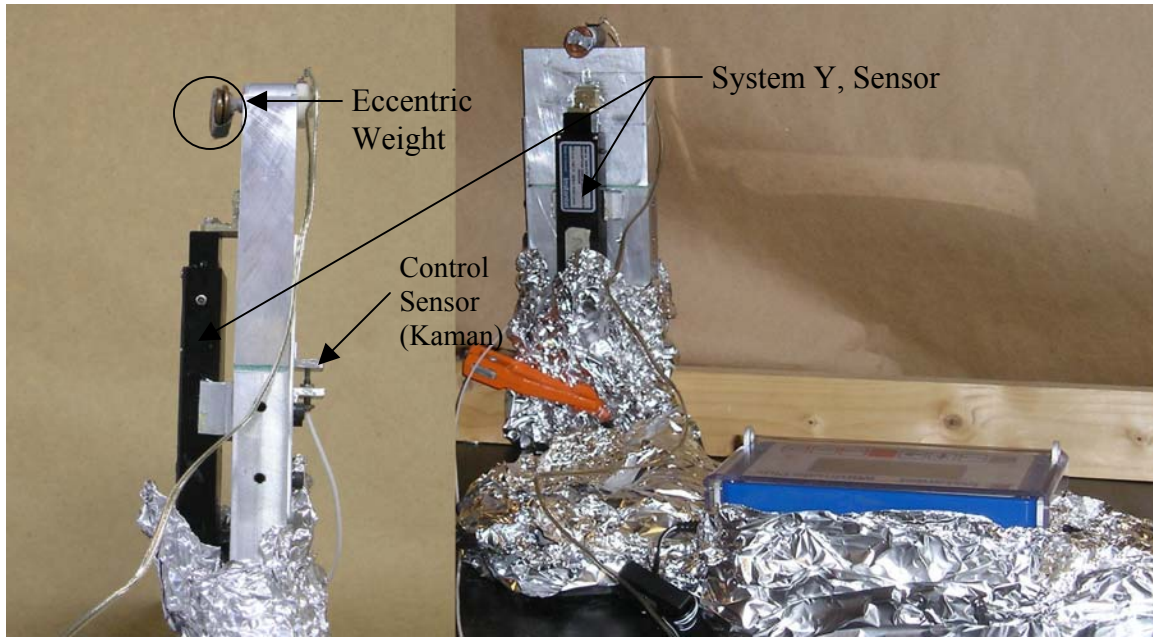


Figure 6.4 Modified dynamic testing apparatus for System Y testing.

The system Y sensor and the control Kaman sensor were attached to opposite sides of the aluminum block assembly. Both systems were set to record dynamic data for up to 15 seconds. The electric motor was activated by a 1.5 volt source to vibrate the upper block with respect to the lower block and the corresponding dynamic crack movement was then recorded by each system. Dynamic excitation was initiated with the eccentric weight spaced farthest away from the motor shaft. Subsequently excitation was reduced by placing the eccentric weight closer to the motor shaft.

During testing, differences in the dynamic response of the control sensor and test sensor were observed. Differences in the sensor responses such as non-uniform displacements and phase shifts could be attributed to limitations in the testing equipment. These limitations included equipment alignment, connection and size effects. Uniform displacement of the upper block with respect to the lower block was anticipated. However, it appears that either lack of horizontal support or difficulty in the alignment of the eccentric

motor to the center of gravity of the upper block or both occurred. This caused a small rocking motion of the upper block and non-uniform displacements at the face of the upper block as shown in Figure 6.5. Any slight deviations in the alignment affected the magnitudes of the displacements measured by the sensors as well as a phase shift between time histories of the sensors on opposite sides.

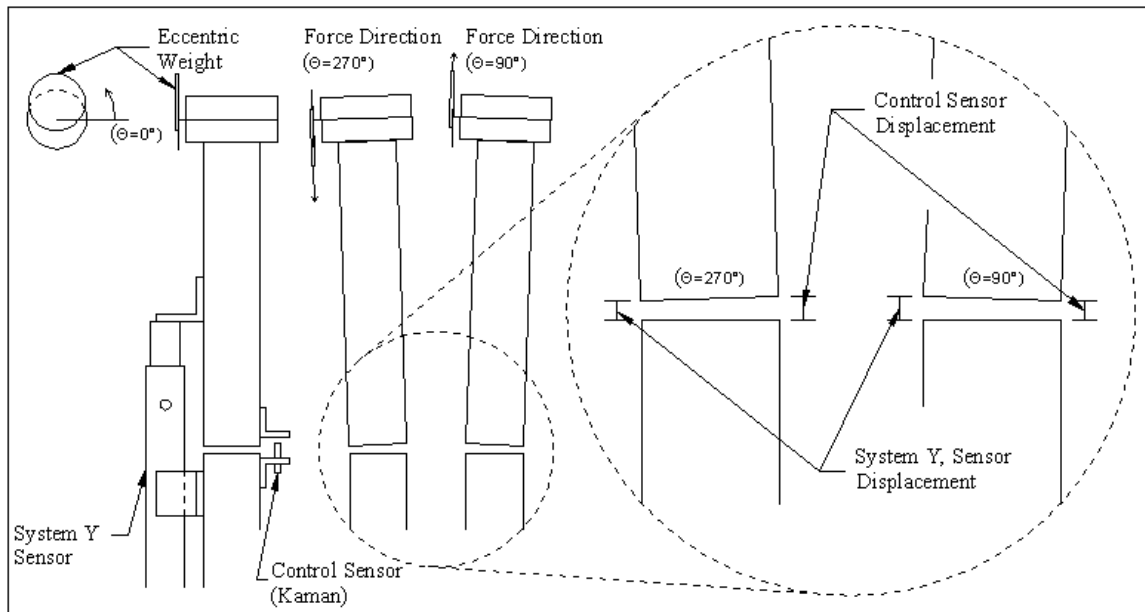


Figure 6.5 Description of how a phase shift was created in the waveforms, during dynamic testing.

In addition to equipment alignment, the size or the sensor and type of connection could affect the amplitude of the recorded waveform during the small force laboratory excitation. System Y sensor required a large force to displace which can dampen the response of the system. During dynamic evaluation it was found that the system Y sensors dampen out the smaller applied forces and only responded to the larger eccentric forces. The much smaller Kaman control sensor, on the other hand, does not require a connection

between the sensor tip and target. Without a direct connection between the tip and housing of the Kaman sensor there are no frictional losses during testing small amplitudes. However, because Kaman sensors are fragile and expensive they are not very field worthy. During dynamic testing, because of the slight rocking motion which occurred from the eccentric weight, the sensor body can bind creating frictional losses. Any binding that would occur during testing should reduce the amplitude of the waveform recorded by system Y.

These lab related damping effects of the system Y sensor during small excitations were not apparent in field testing discussed in Chapter 7. Had the lab evaluation been accomplished on set of much larger aluminum blocks, this dampening effect would not have been apparent since the inertia of the wall is orders of magnitude greater than that of the sensors. However, during field deployment of this system on a residential crack, the dampening effect of the system Y sensor should be considered when selecting an appropriate crack for monitoring.

Dynamic Evaluation Results – Amplitude Comparison

Dynamic response of the linear potentiometer from system Y, was compared to the control system in terms of both frequency and amplitude as shown by the time histories in Figure 6.6. The amplitude of the waveform recorded by system Y was always found to be larger than that recorded by the Kaman sensor. During low amplitude dynamic tests, the system Y sensor was found to absorb typical displacement created by low force excitation and only responded to the larger excitation forces. Table 6.1 summarizes the comparison of the maximum amplitudes collected during the dynamic tests completed on system Y. On average, the system Y linear potentiometer reported 2.8 times the maximum and 2.2 times

the minimum recorded value of the Kaman sensor when using the factory supplied conversion of voltage to displacement. From Figure 6.7 it can be seen that the ratio of the displacement of the linear potentiometer to the Kaman sensor was constant during testing. Since the ratio of the maximum crack displacement was found to be relatively constant throughout a wide range of excitation amplitudes, the sensor was considered to be operating properly and within tolerances. The large difference in crack movement recorded by system Y, compared to the control was attributed to the testing apparatus or the conversion constant of the sensor.

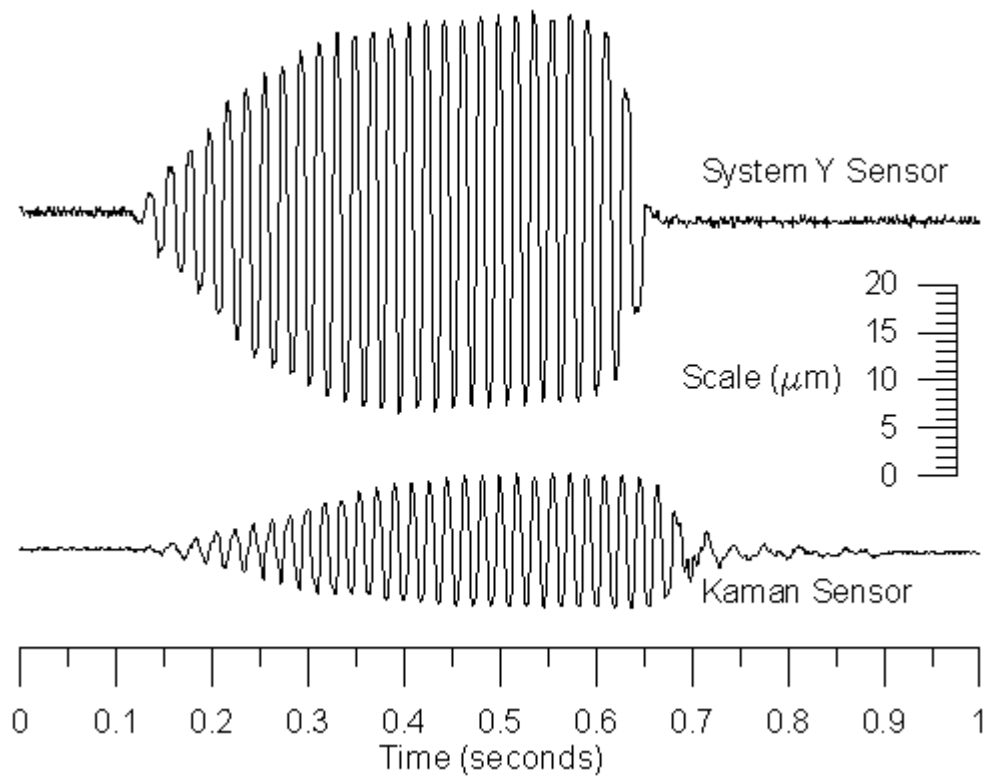


Figure 6.6 Typical waveform recording during the dynamic testing of system Y.

Test Number	Event Number	Kaman Min Amp. (μm)		System Y Min Amp. (μm)		Amp. Ratio System Y/Kaman	
		Min	Max	Min	Max	Min	Max
1	1	-3.80	3.69	-7.94	5.44	2.09	1.47
1	2	-4.01	3.76	-7.92	6.12	1.98	1.63
1	3	-3.91	3.42	-8.00	4.74	2.05	1.39
1	4	-3.92	3.90	-7.50	5.24	1.91	1.34
1	5	-4.36	3.98	-7.94	4.46	1.82	1.12
2	1	-4.62	4.26	-12.64	10.86	2.74	2.55
2	2	-4.34	3.85	-12.37	9.83	2.85	2.55
2	3	-4.52	4.22	-11.95	9.92	2.64	2.35
2	4	-4.25	4.22	-11.85	9.69	2.79	2.30
2	5	-4.09	4.11	-11.60	9.29	2.84	2.26
2	6	-4.08	4.02	-11.93	8.31	2.92	2.07
3	1	-4.85	8.77	-16.45	23.05	3.39	2.63
3	2	-5.79	8.16	-17.68	20.84	3.05	2.55
3	3	-5.88	8.14	-20.67	21.44	3.52	2.63
3	4	-6.69	7.65	-21.32	20.13	3.19	2.63
3	5	-6.30	8.15	-21.65	19.15	3.44	2.35
3	6	-5.26	6.57	-19.65	18.87	3.74	2.87
3	7	-4.84	5.48	-18.65	15.3	3.85	2.79
Standard Deviation All Data						0.64	0.55
Average Ratio During an Event						2.82	2.19

Table 6.1 Summary of the dynamic tests completed for system Y.

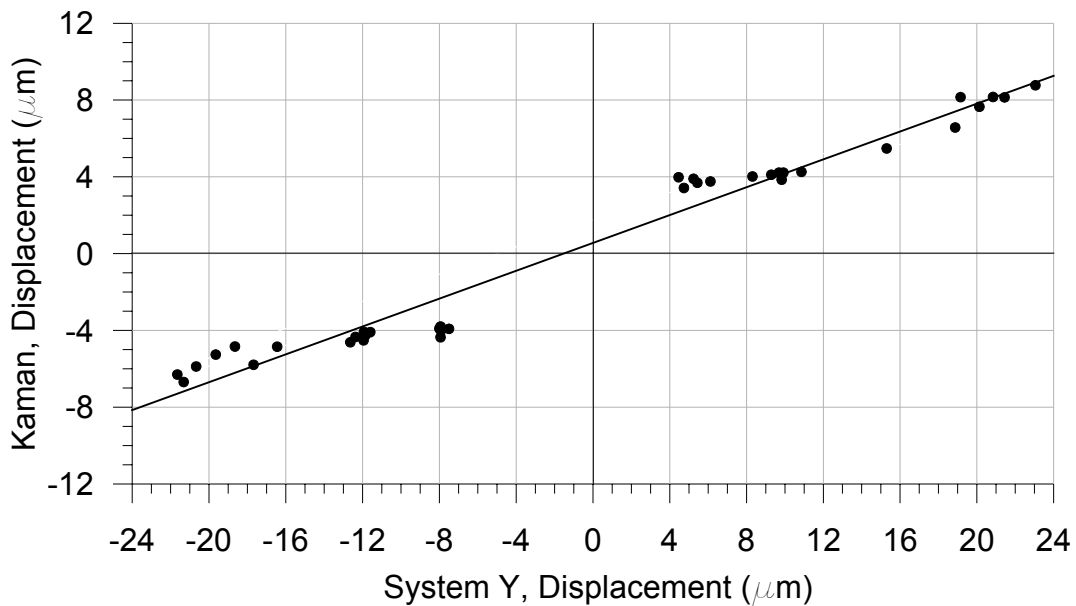


Figure 6.7 Maximum and minimum displacements of the Kaman and system Y sensors during dynamic testing.

Dynamic Testing Results – Frequency Comparison

The measured response frequency of the system Y sensor was compared to the standard Kaman sensor. During testing, the apparatus was operated at a frequency of approximately 100 Hz, this is well above the 10 – 50 Hz range necessary for field operation. Equipment that can capture waveforms accurately at a high frequency can readily capture waveforms at lower frequencies. However, briefly during the start-up of the eccentric weight rotation, the excitation frequencies were lower than during constant operation as shown in Figure 6.8. During both start-up and at constant angular velocity, the measured response frequency of system Y was comparable to that of the control system.

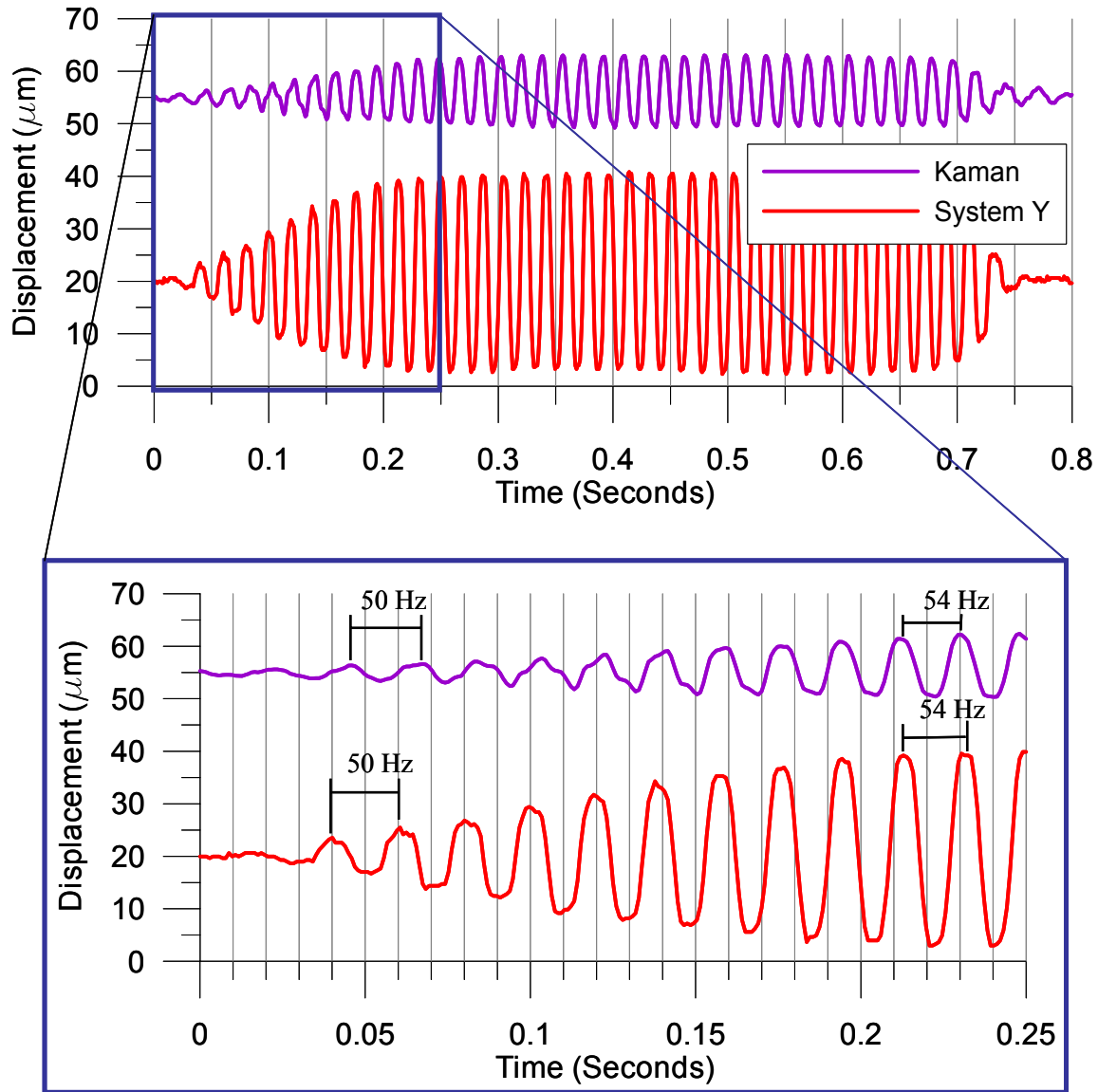


Figure 6.8 Frequency comparison of system Y to the control system.

Dynamic Testing Results – Offsets

Baseline shifts or temporary offsets of a crack can occur during a dynamic event. An important feature for crack monitoring devices is being able to capture these events. Use of the data collected can be used as evidence of the magnitude and causes of a crack opening or closing during excitation. Figure 6.9 shows a typical waveform time history when a baseline

shift or offset has occurred. This waveform shows that system Y was able to capture crack offsets during dynamic testing when recorded by the control system.

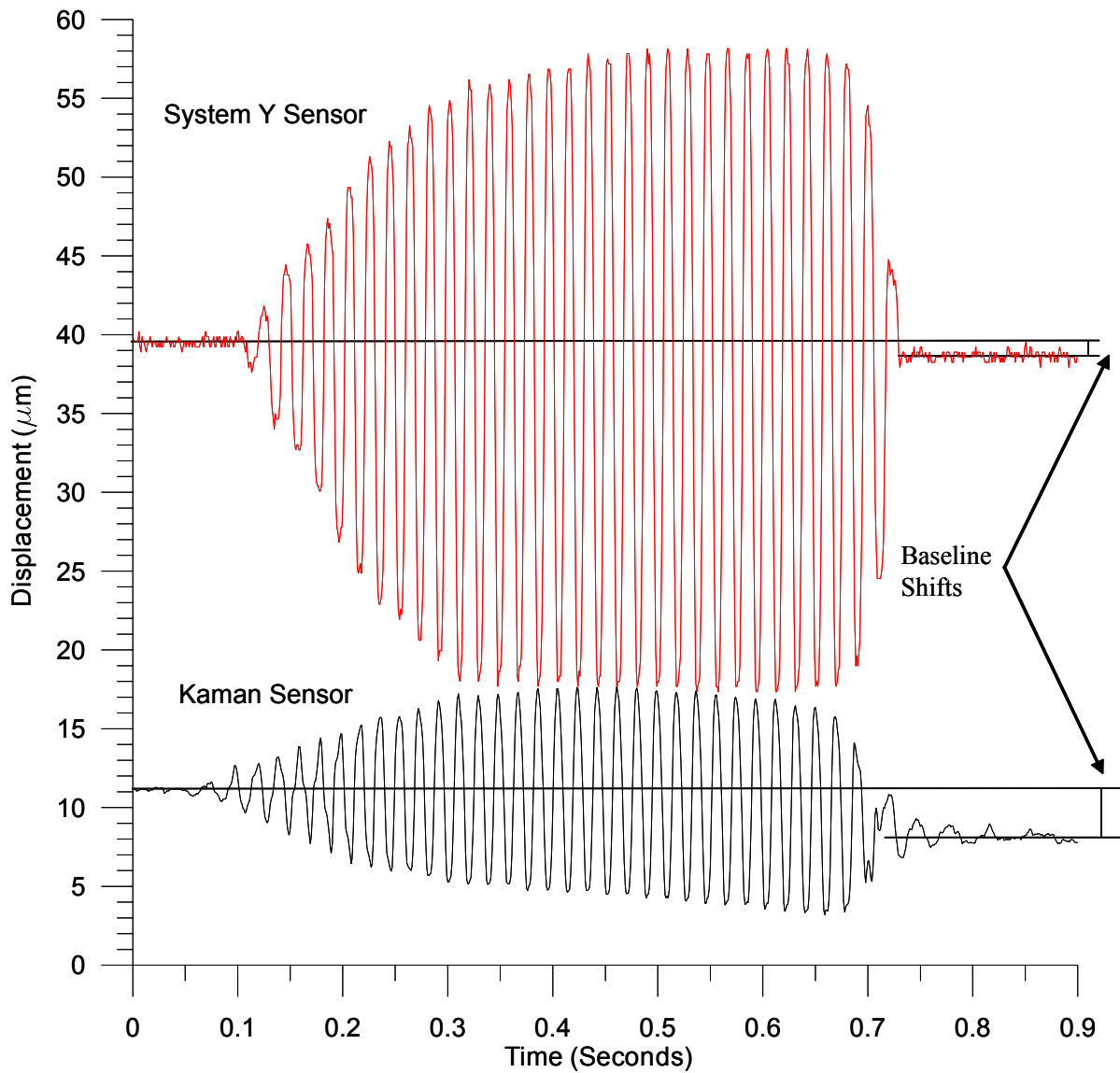


Figure 6.9 Typical waveform time history of the control system and system Y during a baseline shift.

Chapter 7

Field Testing of Crack Monitoring System Y

The field testing of Autonomous Crack Monitoring (ACM) system Y in a blasting environment is described in this chapter. Two modes of monitoring operations were evaluated for this system. These operation modes or types of trigger operation included both level I and II operation. Level I operation requires recording crack displacement at a regular interval. Level II operation requires the recording of dynamic crack response at unknown times when a preset intensity of ground motion is exceeded. A field installation across a crack in a house located near an active limestone quarry was selected to test the performance of this system in both of these modes. Additionally, all procedures were reviewed to ensure that the system was easy to use by the average field technician.

Field Trial Blast Vibrations

Performance of system Y was evaluated at both levels I & II in the field by installing the equipment in the Milwaukee test house. The active limestone quarry adjacent to the test house blasted more or less weekly during the monitoring period, which provided a realistic environment. As a level I system, the unit recorded only the long term crack response, which could be compared to long term changes in temperature and humidity as well as the long term response of various Northwestern University (NU) benchmark systems. As a level II

system, the unit not only recorded the long term crack response, but also the dynamic crack response to blast induced ground motion and air over pressure.

Level I Operation

During level I operation, the system records peak micrometer changes in crack width at preset time intervals. System Y offers a choice of six different time intervals. These range from every two seconds up to every 15 minutes. Selecting a sampling rate smaller than every minute would not be recommended for remote operation of an ACM system when the data stored on the unit is not downloaded regularly. For most ACM applications sampling every 15 minutes is sufficient for capturing long term trends. Long term patterns of crack response can be compared to environmental effects to determine if dynamic excitation due to blasting, mining or construction activities have caused permanent changes to the crack displacement. However, level I operation alone does not include the needed measurement of the dynamic response of the crack during a blast event.

Level I Equipment Setup

System Y's performance was evaluated by comparison with the NU system which concurrently monitors the same crack. The temperature and humidity data were collected with the NU system. System Y was setup to record level I responses as described previously in Chapter 5. During setup, the histogram function on the unit was set to record the peak displacement of the crack and null sensor every 15 minutes.

Level I Data Collection

Level I data were collected from February to July of 2005. While collecting level I data the unit's functionality was evaluated during the extreme changes in temperature and humidity observable during both heating and cooling seasons common for Milwaukee, WI. Temperature and humidity during the winter months were relatively low and in the spring and summer they were higher with varying levels of humidity, which varied with the passage of various weather fronts encountered. Varying levels of indoor humidity were expected during the spring when most people open the windows in their homes. In all cases the indoor temperature fluctuated within a few degrees of 21°C.

During most of the monitoring period, the inside temperature and humidity were maintained within a cyclically narrow range, which is normal for most homes heated with a gas furnace and cooled with a central air conditioner. The temperature and humidity data and the long-term crack data collected by system Y and the NU LVDT are compared in Figure 7.1. This figure shows similar trends in the crack displacements recorded by the NU LVDT and system Y linear potentiometer.

The thermal expansion experienced by the drywall ceiling was found to be heavily influenced by changes in indoor temperature as seen in the comparison of trends in crack displacement and temperature in Figure 7.1. Trends in Figure 7.1 also validate sufficient operation of system Y by comparing the peak displacements of the NU LVDT and system Y linear potentiometer. To remove noise spikes in the data, the time histories are averaged over a 24 hour period. Peaks and valleys in the time histories of the two sensors occur at approximately the same times. Maximum peaks in displacement occur at the same time as minimum indoor temperatures. When comparing the 15 minute data shown in grey in Figure

7.1, it is shown that the magnitude of the system Y peaks and valleys were larger than those of the NU LVDT by a factor of two. The ratio of the peaks in the 24 hour averaged data tends to be similar in magnitude for both sensors, with system Y being only slightly higher.

During operation an ACM system must be to maintain a constant ratio of long term to dynamic movement. A constant ratio is needed in order to directly compare dynamic crack excitation to long term crack movement to determine the significance of dynamic events. During level I or long term data collection the ratio of the NU LVDT to the system Y sensor was found. The peak data points collected, denoted with red dots, in Figure 7.1 are presented in Table 7.1 and graphically in Figure 7.2. The NU LVDT has been used previously in ACM applications and has been tested for compliance and is therefore used as baseline for comparison. The ratio of measure displacement of the NU LVDT to system Y was found to be 0.52 during long term operation.

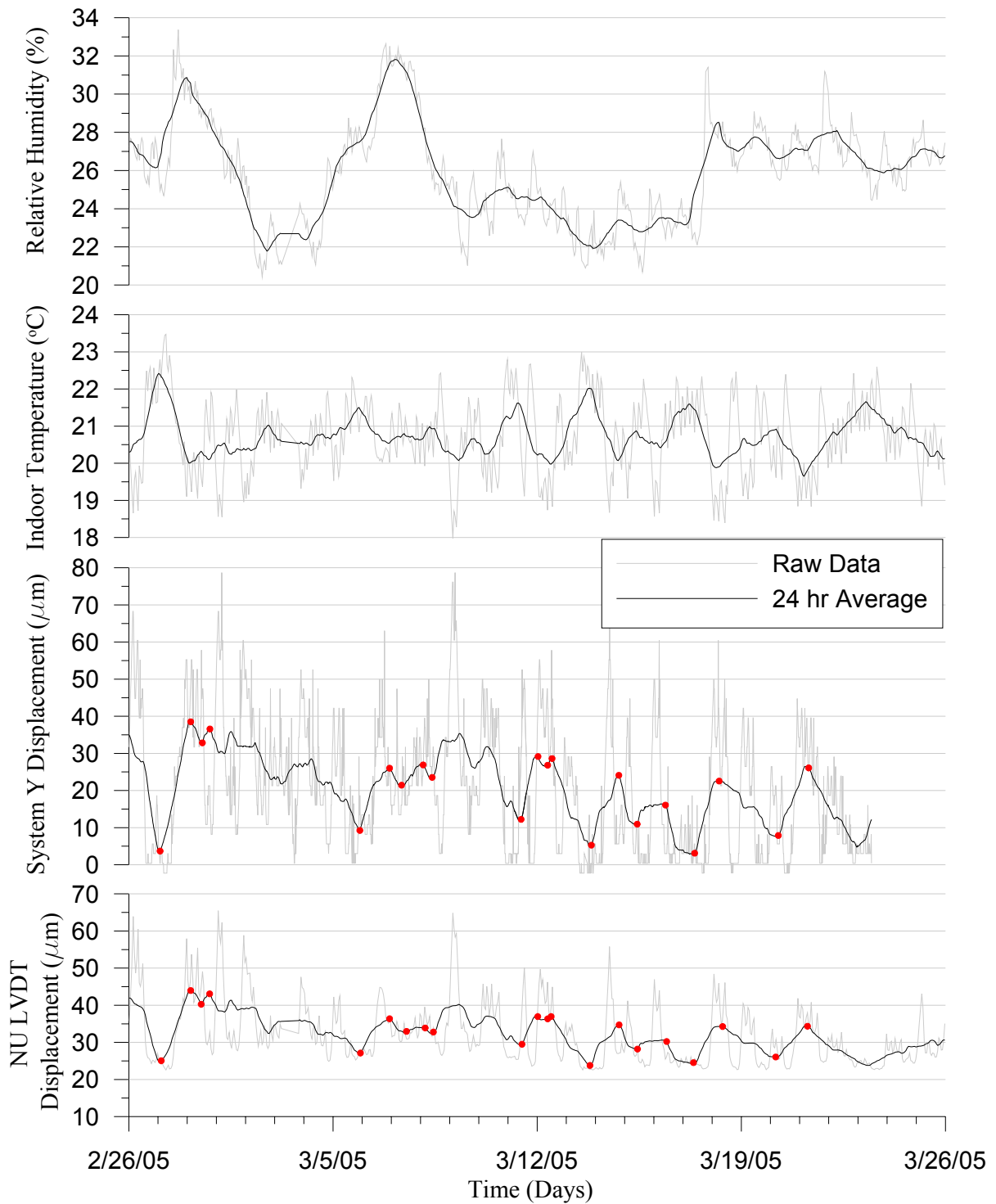


Figure 7.1 Comparison of the displacement time histories for the NU LVDT, System Y linear potentiometer crack gauge and indoor temperature. Gray jagged lines are a 1 hour rolling average; and the black lines are a 24-hour rolling average. (red dots indicate points used to calculate the long term static ratio.)

NU LVDT Δ Displacement (μm)	System X Δ Displacement (μm)	Ratio NU/X
18.91	34.84	0.54
-3.7	-5.68	0.65
2.81	3.72	0.76
9.24	16.76	0.55
-3.4	-4.57	0.74
0.92	5.46	0.17
-1.1	-3.36	0.33
7.46	16.93	0.44
-0.61	-2.34	0.26
0.61	1.8	0.34
-13.16	-23.34	0.56
10.92	18.82	0.58
-6.51	-13.16	0.49
2.03	5.14	0.39
-5.69	-12.98	0.44
9.73	19.44	0.50
-8.21	-14.65	0.56
8.28	18.2	0.45
Average		0.49
Slope linear best line		0.52

Table 7.1 System Y and NU LVDT calculated changes in displacement from the data collected in Figure 7.1.

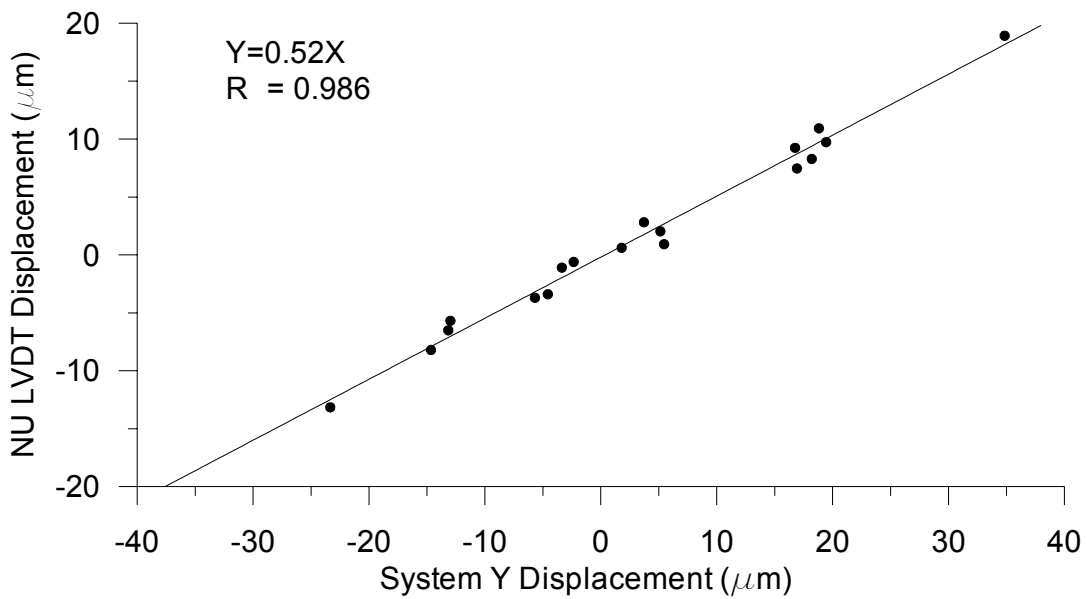


Figure 7.2 Long term system Y versus NU LVDT data used to determine the system X long term or static ratio

To determine if displacement recorded by system Y is caused by the thermal expansion of the ceiling material or the crack, the response of null gauge must be compared to that of the crack gauge. Figure 7.3 is a comparison of the displacements recorded by both the crack and null sensors mounted on the same piece of drywall and spaced within 0.5m of each other. The System Y null gauge was mounted on an uncracked section of ceiling. As expected, the null gauge showed little to no response during testing. Any small spikes in data as shown by grey line in the null displacement on Figure 7.3, could be attributed to electronic noise. Since the readings of the null gauge were so low, it was confirmed that the crack sensor was measuring the displacement of the crack and not the displacement of the ceiling material or temperature response of the sensor body. Upon removal it was discovered that the null gauge was not operable and therefore it is not absolutely certain that the zero response in Figure 7.3 results from low thermal response of the system.

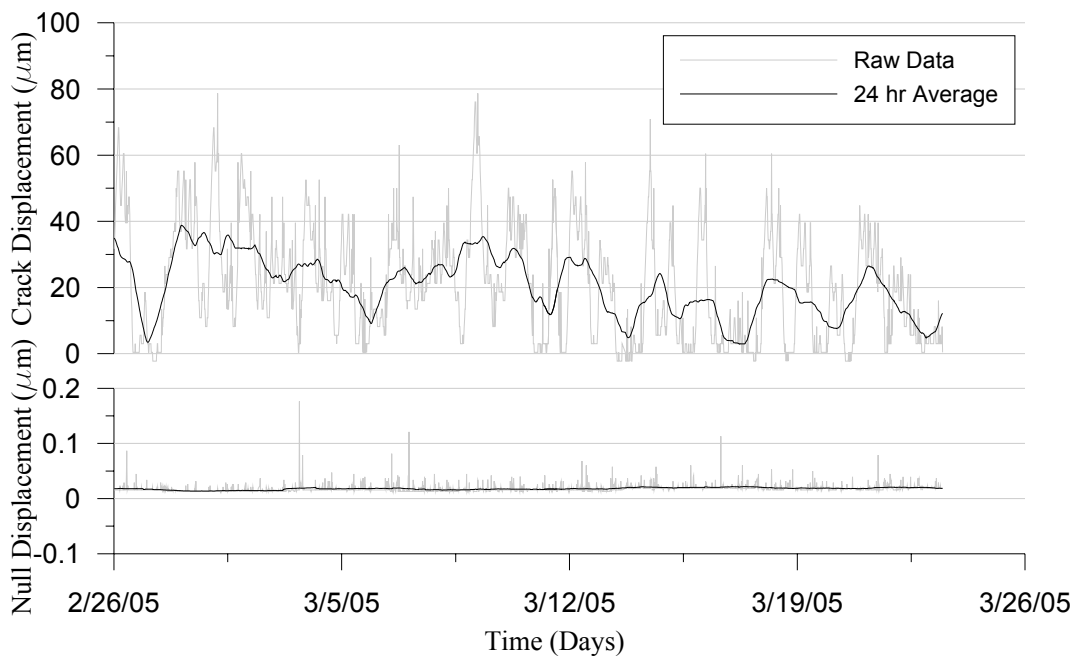


Figure 7.3 Comparison of the System Y Crack and Null gauges over two-month duration of testing

Level II Operation

Level II systems record simultaneously long term crack response and ground motion and dynamic crack response during blast events. The system begins recording dynamic response when the ground velocity exceeds the trigger value. Crack responses are measured as micrometer changes in crack width at high sampling rates (normally 1000 Hz). Long term crack width is recorded at regular time intervals ranging from every 15 minutes to once an hour for comparison with the long term environmental and dynamic effects. Collection of the long term data during level II operation was identical to level I system operation.

Level II evaluation was also conducted in the Milwaukee test house by comparing the response of system Y across a ceiling crack with that of the NU system. During simultaneous operation of system Y and the NU system, it was found that the NU system introduced higher noise levels to system Y. As a result of this conclusion, system Y was operated both with and without the NU system. Data collected during the operation of system Y was evaluated by comparing to the historical data from the NU system.

Level II Equipment Setup

To evaluate the operation of system Y at level II, the equipment was installed to record data as described in Chapter 5. Long term data collection was enabled by setting the histogramcombo function to record the peak crack displacement every 15 minutes. The system was set to record ground motion and trigger the crack monitor to dynamic time histories when the ground motion exceeded 1.02 mm/sec (0.04 in/sec).

Level II Data Collection

Level II data were collected over two months of operation in May and June of 2005. During the construction season, blasts occurred about once a week. On days when blasting did occur, two or three individual blasts would be observed within approximately an hour. As shown in Table 7.2, 19 blasts were recorded during level II evaluation of system Y. During monitoring, the peak particle velocity (PPV) of the ground motion ranged from 1.02 to 6.73 mm/sec with an average PPV of 1.84 mm/sec. The largest blast recorded during monitoring occurred on May 19, 2005. During the largest event the system Y geophone, inside on the basement floor, recorded a PPV of 6.73 mm/sec. The NU geophone position outside of the test house located closer to the quarry, recorded a PPV of 8.20 mm/sec and the even closer quarry geophone recorded a PPV of 9.73 mm/sec. Since the design of system Y for capturing ground motion is well documented, it will not be evaluated.

Records obtained from the quarry indicated 24 blasts occurred during the two months of evaluation of system Y. Approximately 80% of blasts were large enough to trigger system Y. Any blast that did not trigger system Y during testing had attenuated below the trigger value of 1.02 mm/sec by the time the ground motion reached the test house basement.

During level II testing of system Y, the unit was operated in two crack noise environments while in the same blasting environment. The first noise environment occurred when the NU equipment was operating and the noise levels averaged 5.3 μm . At this noise level the crack displacement during an event was completely masked by the noise. Any data collected when the NU equipment was operating required frequency filtering before it could be analyzed. When the nearby NU equipment was deactivated the noise level decreased to 1.3 μm .

Date	Longitudinal		Transverse		Vertical		Max PPV		Crack Displacement Zero to Peak (µm)	
	PPV (mm/sec)	Freq. (Hz.)	PPV (mm/sec)	Freq. (Hz.)	PPV (mm/sec)	Freq. (Hz.)	PPV (mm/sec)	Freq. (Hz.)	Ground Motion	Air Blast
5/4/2005	2.29	N/A	2.16	12	1.90	N/A	2.29	N/A	<2.6 ¹	<2.6 ¹
5/19/2005	5.08	34	2.16	28	6.73	32	6.73	32	<2.6 ¹	<5.2 ¹
5/19/2005	1.27	12	1.65	6	1.40	37	1.65	6	<2.6 ¹	<2.6 ¹
5/27/2005	1.27	34	1.14	32	1.02	37	1.27	34	<2.6 ¹	<2.6 ¹
5/27/2005	1.40	22	1.02	19	1.27	32	1.40	22	<2.6 ¹	<2.6 ¹
5/27/2005	1.90	11	1.27	17	1.90	28	1.90	11	<2.6 ¹	<2.6 ¹
6/2/2005	1.14	21	1.14	30	1.40	34	1.40	34	2.2	4.2
6/2/2005	2.16	17	1.40	14	1.78	20	2.16	17	1.6	3.0
6/2/2005	1.02	15	1.14	32	1.40	39	1.40	39	1.1	1.4
6/2/2005	1.52	37	1.14	37	1.40	47	1.52	37	1.3	7.2
6/9/2005	0.76	34	0.89	22	1.14	51	1.14	51	<0.5*	1.6*
6/9/2005	1.90	22	1.14	10	2.79	30	2.79	30	0.9*	1.6*
6/20/2005	1.14	34	1.02	30	1.02	26	1.14	34	1.3*	4.6*
6/20/2005	0.89	27	1.14	27	1.52	37	1.52	37	1.0*	2.2*
6/20/2005	1.14	11	1.02	11	1.40	11	1.40	11	1.3*	2.9*
6/30/2005	1.65	26	1.14	28	1.52	30	1.65	26	1.0*	1.3*
6/30/2005	1.27	24	1.14	17	1.27	22	1.27	24	<0.5*	1.3*
6/30/2005	1.14	37	1.02	16	1.14	43	1.14	37	<0.5*	1.9*
6/30/2005	1.14	37	0.89	30	1.02	39	1.14	37	1.0*	2.6*

Table 7.2 Summary of blast data collected during level II testing of system Y. ¹Denotes events record with the gain set to 1x. *Denotes events that did not require noise filtering. (NU system inactive)

Level II Performance

Peak dynamic crack displacements measured by the system Y linear potentiometer was compared to the NU LVDT and Kaman sensor. The evaluation of the sensors included a direct comparison of the shape and amplitudes of the waveforms. Figure 7.4 compares the dynamic response of the NU LVDT and Kaman sensors to the system Y linear potentiometer, for the same blast event. To create a direct level II comparison of system Y to the NU system, the system Y waveform was filtered to remove frequencies above 50 Hz. The shape of the waveform captured in Figure 7.4 by system Y, was similar to the waveform captured

by the NU LVDT and Kaman. All waveforms showed a peak crack displacement due to ground vibration 0.5 second into the blast. Additionally, all waveforms have a large low frequency peak at approximately 1.25 seconds from the air overpressure wave of the blast event. The system Y waveform displayed a larger peak crack displacement than the LVDT and Kaman sensors after filtering.

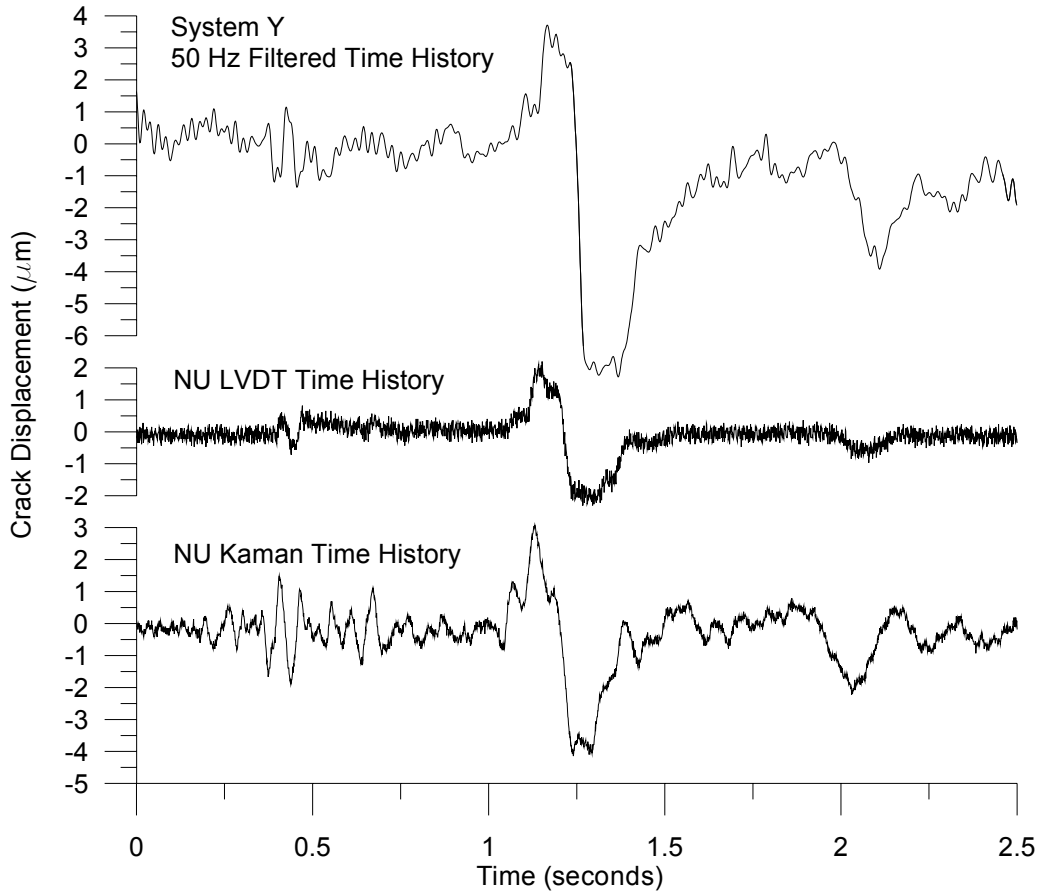


Figure 7.4 Direct comparisons of the crack time histories for system Y, NU LVDT and NU Kaman. Blast June 2, 2005. System Y data filtered to remove all frequency content greater than 50 Hz.

An adequate ACM system should have a consistent ratio of crack displacement for dynamic and long term responses. In addition, the ratio between one ACM system and another should remain relatively constant. Therefore, there are two measures of consistency

for an ACM system. First consider the average ratio of the dynamic responses shown in Figure 7.5 where four different blasts that occurred on June 2, 2005 are compared. Second, the ratio during long term response found during level I evaluation can be compared. Figure 7.5 shows data points that correspond to the maximum displacement response from ground motion and air overpressure of the system Y and NU LVDT sensors. During each event one of the peaks represents the ground motion induced crack response and the other represents the peak air overpressure induced crack response. In this case, the air blast response is always the largest.

Interpretation of ratios of the NU LVDT to system Y response is very complicated. For instance, the ratio for long term effects (shown in Figure 7.2 as 0.52), is 40% of the ratio of dynamic effects (shown in Figure 7.5 to be 0.32). While these ratios could be used to adjust the dynamic response to be comparable to the long term response, it may not be the proper adjustment because of filtering and the difference in noise compared to signal for dynamic and long term response. Unfortunately, to obtain a comparison requires simultaneous operation of the NU system, which induces high noise levels.

The required filtering of the system Y waveforms to reduce the effects of noise reduces the amplitude of the signal. Thus, had filtering not been required, the resulting waveforms would have had larger system Y crack response amplitudes and thus, a smaller dynamic ratio of the NU LVDT to system Y.

The noise level of system Y while the NU system was operational was much larger than the dynamic crack response amplitude but small with respect to the long term crack response amplitudes. For example during a blast event with a ground motion of 0.1 PPV there was only 1 μm of crack displacement (zero to peak) while the noise with the NU

system operational was $5.3 \mu\text{m}$ (zero to peak) or a 530 % of the signal. This high noise level shown in Figure 5.5 of Chapter 5 required filtering to obtain any signal relating to crack displacement, which complicates the comparison as discussed above. On the other hand the noise level is only 10% of the signal for a typical long term, weather induced crack response shown in Figure 7.3.

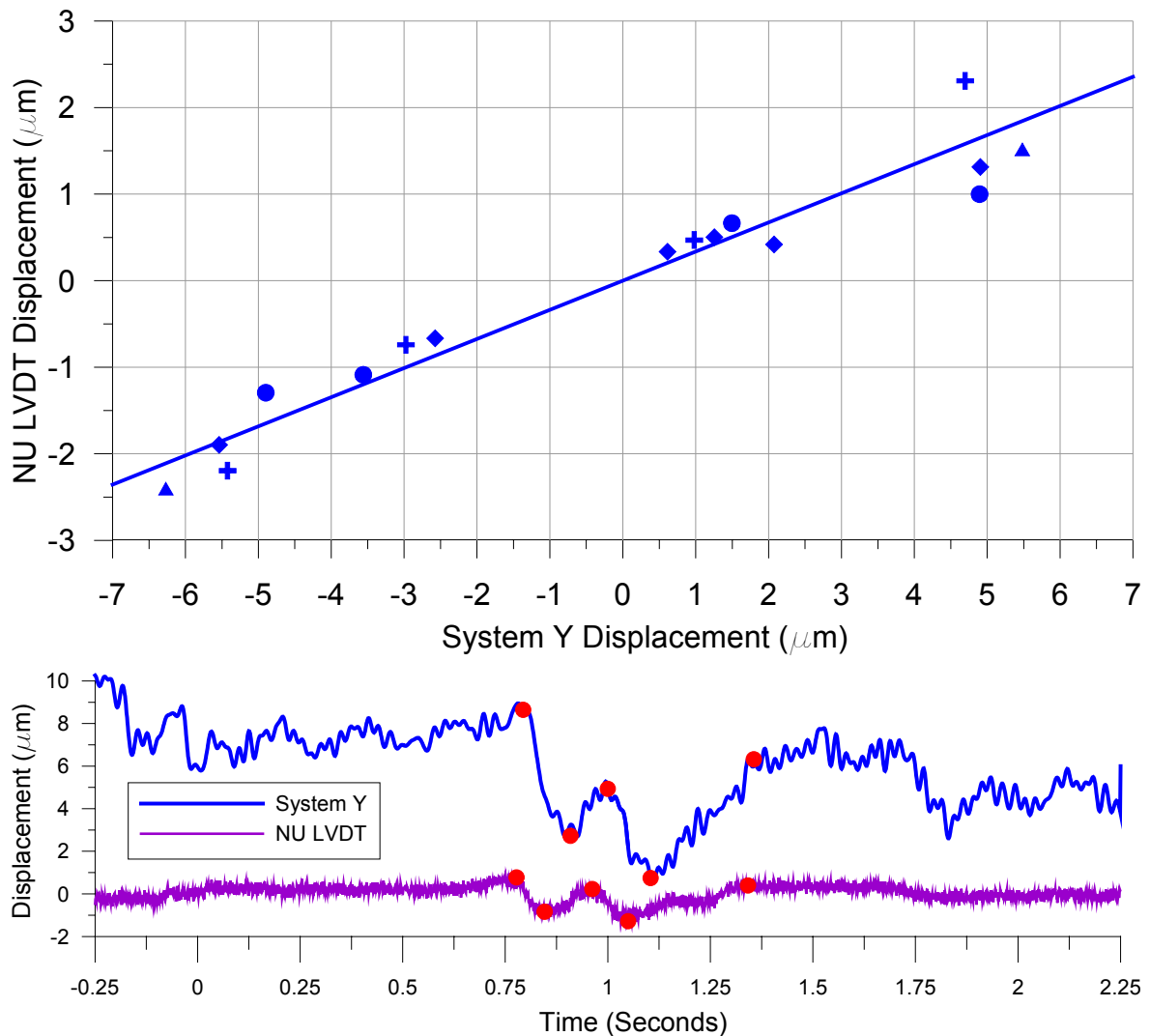


Figure 7.5 (Top) Comparison of the maximum and minimum displacements of system Y with the NU LVDT sensor during dynamic recording. These four events (denoted by symbols) occurred on June 2, 2005. (Bottom) Example of how the dynamic ratio was selected for a given filtered waveform.

To illustrate system Y's ability to capture a complete blast response, two different examples of the data captured by the system are reviewed. These events can be used to determine the overall effectiveness of the system's ability in capturing level II data as an independent system. The first event shown in Figure 7.6 depicts a blast event that occurred on June 9, 2005 and resulted in a temporary offset of the crack baseline. During this blast the geophone recorded a PPV of 2.79 mm/sec on the vertical channel. The corresponding crack displacement due directly from the ground motion was less than $2\mu\text{m}$, peak to peak, which is barely above the noise level of $1.3\mu\text{m}$ peak to peak. The larger crack response shown in Figure 7.6 due to the air overpressure wave that reached the structure approximately a second after the ground motion was $2.6\mu\text{m}$ peak to peak.

The long term and dynamic data collected with system Y during the day of the June 9th blast, can be compared to determine the significance of magnitude of the dynamic response of this blast to the total crack displacement due to all effects including the weather. The long term movement of the crack and dynamic displacement during the June 9th blast are shown together in Figure 7.7. Peak to peak displacement of the crack due to the blast air over pressure of $2.6\mu\text{m}$ is relatively insignificant. The dynamic crack movement is an order of magnitude higher compared to the daily movement of the crack at $25\mu\text{m}$ due to the various environmental effects.

System Y captured a small temporary baseline shift of $0.9\mu\text{m}$ in the crack time history shown in Figure 7.6. The June 9th blast was the second largest recorded during the entire monitoring period with PPV of 2.79 mm/sec. The time history captured showing the offset shown in Figure 7.6 is only three seconds long. As seen in Figure 7.7, temporary offset does not change the overall sinusoidal response pattern and is thus not an offset in any

permanent sense. Compared to the daily long term movement of the crack, the temporary change was only 3.6% of the daily movement in the displacement as shown in the figure.

The second example to illustrate system Y's ability to capture the cracks response to a blast is shown in Figure 7.7. This blast event recorded with system Y, on June 30, 2005 was more typical of the blasts seen during monitoring and had PPV of 1.14 mm/sec on the vertical channel of the geophone. This blast shows a small peak crack displacement due to the blast vibration when compared to the June 9th blast, but a large low frequency crack displacement due to the air overpressure. The June 30th blast shown in Figure 7.8 which has far lower ground particle velocities compared to the June 9th blast, shown in Figure 7.6, has an equivalent peak to peak crack displacement of 2.4 μm due to air overpressure.

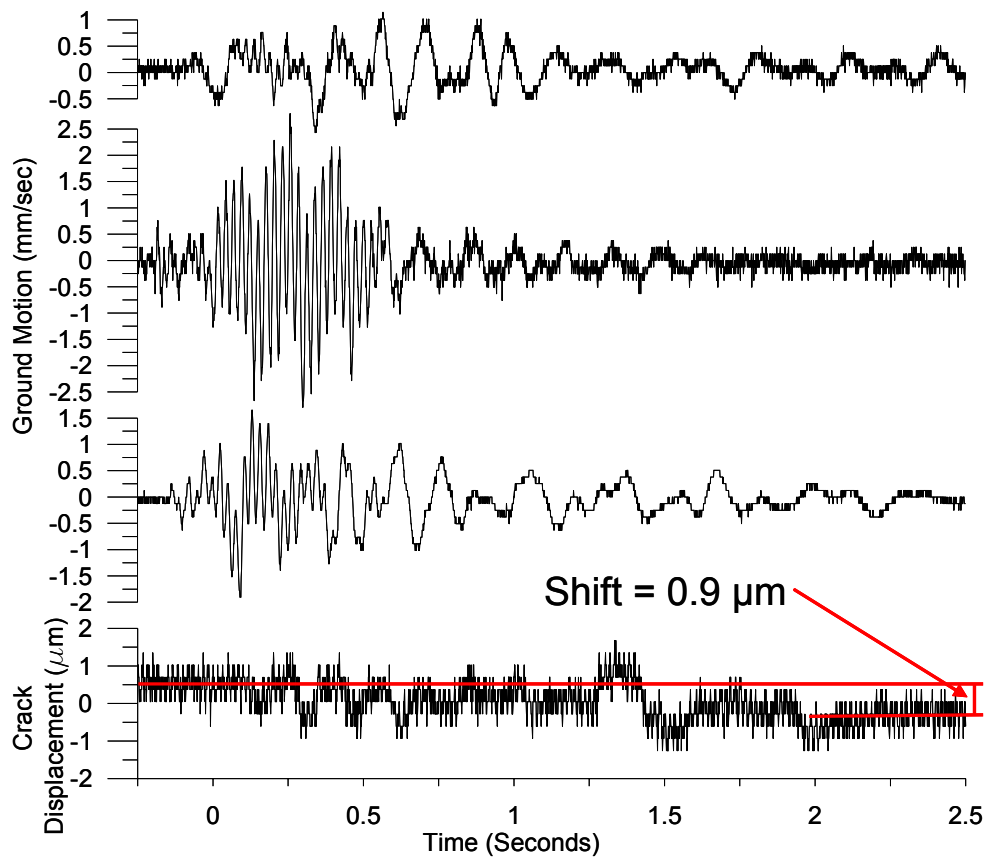


Figure 7.6 System Y recorded crack displacement from a blast occurring June 9, 2005 where a temporary offset occurred.

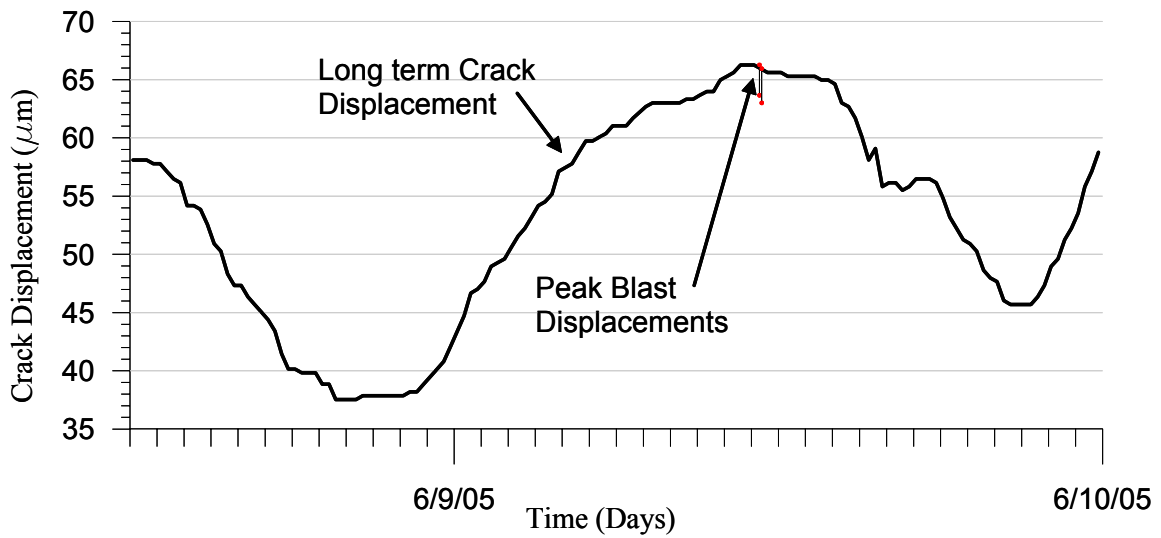


Figure 7.7 Comparison of the crack displacement captured by system Y both long term and dynamically during blasting on June 9, 2005 where an insignificant temporary offset occurred.

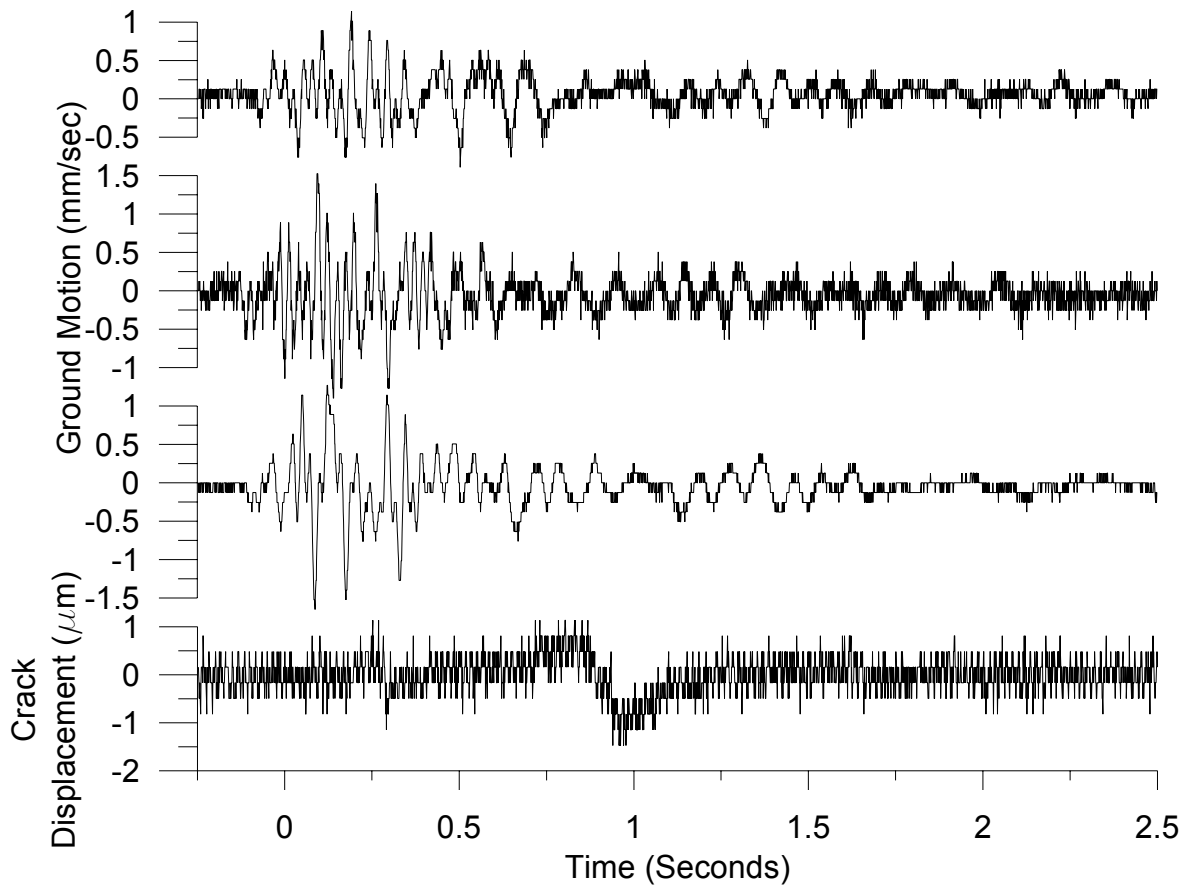


Figure 7.8 System Y recorded crack displacement from a blast occurring June 30, 2005 during which the crack responded primarily to the air blast.

Chapter 8

Conclusion

This thesis summarized the qualification and testing of two commercial Autonomous Crack Monitoring (ACM) systems for use in measuring micrometer displacement of cracks. Qualification involved the assessment of both laboratory and field performance in a residential structure subjected to nearby quarry blasting for the production of roadway aggregate. Aggregate and construction industries are dependant on procedures that cause vibratory ground motion and would benefit from a commercial ACM system. Currently, only research grade equipment is available for ACM monitoring which is expensive, unwieldy and requires specialized knowledge to operate.

Performance at three levels of monitoring has been evaluated. During level I monitoring only long term crack displacement response to environmental effects was recorded. During level II monitoring both long term and dynamic (triggered by ground motion) crack displacements are recorded. At the highest level of monitoring, level III, long term and dynamic crack displacements are recorded with dynamic response triggered by crack response and/or ground motion. Crack displacement triggering allows recording of crack responses to occupant activities or other non ground motion events such as wind gusts.

Conclusions regarding each system are subdivided into the following categories: installation, laboratory testing and field testing for each system. Their capabilities are

compared to the, Northwestern (NU) system response, which serves as a base line for performance. Evaluation of system X, is summarized first, followed by that of system Y.

System X

Analysis of the installation, software and literature

- Installation of system X in a residential structure can be completed in one day to measure ground motion, air overpressure and crack response.
- Crack displacements can be recorded in level I, II and III monitoring modes.
- Electromagnetic interference occurred at the 60 Hz, which is a common household power frequency.
- When employed in close proximity with the NU instrumentation system, noise levels increased.
- On-site programming can be completed via the key pad or a laptop computer through a serial connection, which may require a USB to serial converter for most laptops.
- Remote programming can be accomplished with the “get and set” method, because the easier to program TTY mode is less stable.
- Two software packages, Seismic Analysis and Event Manager, are required to view and process the data collected.
- Current literature for operation focused on ground motion monitoring; more ACM specific literature would be helpful.

Laboratory testing

- Long term temperature induced displacement responses were linear with minimal hysteresis.
- Dynamic excitation responses were similar to the control system in both frequency and magnitude.
- Temporary offsets in crack displacement can be captured during operation with the DC coupled channel.

Field testing (by level of operation)

Level I

- Long term crack displacement followed the changes in temperature and humidity in a pattern similar to that followed by the NU control system.
- Ratios of measured long term displacements (NU LVDT/system X) were constant, but greater than one throughout the qualification.
- Long term linearity and hysteresis remained similar during separate studies of the same crack response.

Level II

- During level II testing, ground motion triggered crack responses were similar to the NU control system response, yet smaller in magnitude.
- Only filtered dynamic data can be compared to that measured by the NU LVDT, because of the high level of noise produced by the NU system combined with the low signal.

- Two channels must be reviewed during level II operation; a DC coupled channel for long term crack response and an AC coupled channel for dynamic crack response.
- Calculation of ratios of dynamic response required filtering, to remove noise and allow a direct comparison to the NU system.
- Ratios of (NU system/system X) displacements for long term and dynamic responses of the same crack were within 25% of each other, despite the complexities imposed by high noise levels and filtering.

Level III

- Many crack responses triggered by occupant and environmentally induced events were captured.
- Crack trigger levels at specific locations may have to be varied because of large numbers of occupant generated events.
- Crack responses with small temporary offsets can be compared to the long term trends in the crack displacement to show their insignificance.
- Deliberate occupancy events were initiated to obtain time histories whose signatures could be correlated with otherwise unknown dynamic event time histories.
- Wind gust velocity, collected from the nearby airport correlated in time with dynamic crack displacement.
- Dynamic crack response studies can be under taken to identify trends in the occupant's daily activities and their effects on crack displacement.

System Y

Installation, software and literature

- Installation of system X in a residential structure can be completed in one day to measure ground motion, air overpressure and crack response.
- Crack displacements can be recorded in level I and II monitoring modes.
- Electromagnetic interference occurred at the 60 Hz, which is a common household power frequency.
- When employed in close proximity with the NU instrumentation system, noise levels increased.
- On-site programming can be completed via the key pad or a laptop computer through a serial connection, which may require a USB to serial converter for most laptops.
- Remote programming can be accomplished with the system specific software and an internet or mode connection.
- One software package was required to view and process the data collected.
- Current literature for operation focused on ground motion monitoring; more ACM specific literature would be helpful.

Laboratory testing

- Long term temperature induced displacement responses were linear with modest amounts of hysteresis.
- Dynamic excitation responses were similar to the control system in both frequency and magnitude.

- Temporary offsets in crack displacement can be captured during operation with the DC coupled channel.
- It was discovered that the null crack gauge supplied by the manufacturer was inoperable.
- During low amplitude dynamic tests, the system Y sensor was found to absorb typical displacement created by low force excitation and only responded to the larger excitation forces.

Field testing (by level of operation)

Level I

- Long term crack displacement followed the changes in temperature and humidity in a pattern similar to that followed by the NU control system.
- Ratios of measured long term displacements (NU LVDT/system Y) were constant, but less than one throughout the qualification.
- Long term crack displacement was found to follow the changes in temperature and humidity in a pattern similar to that followed by the NU control system.
- Lower than expected null displacement was recorded during monitoring, which may or may not have resulted from a malfunctioning null gauge.

Level II

- During level II testing, ground motion triggered crack responses were similar to the NU control system response, yet smaller in magnitude.

- Only filtered dynamic data can be compared to that measured by the NU LVDT, because of the high level of noise produced by the NU system combined with the low signal.
- Calculation of ratios of dynamic response required filtering, to remove noise and allow a direct comparison to the NU system.
- Ratios of (NU system/system Y) displacements for long term and dynamic responses of the same crack were within 40% of each other, despite the complexities imposed by high noise levels and filtering.
- Each event's, ground motion, air overpressure and crack displacement are contained within one record.

This study has made significant progress in the commercialization of ACM systems by verifying the operation of two commercial ACM systems in both the laboratory and field. Based on the measured data and the field experience from this study the following recommendations for future work are suggested. Further development of the manuals, literature and software that would accompany a commercial ACM system is needed. Improved literature and software would allow for ACM system to be installed and operated efficiently by a field technician with minimal experience. ACM systems should add the capability of autonomously collecting temperature and humidity data. Integrated temperature and humidity sensors would reduce the current dependency of these systems on external, stand alone temperature and humidity loggers. Finally, improved displacement sensors could reduce signal noise and increase recording resolution.

References

- Aimone-Martin, C. (2005). *Structural Response Study; Crystal Ridge, MacDonald Ranch and MacDonald Highlands*, Aimone-Martin Associates, LLC.
- Baillet, R. (2005). *Crack Response of a Historic Structure to Weather Effects and Construction Vibrations*, M.S. Thesis, Department of Civil and Environmental Engineering, Northwestern University, Evanston, IL.
- Dowding, C.H. (1996). *Construction Vibrations*, Prentice Hall, Upper Saddle River, NJ.
- Louis, M. (2000). *Autonomous Crack Comparometer Phase II*, M.S. Thesis, Department of Civil and Environmental Engineering, Northwestern University, Evanston, IL.
- McKenna, L.M. (2002). *Comparison of Measured Crack Response in Diverse Structures to Dynamic Events and Weather Phenomena*, M.S. Thesis, Department of Civil and Environmental Engineering, Northwestern University, Evanston, IL.
- National Climatic Data Center (2005). <http://cdo.ncdc.noaa.gov/ulcd/ULCD>, U.S. Department of Commerce, Federal Building, 151 Patton Avenue, Asheville, NC 28801
- Ozer, H. (2005). *Wireless Sensor Networks for Crack Displacement Measurement*, M.S. Thesis, Department of Civil and Environmental Engineering, Northwestern University, Evanston, IL.
- Petrina, M.B. (2004) *Standardization of Automated Crack Monitoring Apparatus for Long-Term Commercial Applications*, M.S. Thesis, Department of Civil and Environmental Engineering, Northwestern University, Evanston, IL.
- Siebert, M.L. (2000) *Autonomous Crack Comparometer*, M.S. Thesis, Department of Civil and Environmental Engineering, Northwestern University, Evanston, IL.
- Waldron, M. (2006) *Residential Crack Response to Vibrations from Underground Mining*, M.S. Thesis, Department of Civil and Environmental Engineering, Northwestern University, Evanston, IL.